Cover Page



Universiteit Leiden



The handle http://hdl.handle.net/1887/19155 holds various files of this Leiden University dissertation.

Author: Happé, Hester
Title: Cyst initiation, cyst expansion and progression in ADPKD
Date: 2012-06-27

Cyst initiation, cyst expansion and progression in ADPKD

Hester Happé

Cyst initiation, cyst expansion and progression in ADPKD

Thesis, Leiden University, Leiden, the Netherlands

© H. Happé, 2012, Leiden, the Netherlands
Copyright of the individual chapters rests with the authors, with the following exception: Chapter 4 was used with kind permission from Springer Science and Business Media.
No part of this thesis may be reproduced, stored or transmitted in any form or by any means, without prior written permission of the author and corresponding journal.

Lay-out and printing: Gildeprint Drukkerijen – Enschede, the Netherlands

Cover: Artistic representation of PAS stained section of a murine cystic kidney.
Design: Thomas Prins.

ISBN: 978-94-6108-309-8

Cyst initiation, cyst expansion and progression in ADPKD

Proefschrift

ter verkrijging van
de graad van Doctor aan de Universiteit Leiden,
op gezag van Rector Magnificus prof.mr. P.F. van der Heijden,
volgens besluit van het College voor Promoties
te verdedigen op woensdag 27 juni 2012
klokke 15.00 uur

door

Hester Happé
geboren te 's-Hertogenbosch in 1981

Promotiecommissie

Promotor:	Prof. Dr. M.H. Breuning
Co-promotores:	Dr. E. de Heer
	Dr. D.J.M. Peters
Overige leden:	Prof Dr. R.T. Gansevoort[1]
	Prof. Dr. N.V. Knoers[2]
	Prof. Dr. B. van de Water

[1] Divisie Nefrologie, Afdeling Interne Geneeskunde, Universitair Medisch Centrum Groningen, Universiteit Groningen, Groningen, Nederland
[2] Afdeling Medische Genetica, Universitair Medisch Centrum Utrecht, Utrecht, Nederland

The studies described in thesis have been performed at the Leiden University Medical Center, department of Human Genetics and Pathology (head Prof. Dr. G.J.B. van Ommen and Prof. Dr. G.J. Fleuren, respectively).

Publication of this thesis was financially supported by:
J.E. Jurriaanse Stichting

Contents

Chapter 1	General introduction	7
Chapter 2	Polycystic kidney disease: The complexity of planar cell polarity and signaling during tissue regeneration and cyst formation *Biochim Biophys Acta 2011; 1812: 1249-1255.*	23
Chapter 3	Toxic tubular injury in kidneys from *Pkd1*-deletion mice accelerates cystogenesis accompanied by dysregulated planar cell polarity and canonical Wnt signaling pathways *Hum Mol Genet 2009; 18: 2532-2542.*	39
Chapter 4	Morphometric analysis of centrosome position in tissues *Methods Mol Biol. 2012;839:249-55*	61
Chapter 5	Altered Hippo signaling in polycystic kidney disease *J Pathol 2011; 224: 133-142.*	71
Chapter 6	Cyst expansion and regression in a mouse model for polycystic kidney disease *Kidney International, under revision*	93
Chapter 7	Summarizing discussion	117
Chapter 8	Nederlandse samenvatting voor niet-ingewijden	129
Chapter 9	Curriculum Vitae	135
Chapter 10	List of Publications	139
Chapter 11	Dankwoord (Acknowledgements)	143

1

General introduction and thesis outline

General introduction

Autosomal Polycystic Kidney Disease (ADPKD) is one of the most common inherited diseases with an incidence of 1 in 400 to 1 in 1000 in Caucasians.[1-4] In 50% of the ADPKD patients the disease leads to end stage renal disease (ESRD) around the age of 55 years and patients require dialysis and renal transplantation. In fact, ADPKD accounts for up to 10% of the ESRD cases.[5] ADPKD is characterized by the formation of fluid filled cysts in both kidneys eventually replacing almost all normal renal parenchyma leading to a decline in renal function (Fig. 1). The disease is, however, a systemic disease. Extra-renal manifestations are hypertension, cardiac valvular abnormalities, cerebral aneurysms and cysts in liver and pancreas.[6]

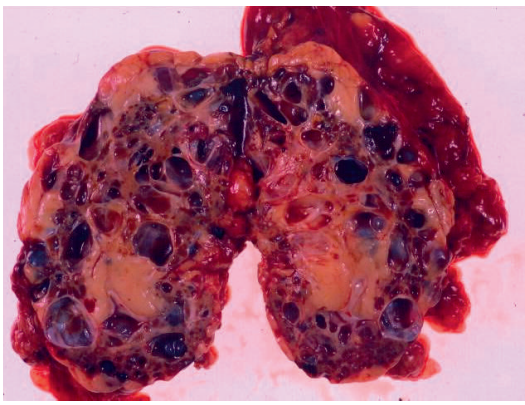


Figure 1. Polycystic kidney showing many cysts and fibrotic tissue.

Genetics of ADPKD

In 85% of the ADPKD patients the Polycystic Kidney Disease 1 (*PKD1*) gene, encoding the protein polycystin-1 (PC1), is mutated. In the remaining 15% of the patients the disease is caused by a mutation in the Polycystic Kidney Disease 2 (*PKD2*) gene, encoding polycystin-2 (PC2).[7-9] The *PKD1* gene is located on chromosome 16 and contains 46 exons, spanning 50 kb of genomic DNA, encoding a large 14.1 kb mRNA transcript. *PKD2* has 15 exons, spanning 68 kb of genomic sequence, encoding a 5.1 kb mRNA transcript.

No mutation hot spot has been found for *PKD1* and *PKD2*, which means that mutations are spread throughout the entire gene.[10]

The polycystin proteins

PC1 protein is a large transmembrane glycoprotein of 4303 amino acids. It has a large extracellular N-terminal domain, 11 transmembrane domains and a short cytoplasmic C-terminus.[11-13] The extracellular portion contains many domains, several of them implicated in protein-protein

interactions. In addition, the extracellular part contains a proteolytic G protein-coupled receptor (GPCR) proteolytic site domain (GPS) that was shown to be functionally active; cleavage activates signal transducer and activator of transcription-1 (STAT-1) and induces tubulogenesis in vitro.[14]
The intracellular C-terminus of PC1 contains a coiled-coil domain that interacts with PC2[15-17] (Fig. 2). The C-terminus has also been shown to be cleaved at least two different sites, generating two products. These products can interact with transcription factors, β-catenin or STAT6, and translocate into the nucleus to modulate gene expression.[18, 19]
PC2 is with 968 amino acids a smaller protein than PC1. This protein forms a nonselective cation-channel that is highly permeable for Ca^{2+} (Fig. 2).

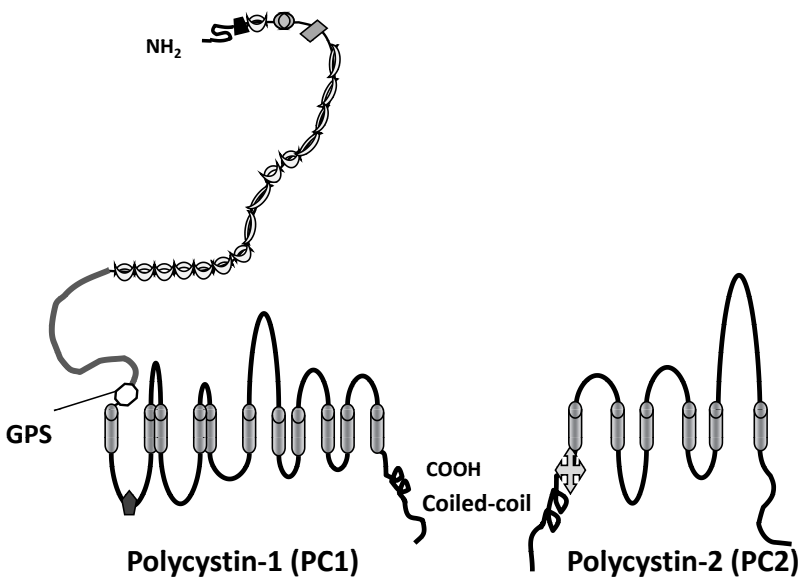


Figure 2. Schematic representation of polycystin-1 and polycystin-2 and the different domains.

The polycystins are abundantly expressed in renal tubular epithelial cells where a balanced level of PC1 and 2 is required to maintain renal epithelial architecture. The polycystins are localized in several sub-cellular compartments such as the primary cilium, cell-cell contacts and cell extracellular matrix (ECM) contacts.
The primary cilium is a cellular organelle that protrudes from the plasma membrane in non-dividing cells, with one of the two centrosomes, the basal body, at its base. A primary cilium can be found on almost, if not all, cell types. Also renal epithelial cells have a primary cilium, which protrudes into the tubule lumen where it is thought to sense the extra-cellular environment. PC1 and PC2 are considered to act as mechanosensors here; upon bending of the cilium, as the result of flow, PC2 mediates a calcium-influx. How exactly this signal is transduced further into

the cell is not exactly known. However, ciliary signaling seems to be involved in cyst formation as mutations in many ciliary proteins result in renal cyst formation.

At cell-cell and cell-ECM contacts, they form different multimeric protein complexes, modulating several signaling pathways, which in concert control essential cellular functions such as proliferation, apoptosis, cell adhesion, and differentiation.[2] Disruption of any of these processes can lead to cyst formation, as demonstrated by a variety of mouse models.[20-24]

Mechanism of cyst formation

In general, ADPKD patients carry one inherited mutated allele of *PKD1* or *PKD2* (germ-line mutation), and one healthy *PKD1* or *PKD2* allele. It is thought that renal epithelial cells of patients function normally, but when the expression of PC1 or PC2 drops below a critical threshold, cysts arise. This decrease in expression can be caused by a somatic mutation in the remaining healthy allele, called a "second hit" or due to haploinsufficiency, stochastic fluctuations in gene expression as a result of the inactivation of one allele.[25] Somatic mutations are often found in renal epithelial cells and increase with age.[26] The second hit model is also in agreement with the fact that only 1% of the nephrons is involved in cyst formation and that mice heterozygous for mutated *Pkd1* or *Pkd2* don't show renal cyst formation. Furthermore cysts of clonal origin have been observed.[27] Whereas the second hit model assumes that cystic epithelia lack PC1 or PC2 expression, the haploinsufficiency model fits with the expression of PC1 and PC2 in cystic epithelia that has been reported. However, it was also shown that overexpression of the polycystins results in cysts. This suggests that expression of polycystins within a critical window, not too high or too low, or a correct balance between PC1 and PC2 expression is required for normal tubular morphology.

Following the acquired misbalance of PC1 and PC2 it was hypothesized that these cells then become hyper proliferative and show deregulation of many signaling pathways resulting in depolarization, increased fluid transport and extracellular matrix production.

However, complete inactivation of *Pkd1* at adult age resulted in a mild cystic phenotype after 3-5 months, while inactivation during renal development resulted in massive cystic kidneys after 1 month.[28, 29] As a result, it was hypothesized that developmental and/or proliferative status of renal epithelial cells was important for cyst formation upon complete *Pkd1*-gene inactivation. This hypothesis is further discussed in chapter 2 of this thesis and is part of investigation in chapter 3. Figure 3 shows a schematic representation of the proposed mechanism.

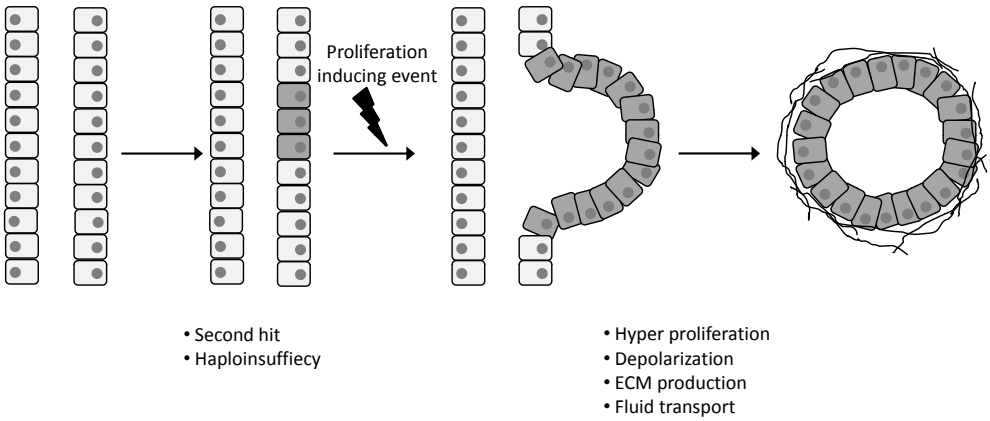


Figure 3. Schematic representation of the proposed mechanism of cyst formation in ADPKD. All tubular epithelial cells contain one mutated *PKD1* or *PKD2* allele and one unaffected allele. During life, in a subset of cells, protein levels of PC1 and/or PC2 become misbalanced due to a second hit or haploinsufficiency (dark grey). When these cells proliferate, cyst formation is initiated and many signaling pathways become deregulated. The epithelial cells become hyper proliferative and depolarized. Increased fluid transport into the isolated cyst contributes to expansion.

Signaling pathways involved in ADPKD

Many signaling pathways are modulated by PC1 or 2 or are implicated in ADPKD and cyst formation. Both PC1 and PC2 are expressed in several sub-cellular compartments such as the primary cilium, cell-cell contacts and cell-extracellular matrix contacts. They form different multimeric protein complexes in the cell, modulating several signaling pathways, which in concert control essential cellular functions such as proliferation, apoptosis, cell adhesion, and differentiation.[2, 30] Additionally, reduced Ca^{2+} influx, cAMP accumulation and aberrant Ras/Raf/ERK activation are implicated in cyst growth [31, 32] as well as activation of mTOR, PI3-kinase, and Jak2-STAT1/3 signaling.[33-35] However, this thesis focuses on canonical Wnt signaling, the planar cell polarity signaling and the Hippo pathway.

Canonical Wnt signaling

The canonical Wnt signaling pathway, also known as β-catenin mediated Wnt signaling pathway, signals through binding of the Wnts ligands to the frizzled receptors. In the absence of Wnt-ligands, β-catenin, an integral cell-cell adhesion adaptor protein as well as transcriptional co-regulator, is targeted for degradation via the ubiquitin pathway by a destruction complex. This destruction complex contains APC and GSK-3β among others (Fig. 4A).

Upon binding of Wnt-ligand, the protein Dishevelled is activated and GSK-3β is recruited away from the degradation complex. This allows for stabilization of β-catenin levels and subsequent nuclear translocation where it acts as an activator for transcription (Fig 4B). Well known β-catenin

target genes are *C-myc*, *Axin2*, *CyclinD1*, *Cd44*, *Ppar-δ and Mmp7*. In addition to canonical Wnt signaling, also non-canonical Wnt-signaling routes, independent of β-catenin were discovered. These non-canonical pathways have also been termed the Wnt/Calcium and Wnt/JNK pathways in vertebrates and planar cell polarity pathway in *Drosophila.* The Wnt/JNK and PCP pathways appear to be similar in the use of Frizzled receptors, and several downstream components.

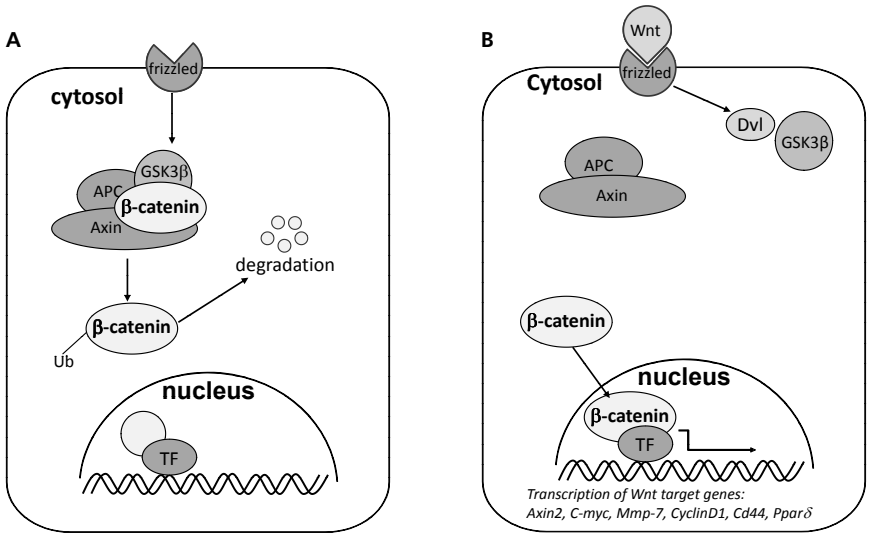


Figure 4. Simplified diagram of canonical Wnt signaling. (A) In absence of Wnt-ligand binding to the frizzled receptor, β-catenin is targeted for degradation via the ubiquitin pathway by the destruction complex containing APC, GSK3β and Axin. (B) In presence of Wnt-ligand binding, activated Dishevelled (Dvl) inactivates the destruction complex by recruiting GSK3β away from the destruction complex. β-catenin can now enter nucleus and mediate transcription of Wnt-target genes.

Planar cell polarity signaling

Epithelial cells do not only show apical-basal polarity but also show orientation within the plane of the epithelial cell sheet. This is called planar cell polarity (PCP).

Planar cell polarity is clearly visible on the wings of *Drosophila* where all the hairs point in the same direction (Fig. 5A). Mutations in the PCP pathways core components disturb this pattern (Fig. 5B). Also during renal development the PCP pathway is important; it ensures lengthening of the tubules while maintaining correct tubular diameter. Defects in PCP signaling may therefore cause an increase in tubular diameter.[36, 37]

The PCP pathway is the signaling pathway that affects planar polarization of cells and is also known as the non-canonical Wnt pathway in *Drosophila*. This pathway also includes the frizzled receptor and the protein Dishevelled as well as the cadherins Dachsous (Ds) and Four-jointed (Fj) (reviewed by McNeill[38]). Although much knowledge about the PCP pathway has been gained

from *Drosophila* wing and eye, it is not exactly known how planar cell polarity executed and regulated in vertebrates. In vertebrates the regulation is more complex and planar polarization is influenced by more signaling cascades than non-canonical Wnt signaling as discussed in chapter 2.

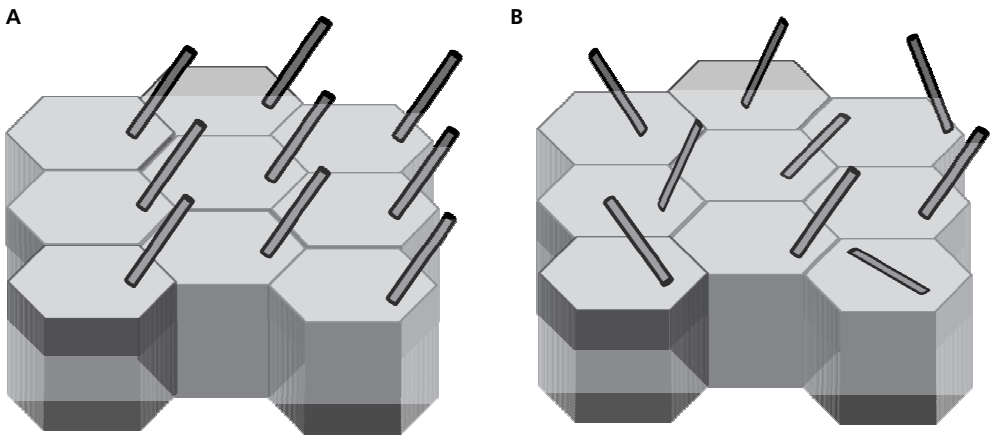


Figure 5. Planar cell polarity (PCP) in cells of the wing of Drosophila. (A) Normal PCP in wild type cells; hairs point in the same direction. (B) Disturbed PCP; hairs point in random direction.

Hippo signaling pathway

Finally, the Hippo pathway is also a major subject in this thesis. The Hippo pathway has extensively been studied in *Drosophila*, where it is involved in control of cell proliferation and apoptosis.[39-41] In addition, an important role for the Hippo pathway has been suggested in the regulation of organ and tissue size control. Hippo pathway mutants show dramatic alterations in e.g. wing size.[39-42] The pathway is named after the core pathway component, the kinase Hippo. Via several phosphorylation steps eventually, the non-DNA binding transcriptional co-activator Yorkie (Yki) is phosphorylated and retained in the cytoplasm. This prevents Yki target genes from being transcribed (Fig. 6A).

The core components of the *Drosophila* Hippo pathway are well conserved and also function as tumor suppressors in mammals in addition to regulating growth in terms of organ size control.[43] In mammals, the Hippo signaling pathway exerts its actions by controlling the transcription of genes through the Yki ortholog YAP and its paralog TAZ (Fig. 6B).
FJ is not only involved in PCP signaling but is also a regulator of the Hippo pathway together with Ds, via a complex and currently not completely understood mechanism.[44]

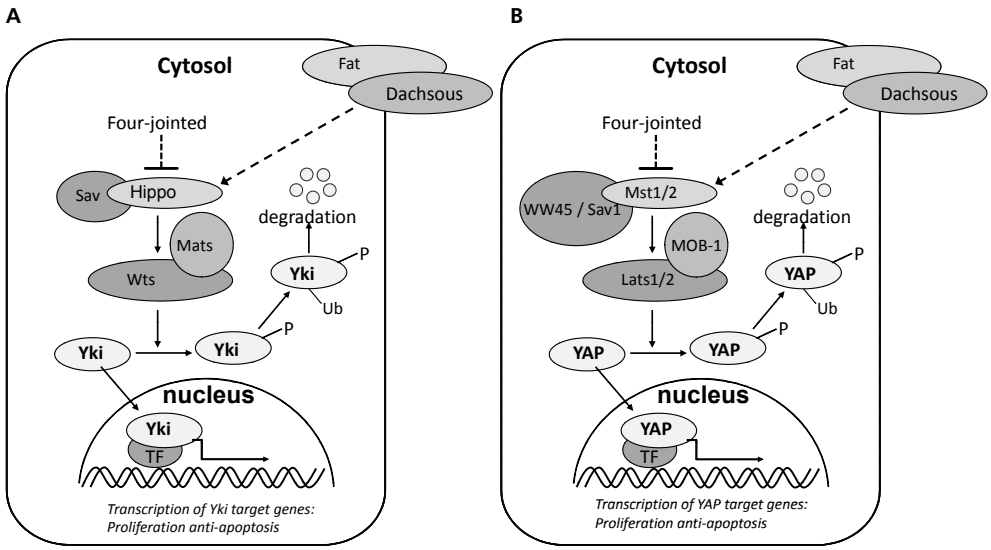


Figure 6. Simplified diagram of Hippo signaling in (A) *Drosophila* and (B) mammals. (A) The kinase Hippo is at the top of a cascade of phosphorylation events leading to the phosphorylation of the transcriptional co-activator Yki. Thereby targeting it for degradation through ubiquitination and preventing nuclear localization of YAP. Thus diminished activation of the Hippo pathway leads to nuclear localization of Yki and transcription of Yki targets genes. (B) In mammals the Hippo pathway in general functions the same way as in *Drosophila*. Here the effector molecule of the Hippo pathway is called YAP.

Mouse models used in this thesis to study cyst formation and disease progression

In order to study the mechanism of cyst formation and disease progression in ADPK, several murine models are available.[45-54] To overcome embryonic lethality homozygous knock-out mice and to study tissue specific effects of *Pkd1*-inactivation, inducible *Pkd1* and *Pkd2* deletion mice have been created, using the Cre/LoxP system.[28, 29, 55-59]

The inducible *Pkd1*-deletion model

One of the models used in this thesis is the tamoxifen-inducible *KspCad-CreER^{T2};Pkd1$^{del2\text{-}11/lox2\text{-}11}$* model. This is a model using the Cre/LoxP system; In this mouse model one *Pkd1* allele contains a germ-line deletion; exons 2-11 are deleted (*Pkd1$^{del2\text{-}11}$*). The second *Pkd1* allele contains two LoxP sites which are located in introns 1 and 11 respectively (*Pkd1$^{lox2\text{-}11}$*) The inactivation of the second *Pkd1* allele is based on excision of exons 2-11 by homologous recombination mediated by the Cre-recombinase (Fig. 7A). When Cre-recombinase is not active, exons 2-11 are not excised, resulting in a normal PC1 protein.

The *Pkd1*$^{del2\text{-}11/lox2\text{-}11}$ mice are crossed with mice that contain a construct encoding a genetically engineered Cre-recombinase that is driven by the kidney specific cadherin promoter (KspCad), thereby only expressing Cre in renal epithelial cells. In addition, this Cre-recombinase is modified in such a way that it is inactive in absence of the chemical compound tamoxifen (Cre-ER^{T2}). Thereby, excision of the by loxP sites flanked sequence, i.e., inactivation of the gene, can be achieved at any desired time point by administration of tamoxifen.
Thus, in the generated transgenic mouse model (Fig. 7B) the second *Pkd1* allele can be inactivated in renal epithelial cells specifically at any desired moment using tamoxifen.

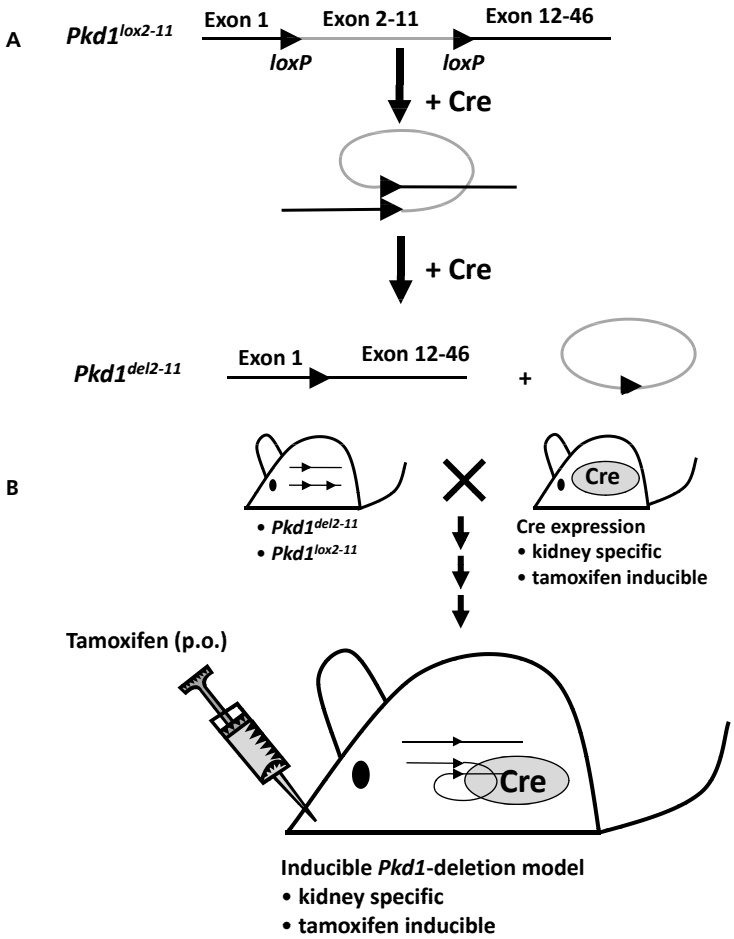


Figure 7. Schematic representation of the inducible *Pkd1*-deletion model. (A) Schematic representation of the *Pkd1* allele containing loxP sites in intron 1 and 11. When the recombinase Cre is active, the part between the loxP sites is then excised. (B) The *Pkd1* inducible conditional knockout model is generated by breeding mice containing one *Pkd1*$^{del2\text{-}11}$ allele and one *Pkd1*$^{lox2\text{-}11}$ allele with mice in which a modified Cre is expressed in renal epithelial cells. The modified Cre-recombinase becomes active in presence of tamoxifen. In this way a mouse model is generated in which *Pkd1* inactivation is achieved in renal epithelial cells at any desired time point.

The *Pkd1*^{nl,nl} mouse model

The second mouse model that was used in this thesis, is the *Pkd1*^{nl,nl} model. These mice are homozygous for mutated *Pkd1*. This mouse model shows reduced expression of the normal *Pkd1* transcript caused by the insertion of a selection cassette containing the neomycin resistance gene (neo) flanked by loxP sites in intron 1 of *Pkd1*. This results in alternative splicing leading to a mixture of normal and mutant transcript, the latter predicted to result in a premature translational stop[60] (Fig. 8).

These mice develop cystic kidneys within 3-4 weeks and also show extra-renal manifestations such as cysts in the liver and pancreas and dissecting aortic aneurysms were observed.[60, 61] However, the severity of the phenotype and lifespan is dependent on the genetic background of the mouse strain as is discussed in chapter 6.

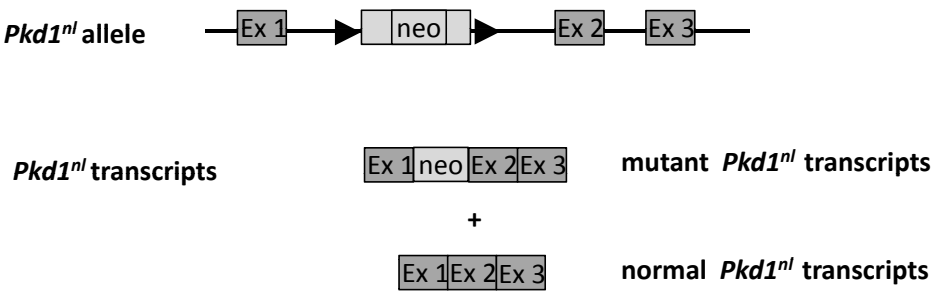


Figure 8. Schematic representation of the *Pkd1*^{nl} allele containing a selection cassette containing the neomycin resistance gene (neo) flanked by loxP sites in intron 1 of *Pkd1*. Alternative splicing of *Pkd1* results in a mixture of normal and mutant transcripts. Ex; exon (only exon 1 to 3 of the 46 *Pkd1* exons are shown).

Outline

Chapter 2 of this thesis reviews the signaling pathways involved in the different phases of ADPKD pathogenesis. The initiation phase, with hyper proliferative epithelial cells as a hallmark, is followed by a phase of cyst growth and cyst expansion. Later on, proliferation of cystic epithelia ceases and interstitial fibrosis and inflammation become apparent. This literature review focuses on the initiation phase and the involvement of planar cell polarity (PCP) signaling pathway, while briefly discussing other signaling cascades involved during this and following phases. In this thesis the different phases, as described in **chapter 2,** are studied. In **chapter 3** the initiation of cyst formation is studied. In contrast to patients with ADPKD, heterozygosity for mutated *Pkd1* in mice does not lead to cyst formation. Complete inactivation of *Pkd1* in kidneys of conditional knockout mice, however, induces massive cyst formation when *Pkd1* deletion occurs when renal development is not completed fully and proliferation of tubular epithelial cells is present. This suggests a role for proliferation in cyst formation. We investigated the role of tubular epithelial proliferation in cyst formation by induction of renal injury in adult mice, thereby inducing epithelial proliferation as a result of repair. In addition, canonical Wnt-signaling (β-catenin mediated) as well as PCP signaling were investigated as these pathways are involved in cyst formation.
In chapter 3 we used measurement of the position of the centrosome as read-out system for PCP. **Chapter 4** describes in detail the method used for measuring centrosome position.

The results in chapter 3 showed differential expression of a component of the PCP pathway and Hippo-signaling pathway. Therefore, in **chapter 5** the involvement of the Hippo signaling pathway in cyst formation and growth is examined. The Hippo signaling pathway is known for its role in *Drosophila* organ size control and involvement in several forms of cancer. Because of these characteristics this pathway provides a potential additional participant and therapeutic target in cyst formation and growth.
The later phase of ADPKD pathogenesis is subject of investigation in **chapter 6**. Here ADPKD disease progression is studied in the *Pkd1*$^{nl/nl}$ mouse model on a mixed genetic background of 50% C57Bl/6J and 50% 129Ola/Hsd. The prolonged survival of these mice, compared to survival previously reported for this model on full C57Bl/6J genetic background, allowed us to examine several aspects of disease progression such as changes in renal volume and renal function, fibrosis and inflammation. Finally, the results described in the individual chapters of this thesis are concluded with a summarizing discussion in **chapter 7.**

References

1. Igarashi,P. & Somlo,S. Genetics and pathogenesis of polycystic kidney disease. *J. Am. Soc. Nephrol.* **13**, 2384-2398 (2002).
2. Wilson,P.D. Polycystic kidney disease. *N. Engl. J. Med.* **350**, 151-164 (2004).
3. Torres,V.E. New insights into polycystic kidney disease and its treatment. *Curr. Opin. Nephrol. Hypertens.* **7**, 159-169 (1998).
4. Calvet,J.P. & Grantham,J.J. The genetics and physiology of polycystic kidney disease. *Semin. Nephrol.* **21**, 107-123 (2001).
5. Gabow,P.A. Autosomal dominant polycystic kidney disease. *N. Engl. J. Med.* **329**, 332-342 (1993).
6. Gabow,P.A. Autosomal dominant polycystic kidney disease--more than a renal disease. *Am. J. Kidney Dis.* **16**, 403-413 (1990).
7. Peters,D.J. & Sandkuijl,L.A. Genetic heterogeneity of polycystic kidney disease in Europe. *Contrib. Nephrol.* **97**, 128-139 (1992).
8. The European Polycystic Kidney Disease Consortium. The polycystic kidney disease 1 gene encodes a 14 kb transcript and lies within a duplicated region on chromosome 16. *Cell* **77**, 881-894 (1994).
9. Mochizuki,T. *et al.* PKD2, a gene for polycystic kidney disease that encodes an integral membrane protein. *Science* **272**, 1339-1342 (1996).
10. Tan,Y.C., Blumenfeld,J., & Rennert,H. Autosomal dominant polycystic kidney disease: genetics, mutations and microRNAs. *Biochim. Biophys. Acta* **1812**, 1202-1212 (2011).
11. Nims,N., Vassmer,D., & Maser,R.L. Transmembrane domain analysis of polycystin-1, the product of the polycystic kidney disease-1 (PKD1) gene: evidence for 11 membrane-spanning domains. *Biochemistry* **42**, 13035-13048 (2003).
12. Sutters,M. The pathogenesis of autosomal dominant polycystic kidney disease. *Nephron Exp. Nephrol.* **103**, e149-e155 (2006).
13. Sutters,M. & Germino,G.G. Autosomal dominant polycystic kidney disease: molecular genetics and pathophysiology. *J. Lab Clin. Med.* **141**, 91-101 (2003).
14. Qian,F. *et al.* Cleavage of polycystin-1 requires the receptor for egg jelly domain and is disrupted by human autosomal-dominant polycystic kidney disease 1-associated mutations. *Proc. Natl. Acad. Sci. U. S. A* **99**, 16981-16986 (2002).
15. Hanaoka,K. *et al.* Co-assembly of polycystin-1 and -2 produces unique cation-permeable currents. *Nature* **408**, 990-994 (2000).
16. Qian,F. *et al.* PKD1 interacts with PKD2 through a probable coiled-coil domain. *Nat. Genet.* **16**, 179-183 (1997).
17. Yu,Y. *et al.* Structural and molecular basis of the assembly of the TRPP2/PKD1 complex. *Proc. Natl. Acad. Sci. U. S. A* **106**, 11558-11563 (2009).
18. Lal,M. *et al.* Polycystin-1 C-terminal tail associates with beta-catenin and inhibits canonical Wnt signaling. *Hum. Mol. Genet.* **17**, 3105-3117 (2008).
19. Low,S.H. *et al.* Polycystin-1, STAT6, and P100 function in a pathway that transduces ciliary mechanosensation and is activated in polycystic kidney disease. *Dev. Cell* **10**, 57-69 (2006).
20. Sorenson,C.M., Padanilam,B.J., & Hammerman,M.R. Abnormal postpartum renal development and cystogenesis in the bcl-2 (-/-) mouse. *Am. J. Physiol* **271**, F184-F193 (1996).
21. Trudel,M., D'Agati,V., & Costantini,F. C-myc as an inducer of polycystic kidney disease in transgenic mice. *Kidney Int.* **39**, 665-671 (1991).
22. Saadi-Kheddouci,S. *et al.* Early development of polycystic kidney disease in transgenic mice expressing an activated mutant of the beta-catenin gene. *Oncogene* **20**, 5972-5981 (2001).
23. Saburi,S. *et al.* Loss of Fat4 disrupts PCP signaling and oriented cell division and leads to cystic kidney disease. *Nat. Genet.* **40**, 1010-1015 (2008).
24. Shannon,M.B., Patton,B.L., Harvey,S.J., & Miner,J.H. A Hypomorphic Mutation in the Mouse Laminin {alpha}5 Gene Causes Polycystic Kidney Disease. *J. Am. Soc. Nephrol.* **17**, 1913-1922 (2006).
25. Cook,D.L., Gerber,A.N., & Tapscott,S.J. Modeling stochastic gene expression: implications for haploinsufficiency. *Proc. Natl. Acad. Sci. U. S. A* **95**, 15641-15646 (1998).

26. Martin,G.M. *et al.* Somatic mutations are frequent and increase with age in human kidney epithelial cells. *Hum. Mol. Genet.* **5**, 215-221 (1996).
27. Qian,F., Watnick,T.J., Onuchic,L.F., & Germino,G.G. The molecular basis of focal cyst formation in human autosomal dominant polycystic kidney disease type I. *Cell* **87**, 979-987 (1996).
28. Lantinga-van Leeuwen,I.S. *et al.* Kidney-specific inactivation of the Pkd1 gene induces rapid cyst formation in developing kidneys and a slow onset of disease in adult mice. *Hum. Mol. Genet.* **16**, 3188-3196 (2007).
29. Piontek,K., Menezes,L.F., Garcia-Gonzalez,M.A., Huso,D.L., & Germino,G.G. A critical developmental switch defines the kinetics of kidney cyst formation after loss of Pkd1. *Nat. Med.* **13**, 1490-1495 (2007).
30. Nauli,S.M. *et al.* Polycystins 1 and 2 mediate mechanosensation in the primary cilium of kidney cells. *Nat. Genet.* **33**, 129-137 (2003).
31. Yamaguchi,T. *et al.* Cyclic AMP activates B-Raf and ERK in cyst epithelial cells from autosomal-dominant polycystic kidneys. *Kidney Int.* **63**, 1983-1994 (2003).
32. Arnould,T. *et al.* The polycystic kidney disease 1 gene product mediates protein kinase C alpha-dependent and c-Jun N-terminal kinase-dependent activation of the transcription factor AP-1. *J. Biol. Chem.* **273**, 6013-6018 (1998).
33. Bhunia,A.K. *et al.* PKD1 induces p21(waf1) and regulation of the cell cycle via direct activation of the JAK-STAT signaling pathway in a process requiring PKD2. *Cell* **109**, 157-168 (2002).
34. Boca,M. *et al.* Polycystin-1 induces resistance to apoptosis through the phosphatidylinositol 3-kinase/Akt signaling pathway. *J. Am. Soc. Nephrol.* **17**, 637-647 (2006).
35. Shillingford,J.M. *et al.* The mTOR pathway is regulated by polycystin-1, and its inhibition reverses renal cystogenesis in polycystic kidney disease. *Proc. Natl. Acad. Sci. U. S. A* **103**, 5466-5471 (2006).
36. Germino,G.G. Linking cilia to Wnts. *Nat. Genet.* **37**, 455-457 (2005).
37. Fischer,E. *et al.* Defective planar cell polarity in polycystic kidney disease. *Nat. Genet.* **38**, 21-23 (2006).
38. McNeill,H. Planar cell polarity and the kidney. *J. Am. Soc. Nephrol.* **20**, 2104-2111 (2009).
39. Edgar,B.A. From cell structure to transcription: Hippo forges a new path. *Cell* **124**, 267-273 (2006).
40. Harvey,K. & Tapon,N. The Salvador-Warts-Hippo pathway - an emerging tumour-suppressor network. *Nat. Rev. Cancer* **7**, 182-191 (2007).
41. Pan,D. Hippo signaling in organ size control. *Genes Dev.* **21**, 886-897 (2007).
42. Reddy,B.V. & Irvine,K.D. The Fat and Warts signaling pathways: new insights into their regulation, mechanism and conservation. *Development* **135**, 2827-2838 (2008).
43. Badouel,C., Garg,A., & McNeill,H. Herding Hippos: regulating growth in flies and man. *Curr. Opin. Cell Biol.* **21**, 837-843 (2009).
44. Willecke,M., Hamaratoglu,F., Sansores-Garcia,L., Tao,C., & Halder,G. Boundaries of Dachsous Cadherin activity modulate the Hippo signaling pathway to induce cell proliferation. *Proc. Natl. Acad. Sci. U. S. A* **105**, 14897-14902 (2008).
45. Wu,G. *et al.* Somatic inactivation of Pkd2 results in polycystic kidney disease. *Cell* **93**, 177-188 (1998).
46. Lu,W. *et al.* Perinatal lethality with kidney and pancreas defects in mice with a targetted Pkd1 mutation. *Nat. Genet.* **17**, 179-181 (1997).
47. Boulter,C. *et al.* Cardiovascular, skeletal, and renal defects in mice with a targeted disruption of the Pkd1 gene. *Proc. Natl. Acad. Sci. U. S. A* **98**, 12174-12179 (2001).
48. Kim,K., Drummond,I., Ibraghimov-Beskrovnaya,O., Klinger,K., & Arnaout,M.A. Polycystin 1 is required for the structural integrity of blood vessels. *Proc. Natl. Acad. Sci. U. S. A* **97**, 1731-1736 (2000).
49. Muto,S. *et al.* Pioglitazone improves the phenotype and molecular defects of a targeted Pkd1 mutant. *Hum. Mol. Genet.* **11**, 1731-1742 (2002).
50. Wu,G. *et al.* Cardiac defects and renal failure in mice with targeted mutations in Pkd2. *Nat. Genet.* **24**, 75-78 (2000).
51. Pennekamp,P. *et al.* The ion channel polycystin-2 is required for left-right axis determination in mice. *Curr. Biol.* **12**, 938-943 (2002).
52. Allen,E. *et al.* Loss of polycystin-1 or polycystin-2 results in dysregulated apolipoprotein expression in murine tissues via alterations in nuclear hormone receptors. *Hum. Mol. Genet.* **15**, 11-21 (2006).
53. Lu,W. *et al.* Comparison of Pkd1-targeted mutants reveals that loss of polycystin-1 causes cystogenesis and bone defects. *Hum. Mol. Genet.* **10**, 2385-2396 (2001).
54. Wu,G. *et al.* Trans-heterozygous Pkd1 and Pkd2 mutations modify expression of polycystic kidney disease. *Hum. Mol. Genet.* **11**, 1845-1854 (2002).

55. Lantinga-van Leeuwen,I.S. *et al.* Transgenic mice expressing tamoxifen-inducible Cre for somatic gene modification in renal epithelial cells. *Genesis.* **44**, 225-232 (2006).
56. Chatha,R.K. *et al.* Von Hippel-Lindau disease masquerading as autosomal dominant polycystic kidney disease. *Am. J. Kidney Dis.* **37**, 852-858 (2001).
57. Takakura,A., Contrino,L., Beck,A.W., & Zhou,J. Pkd1 inactivation induced in adulthood produces focal cystic disease. *J. Am. Soc. Nephrol.* **19**, 2351-2363 (2008).
58. Shibazaki,S. *et al.* Cyst formation and activation of the extracellular regulated kinase pathway after kidney specific inactivation of Pkd1. *Hum. Mol. Genet.* **17**, 1505-1516 (2008).
59. Kim,I. *et al.* Conditional mutation of Pkd2 causes cystogenesis and upregulates beta-catenin. *J. Am. Soc. Nephrol.* **20**, 2556-2569 (2009).
60. Lantinga-van Leeuwen,I.S. *et al.* Lowering of Pkd1 expression is sufficient to cause polycystic kidney disease. *Hum. Mol. Genet.* **13**, 3069-3077 (2004).
61. Hassane,S. *et al.* Pathogenic sequence for dissecting aneurysm formation in a hypomorphic polycystic kidney disease 1 mouse model. *Arterioscler. Thromb. Vasc. Biol.* **27**, 2177-2183 (2007).

2

Polycystic kidney disease: The complexity of planar cell polarity and signaling during tissue regeneration and cyst formation

Hester Happé[1], Emile de Heer[2] and Dorien J.M. Peters[1]

[1]Department of Human Genetics and,
[2]Pathology, Leiden University Medical Center,
2300 RC Leiden, The Netherlands

Biochim Biophys Acta 2011; 1812: 1249-1255.

Abstract

Autosomal Dominant Polycystic Kidney Disease (ADPKD) is an inherited systemic disease with intrarenal cystogenesis as its primary characteristic. A variety of mouse models provided information on the requirement of loss of balanced polycystin levels for initiation of cyst formation, the role of proliferation in cystogenesis and the signaling pathways involved in cyst growth and expansion.
Here we will review the involvement of different signaling pathways during renal development, renal epithelial regeneration and cyst formation in ADPKD, focusing on planar cell polarity (PCP) and oriented cell division (OCD). This will be discussed in context of the hypothesis that aberrant PCP signaling causes cyst formation.
In addition, the role of the Hippo pathway, which was recently found to be involved in cyst growth and tissue regeneration, and well-known for regulating organ size control, will be reviewed. The fact that Hippo signaling is linked to PCP signaling makes the Hippo pathway a novel cascade in cystogenesis.
The newly gained understanding of the complex signaling network involved in cystogenesis and disease progression, not only necessitates refining of the current hypothesis regarding initiation of cystogenesis, but also has implications for therapeutic intervention strategies. This article is part of a Special Issue entitled: Polycystic Kidney Disease.

General introduction

Polycystic kidney disease presents itself in many different forms. In this review we will focus on Autosomal Dominant Polycystic Kidney Disease (ADPKD). ADPKD is a systemic disease with intrarenal cystogenesis as its primary characteristic. Extra-renal manifestations are hypertension, cardiac valvular abnormalities, cerebral aneurysms, and cysts in liver and pancreas[1]. Usually, in young adults, only a small number of cysts can be detected ultrasonographically, whereas at middle age, thousands of cysts and fibrotic tissue have replaced almost all normal renal parenchyma and renal function declines.

In general, ADPKD patients carry one germ-line mutation and one normal *PKD1,* or *PKD2* allele. Renal cysts develop from somatic inactivation of *PKD1* or *PKD2* by a 'two-hit' mechanism[2]. In addition, haploinsufficiency, stochastic fluctuations in *PKD1*or *PKD2* gene dosage below a tissue-specific threshold, may suffice to cause cyst formation[3]. Importantly, recent studies indicate that the picture can be more complex, since several families have been reported with non- or incompletely penetrant alleles of *PKD1* inherited at a homozygous state, or in *trans* with another mutation[4, 5].

In kidneys the primary defect has been found to occur in the epithelium. A balanced expression level of the *PKD1* and 2 genes, encoding polycystin 1 and 2 (PC1and PC2) is critical to maintain renal epithelial architecture. Both PC1 and PC2 are expressed in several sub-cellular compartments such as the primary cilium, cell-cell contacts and cell-extracellular matrix contacts. They form different multimeric protein complexes in the cell, modulating several signaling pathways, which in concert control essential cellular functions such as proliferation, apoptosis, cell adhesion, and differentiation[6, 7]. Disruption of any of these processes can lead to cyst formation, as demonstrated by a variety of mouse models[8-12]. In this review the role of proliferation, injury and repair in ADPKD, as well as their different signaling pathways will be discussed, with the major focus on planar cell polarity (PCP) and oriented cell division (OCD).

Mechanism of disease

The renal pathogenesis of ADPKD recognizes several phases. In the initiation phase, normal quiescent epithelial cells become hyper-proliferative[13, 14]. Subsequently, a phase characterized by cyst growth and cyst expansion caused by proliferation of cystic epithelial cells and increased fluid secretion, as well as extracellular matrix synthesis, can be recognized. During this phase also additional signaling pathways become either activated, or dysfunctional, resulting in more cyst growth[15]. These cysts detach from the original nephrons and continue to growth as isolated autonomous cysts.

Later on, cysts lining epithelial cells of large cysts stop dividing and apoptotic nuclei can be found in these cysts[16]. In addition, interstitial inflammatory infiltrates become apparent resulting in tubulointerstitial fibrosis and subsequent deterioration of kidney function[17-19].

As the material obtained from kidneys of ADPKD patients mainly allows investigation of the last phase of the disease, mouse models had to be developed in order to study the different stages of the disease.

Genetic mechanism in mice

Different *Pkd1*- or *Pkd2*-mutant mouse models have been created, which are supporting the genetic mechanisms mentioned above. The first support for the second hit model was provided by the *Pkd2*$^{ws25,-}$ model. In this model, with one null allele and one instable *Pkd2* allele, somatic rearrangements are accelerating renal cystic disease[20], while mice that are heterozygous for an inactivating *Pkd1* or *Pkd2* mutation, show only a very mild phenotype. Homozygous *Pkd1*- and *Pkd2*-deficient mice, however, die at about embryonic stage 15.5 or directly after birth because of severe cystic disease, vascular defects, and/or abnormalities of the placental labyrinth[20-29]. On the other hand, mice carrying one *Pkd1* as well as one *Pkd2* mutant allele are viable and show accelerated renal cystic disease compared to the single gene phenotypes[29].

Also hypomorphic mouse models for polycystic kidney disease that express *Pkd1* or *Pkd2* at a reduced level are viable, although they develop severe PKD[30-32]. Extra-renal manifestations such as cysts in liver and pancreas[21-23, 28, 33-35], and aortic dissecting aneurysms have been reported as well[30, 36]. However, the severity of the phenotype and lifespan is dependent on the genetic background of the mouse strain (unpublished results). The models with expanded life span are especially useful for studying the later phases in PKD.

For proper renal development the levels of *Pkd1* and *Pkd2* gene expression are critical, since over-expression leads to a renal cystic phenotype[35, 37-39], although in one model *Pkd2*-overexpression did not cause cystic disease but renal tubulopathy[40]. In addition, extra-renal manifestations similar to those observed in patients have been described in a *Pkd1* over-expression model[38], and over-expression of a truncated *Pkd2* gene caused polycystic kidney disease and retinal degeneration in transgenic rats[41].

Inducible conditional deletion models

To overcome embryonic lethality and to study tissue specific effects of *Pkd1*-inactivation, inducible and conditional *Pkd1* and *Pkd2* deletion mice have been created, using the Cre-*loxP* system [42-48]. These models have provided valuable information on the mechanisms involved in the initiation phase of cyst formation. Inducible *Pkd1*-deletion mice were used to analyze the kinetics of cyst formation upon *Pkd1*-gene disruption at different time-points after birth. In mice the progressiveness of cystogenesis depends on the age of *Pkd1*-gene disruption, e.g. in young mice the highest progression can be observed, while adult mice show a very slow phenotype[43, 45]. The difference in progression of cystic renal disease correlates with the developmental status of the renal tissue at the moment of gene disruption as well as with its proliferative status[43, 45].

Around neonatal day 13, renal development enters its completion in mice and a critical switch in gene expression was observed[45]. Also renal epithelial cell proliferation is dramatically higher in neonatal compared to adult mice[43]. Knocking-out *Pkd1* at postnatal day 4 results in progressive cyst formation with the major involvement of the distal nephron. At the moment of gene-inactivation, the distal nephron is still elongating at that time, and shows many proliferating cells[43]. Interestingly, *Pkd1*-gene disruption in young adult mice, well beyond the above-mentioned developmental switch in gene transcription, leads to a disease progression rate intermediate to that of neonatal and adult mice, while young adults also show levels of renal epithelial cell proliferation between neonatal and adult mice[45, 49]. Therefore, proliferation in the absence of functional polycystins seems to be a trigger for cyst formation [49].

As proliferation seems to be an accelerating factor in cystogenesis in young *Pkd1*-deletion mice, proliferation should also provide an accelerating trigger for cyst formation in the kidneys from adult *Pkd1*-deletion mice with low renal epithelial proliferation rates at the moment of gene disruption. Indeed renal epithelial injury accelerates the progression of cystogenesis in adult *Pkd1*-deletion mice[49, 50]. However, it cannot be excluded that proliferation is not the only accelerating factor, as epithelial regeneration probably shares (parts of) the cellular programs involved in renal development.

Also in non-orthologous inducible, conditional knockout models for renal cystic disease, in which *kif3* or *hnf1β* is inactivated, injury accelerates the cystic phenotype[51, 52]. Although the mechanism underlying cyst formation in the *hnf1β* conditional knock-outs probably differs from the model in which *kif3* was deleted. In all of these models the nephron segment that is targeted by the injury, and in which regeneration occurs, determines the origin of the majority of the cysts.

There are several possible answers to the question why proliferation accelerates cyst formation. One explanation may reside in the fact that in quiescent cells epithelial junction complexes, where also the polycystins can be found, are relatively stable but undergo extensive remodeling, when renal epithelial cells are forced to change their quiescent state into either proliferation, or migration[53]. Another possibility is that the polycystins themselves are not stable, and disappear from the junction complexes, but are crucial for proper (re-)establishment of adhesion complexes[54, 55].

Altered ciliary signaling and planar cell polarity signaling

The primary cilium is a common denominator in renal cystic diseases. This organelle harbors many of the proteins encoded by the genes mutated in a variety of renal cystic diseases[56] i.e. genes mutated in Bardet-Biedl syndrome[57], Meckel-Gruber syndrome[58-63], nephronophthisis[64, 65] or oral-facial-digital-syndrome[66].

During development the primary cilia on renal epithelial cells sense flow upon the start of urine production. This is accompanied by up-regulation and altered localization of the protein inversin. These changes result in a switch from canonical to non-canonical Wnt signaling, also known as the planar cell polarity (PCP) pathway[67].

PCP is polarity within the plane of an epithelial monolayer, parallel to the basement membrane and perpendicular to apical-basal polarity, which represents as the (identical) spatial arrangement of cells or sub cellular structures of cells within an epithelial plane. The PCP pathway is the signaling pathway that affects planar polarization of cells.

In PKD, however, defects in PCP signaling are found, as well as increased canonical Wnt signaling[49, 68, 69]. A proper balance of these pathways may be crucial for normal renal development and maintenance of tissue homeostasis since persistent activation of the β-catenin-mediated Wnt signaling itself also causes renal cyst formation in transgenic mouse models [10, 70].

Ciliary signaling and PCP signaling are closely linked; these two pathways act bidirectional in regulating PCP and cilial/basal body orientation. At least for motile cilia, PCP roughly provides cues for the cilium since PCP dictates the orientation of the basal body, resulting in synchronization of the beating direction of motile cilia in specific tissues. On the other hand, orientation of cilia is optimized by hydrodynamic forces, i.e. flow[71-73], and PCP is required for positioning/proper localization of cilia[74]. From these studies Marshall concluded that the cilia have a role in sensing the direction of fluid flow and by that can provide cues for planar orientation of the cilium/basal body[75]. Correspondingly, proper orientation and positioning of the basal body of non-motile primary cilia may also be regulated by PCP-signaling and hydrodynamic forces, although this remains to be confirmed.

PCP and oriented cell division in development

It is proposed that PCP signaling is needed during renal development in order to ensure the correct morphology and diameter of the nephrons. Defects in PCP signaling may therefore cause an increase in tubular diameter[76, 77]. Fischer *et al.* concluded that renal epithelial cells were planary polarized as cell division was oriented during renal development. Orientation of cell division was indicated by the orientation of the nuclear spindle along the longitudinal tubular axis, depicted as the Y-direction in the tubule shown in Figure 1A[77]. Therefore orientation of the nuclear spindle, measured by determining mitotic angle of the nuclear spindle relative to the tubular longitudinal axis, is now commonly used as a read out for PCP signaling.

Using this method, misoriented cell division was observed in developing kidneys and dilated tubules and in cysts in two murine models for renal cystic disease[51, 77]. These findings are consistent with the concept that aberrant PCP signaling causes cyst formation. This hypothesis was further supported by the development of renal cysts in mice in which Fat4, a PCP component, was knocked-out[11]. In addition, in many mouse models presenting renal cysts, tubular dilation and cyst formation are accompanied by aberrant oriented cell division (OCD). However, these models are non-orthologous models for PKD in which the targeted epithelial cells lack cilia[51, 78], non-canonical Wnt-signaling is influenced by Wnt9b deficiency[79] or in which cysts are formed upon unilateral ureteral obstruction[80].

Also for a *Pkd1* conditional knockout model, misorientation of cell division has been reported in pre-cystic epithelia[81]. This contrasts a parallel publication, in which orientation of cell division was studied in a *Pkd1*, *Pkd2* and *Pkdhd1* model. Aberrant OCD could not be observed in pre-cystic tubules of *Pkd1* and *Pkd2*-deletion mice. It was only observed upon dilation of the tubules[82]. These different findings between two independent studies on *Pkd1* deletion mice may be explained by the differences in analysis methods.

However, it is also possible that the accepted hypothesis, that misoriented cell division is the cause of cyst formation, is incorrect or incomplete, since a quite contrasting observation to the accepted hypothesis was made in the latter study. In *Pkhd1*$^{del4/del4}$ mice, defective OCD, including out of the epithelial plane cell division, into the lumen was found. However, these mice failed to develop dilated tubules or cystic kidneys.

Mitotic angles may deviate from the normal orientation in two directions, described by two angles: the first angle (α1) describes the deviation from the longitudinal tubular axis which is represented by Y in Figure 1A, but parallel to the epithelial plane (XY-plane) as shown in Figure 1B. The second angle (α2) describes the angle between the mitotic spindle axis and the basal membrane, a cell division in the YZ-plane as shown in Figure 1C. Thus α2 defines how much the mitotic spindle axis comes out of the epithelial plane. The paper of Nishio *et al.*, studying OCD in *Pkhd1* mutant and *Pkd1* and *Pkd2*-deletion mice, as discussed above, is the first that (clearly) discriminated between these two angles. They showed that misorientation of cell division occurs in both directions, at least clearly shown for mildly dilated tubules in *Pkd1* and *Pkd2*-deletion mice[82]. In addition, they suggested that cell division out of the plane of the epithelium in *Pkhd1*^{del4,del4}, was probably corrected by a convergent extension-like movement into the epithelial plane of cells, resulting in an increased number of tubular circumferential cells but not in cystic kidneys[82]. It cannot be excluded however, that other factors may explain the lack of cyst formation in *Pkhd1*$^{del4/del4}$, e.g. the complex processing of the *Pkhd1* transcript.

Thus, misorientation of cell division includes cell divisions out of the plane of the epithelium. Not in every model misoriented cell division can be designated as the cause of cyst formation, since cytogenesis can develop without loss of OCD. In addition, aberrant orientation of cell division alone seems not to be sufficient for cyst formation and rather seems to be a permissive condition or an accelerating factor for tubular dilatation.

It cannot be excluded, however, that cyst formation and renal cystic disease in the commonest and more adult-onset form of polycystic disease, ADPKD, are mechanistically different from the processes occurring in other types of (congenital) cystic kidney diseases, particularly the ciliopathies.

PCP and oriented cell division in renal epithelial regeneration

It is likely that the complex interplay of processes involved during renal development; e.g. PCP signaling, OCD, convergent extension and ciliary signaling are also involved during regeneration of tubular epithelia. PCP signaling has already proven to be important for proper tubular epithelial repair[80]. To ensure correct tubular morphology during repair, the majority of the mitotic angles have to be parallel to the tubular longitudinal axis.

Reports in which OCD was examined after injury in two different models for PKD, a *Pkd1* and an *Hnf1β* deletion model, showed that the orientation of mitotic spindles during repair in controls is preferentially directed along the tubular (longitudinal) axis[52, 81]. This suggests that, like in developing nephrons, there is planar polarization of the epithelial cells.

As in renal development, the *Pkd1* and an *Hnf1β* deletion model show misoriented cell division during regeneration[52, 81]. However, measurement of the mitotic angle can only be done in dividing cells. As the centrosomes form the spindle poles during cell division, OCD and centrosome position are linked[78], the position of centrosomes may be used as a read-out for PCP in non-dividing cells. This is supported by the observation that disrupting PCP components, lead to aberrant positioning of the basal body/centrosome and cilium[73, 74, 83, 84]. Also in adult *Pkd1*-deletion mice mispositioning of the centrosome was observed during the pre-cystic phase after completion of repair[49]. These data indicate that aberrant PCP precedes cyst formation, although mispositioning of the centrosome was also found in tubules of adult *Pkd1*-deletion mice that were not subjected to epithelial injury, and develop cysts rather late[49].

Planar cell polarity and apical-basal polarity

OCD is accepted as a read-out for PCP as PCP-signaling regulates OCD. However, OCD is not regulated by the PCP pathway alone. PCP-signaling provides spatial information within the epithelial sheet. Other signaling pathways provide information concerning apical-basal polarity and regulate the direction of cell division perpendicular to the epithelial sheet, depicted as the Z-direction shown in Figure 1A and D (resembling asymmetric cell division known from stem-cell biology and neuronal development[85, 86]). Figure 1D shows a cell division in Y-direction, parallel with the plane of the epithelium, and one in the Z-direction, parallel to apical-basal polarity.

The Par3/Par6 complex, including Cdc42 and aPKC, is required for establishing and maintaining polarized cortical domains in a wide variety of epithelia[87-90]. Thus this complex is implicated in apical-basal polarity and also regulates OCD[91]. Additionally, signaling complexes connected to adherens junctions, and cell-extracellular matrix contacts also provide input for the orientation of cell division[92-95]. At these locations, polycystin-1 and 2 modulate signaling of multi-protein complexes[6].

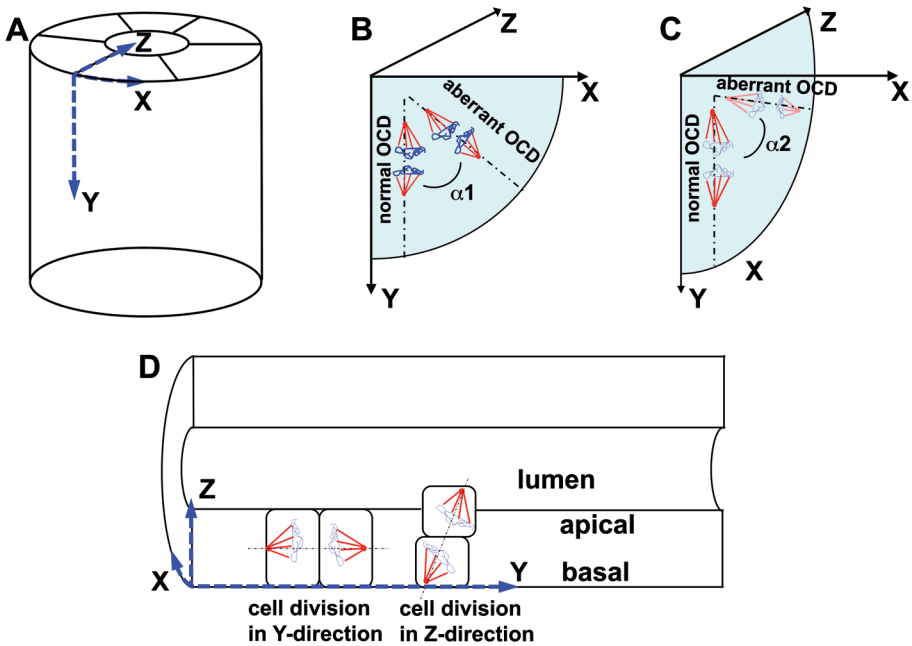


Figure 1. Oriented and misoriented cell division in renal tubules. (A) Cell division within renal tubular epithelium is possible in three directions: in the direction of the Y-axis; parallel to the longitudinal axis of the tubule; in direction of the X-axis parallel to basal membrane and perpendicular to the tubular longitudinal axis or in the direction of the Z-axis; perpendicular to the basal membrane and the tubular longitudinal axis (B) Aberrant OCD with α1 describing the deviation from normal OCD in X-direction within the XY-plane (in the plane of the epithelium). (C) Aberrant OCD with α2 describing the deviation from normal OCD in Z-direction within the YZ-plane (out of the plane of the epithelium). B and C both depict axis as represented in the vertical tubule shown in A. (D) Correct OCD in Y-direction (left) and aberrant OCD with a deviation into Z-direction (right) i.e. cell division out of the epithelial plane. OCD: oriented cell division.

Signaling pathways involved in cyst expansion

A large variety of cellular changes in cyst-lining cells has been observed, and in the last decade it became clear that the polycystins transmit extracellular signals to the nucleus via multiple signaling pathways. A prominent role in cyst growth has been proposed for reduced Ca^{2+} influx, cAMP accumulation and aberrant Ras/Raf/ERK activation[96, 97]. Other proposed mechanisms involve activation of G-proteins, mTOR, PI3-kinase, Jak2-STAT1/3, NFAT (nuclear factor of activated T-cells), and NF-kB (nuclear factor kappa B) signaling[98-100]. It cannot be excluded that some of these pathways or second messengers, e.g. Ca^{2+}, are involved in the early initiation steps of cyst formation. However, these pathways are to a large extend involved in proliferation, and thereby in cyst expansion.

Tubulointerstitial fibrosis is a major process contributing to the pathology towards end-stage renal disease and is a feature of later stages in ADPKD disease progression. A key regulator of fibrosis is the TGFβ-signaling cascade. Indeed, in human tissues and in mouse models phosphorylation and

nuclear translocation of the TGFβ cascade actor, SMAD2 has been detected in more progressive but not in early stages of the disease[101].

Recent data also indicated the involvement of the Hippo pathway in renal cystic disease. This pathway was first known to be important in organ and tissue size control in *Drosophila*. The core components of the *Drosophila* Hippo pathway are well conserved and also function as tumor suppressors in mammals in addition to regulating growth in terms of organ size control[102]. The Hippo signaling pathway exerts its actions in mammals by controlling the transcription of genes involved in proliferation and apoptosis through the transcriptional co-activator and final effector molecule, YAP and its ortholog TAZ.

In PKD, Hippo signaling showed altered activity[103]. YAP, a transcriptional co-activator and final effector molecule of the Hippo pathway, was observed in nuclei of dilated tubules and cyst in injury-induced *Pkd1*-deletion mice. Even more, disturbed Hippo signaling caused by, e.g. deregulation of YAP[104, 105] or TAZ (Wwtr1) deficiency[105-107], resulted in cyst formation. The observed altered activity of the Hippo pathway can provide a proliferative driving force for cyst expansion. Fascinatingly, YAP/TAZ are transcriptional co-activators for a variety of transcription factors, e.g. TEAD, Glis3, SMAD, ErbB4-CTF, p73, Runx2, many of them implicated in polycystic kidney disease[69, 102, 108-110]. Also it has been reported that the canonical Wnt signaling, one of the signaling cascades altered in cystic epithelia, is modulated by Hippo–signaling[49, 68, 69, 111].

As PCP signaling provides directional information, Hippo signaling is known to control organ size, and possibly provides information about the number of tubular circumferential cells. In other words, PCP signaling tells which direction, Hippo signaling dictates how many cells in each direction. In order to coordinate these processes there must be crosstalk between the Hippo-pathway and the PCP pathway. In fact, crosstalk between these pathways is possible since the upstream regulators of the Hippo pathway are shared with the PCP pathway; i.e. Fat, Four-jointed and Dachsous[112].

Although, nuclear YAP was not observed in tubular epithelial cells prior to tubular dilation and cyst formation[103], it cannot be excluded that reduced activity of the Hippo pathway is already involved in the initiation of cyst formation. As mentioned above, Fat4 is in addition to a PCP component, also a regulator of the Hippo pathway. Therefore, it is possible that cyst formation in *fat4*$^{-/-}$ mice may in fact be attributed to a disbalance of Hippo and PCP signaling[11].

Also in tissue regeneration the Hippo pathway is involved. Nuclear and strong cytoplasmic accumulation of YAP is observed during epithelial regeneration in the gut[113] and a similar phenomenon was observed for the kidneys[103]. Overall these data imply that the delicate interplay between PCP and Hippo signaling may also be important for tissue regeneration after injury.

Future prospects in ADPKD research

The animal models showed us the vastness and complexity of signaling pathways involved in cyst formation and disease progression. These pathways act in a concerted fashion as components of an interconnected signaling network. Experimental data also provided us, sometimes, with apparently conflicting results, which can mostly be explained by differences in experimental conditions and data interpretation. The conflicting results concerning PCP-signaling demand us to systematically (re-)analyze our data concerning the orientation of mitotic spindle axis. This will enable us to refine our hypothesis further regarding the role of PCP-signaling in the initiation of cyst formation, and help us dissect the role of the pathways implicated.

The complexity of the involved signaling networks suggest that it may be too ambitious and probably naive to think that prevention of cyst formation and delay of renal failure can be accomplished by targeting a single pathway. In patients cyst formation is not synchronized and areas with different phases of the disease can be found in the kidneys of an individual patient. Probably, therapy with drugs that target more than one signaling pathway will be necessary and probably more successful than treatment with single-target medication.

References

1. Gabow,P.A. Autosomal dominant polycystic kidney disease--more than a renal disease. *Am. J. Kidney Dis.* **16**, 403-413 (1990).
2. Qian,F., Watnick,T.J., Onuchic,L.F., & Germino,G.G. The molecular basis of focal cyst formation in human autosomal dominant polycystic kidney disease type I. *Cell* **87**, 979-987 (1996).
3. Ong,A.C. & Harris,P.C. Molecular basis of renal cyst formation--one hit or two? *Lancet* **349**, 1039-1040 (1997).
4. Rossetti,S. *et al.* Incompletely penetrant PKD1 alleles suggest a role for gene dosage in cyst initiation in polycystic kidney disease. *Kidney Int.* **75**, 848-855 (2009).
5. Vujic,M. *et al.* Incompletely penetrant PKD1 alleles mimic the renal manifestations of ARPKD. *J. Am. Soc. Nephrol.* **21**, 1097-1102 (2010).
6. Wilson,P.D. Polycystic kidney disease. *N. Engl. J. Med.* **350**, 151-164 (2004).
7. Nauli,S.M. *et al.* Polycystins 1 and 2 mediate mechanosensation in the primary cilium of kidney cells. *Nat. Genet.* **33**, 129-137 (2003).
8. Sorenson,C.M., Padanilam,B.J., & Hammerman,M.R. Abnormal postpartum renal development and cystogenesis in the bcl-2 (-/-) mouse. *Am. J. Physiol* **271**, F184-F193 (1996).
9. Trudel,M., D'Agati,V., & Costantini,F. C-myc as an inducer of polycystic kidney disease in transgenic mice. *Kidney Int.* **39**, 665-671 (1991).
10. Saadi-Kheddouci,S. *et al.* Early development of polycystic kidney disease in transgenic mice expressing an activated mutant of the beta-catenin gene. *Oncogene* **20**, 5972-5981 (2001).
11. Saburi,S. *et al.* Loss of Fat4 disrupts PCP signaling and oriented cell division and leads to cystic kidney disease. *Nat. Genet.* **40**, 1010-1015 (2008).
12. Shannon,M.B., Patton,B.L., Harvey,S.J., & Miner,J.H. A Hypomorphic Mutation in the Mouse Laminin α5 Gene Causes Polycystic Kidney Disease. *J. Am. Soc. Nephrol.* **17**, 1913-1922 (2006).
13. Gabow,P.A. Polycystic kidney disease: clues to pathogenesis. *Kidney Int.* **40**, 989-996 (1991).
14. Nadasdy,T. *et al.* Proliferative activity of cyst epithelium in human renal cystic diseases. *J. Am. Soc. Nephrol.* **5**, 1462-1468 (1995).
15. Murcia,N.S., Sweeney,W.E., Jr., & Avner,E.D. New insights into the molecular pathophysiology of polycystic kidney disease. *Kidney Int.* **55**, 1187-1197 (1999).
16. Woo,D. Apoptosis and loss of renal tissue in polycystic kidney diseases. *N. Engl. J. Med.* **333**, 18-25 (1995).
17. Zeier,M. *et al.* Renal histology in polycystic kidney disease with incipient and advanced renal failure. *Kidney Int.* **42**, 1259-1265 (1992).
18. Okada,H. *et al.* Progressive renal fibrosis in murine polycystic kidney disease: an immunohistochemical observation. *Kidney Int.* **58**, 587-597 (2000).
19. Martinez,J.R. & Grantham,J.J. Polycystic kidney disease: etiology, pathogenesis, and treatment. *Dis. Mon.* **41**, 693-765 (1995).
20. Wu,G. *et al.* Somatic inactivation of Pkd2 results in polycystic kidney disease. *Cell* **93**, 177-188 (1998).
21. Lu,W. *et al.* Perinatal lethality with kidney and pancreas defects in mice with a targetted Pkd1 mutation. *Nat. Genet.* **17**, 179-181 (1997).
22. Boulter,C. *et al.* Cardiovascular, skeletal, and renal defects in mice with a targeted disruption of the Pkd1 gene. *Proc. Natl. Acad. Sci. U. S. A* **98**, 12174-12179 (2001).
23. Kim,K., Drummond,I., Ibraghimov-Beskrovnaya,O., Klinger,K., & Arnaout,M.A. Polycystin 1 is required for the structural integrity of blood vessels. *Proc. Natl. Acad. Sci. U. S. A* **97**, 1731-1736 (2000).
24. Muto,S. *et al.* Pioglitazone improves the phenotype and molecular defects of a targeted Pkd1 mutant. *Hum. Mol. Genet.* **11**, 1731-1742 (2002).
25. Wu,G. *et al.* Cardiac defects and renal failure in mice with targeted mutations in Pkd2. *Nat. Genet.* **24**, 75-78 (2000).
26. Pennekamp,P. *et al.* The ion channel polycystin-2 is required for left-right axis determination in mice. *Curr. Biol.* **12**, 938-943 (2002).
27. Allen,E. *et al.* Loss of polycystin-1 or polycystin-2 results in dysregulated apolipoprotein expression in murine tissues via alterations in nuclear hormone receptors. *Hum. Mol. Genet.* **15**, 11-21 (2006).

28. Lu,W. *et al.* Comparison of Pkd1-targeted mutants reveals that loss of polycystin-1 causes cystogenesis and bone defects. *Hum. Mol. Genet.* **10**, 2385-2396 (2001).
29. Wu,G. *et al.* Trans-heterozygous Pkd1 and Pkd2 mutations modify expression of polycystic kidney disease. *Hum. Mol. Genet.* **11**, 1845-1854 (2002).
30. Lantinga-van Leeuwen,I.S. *et al.* Lowering of Pkd1 expression is sufficient to cause polycystic kidney disease. *Hum. Mol. Genet.* **13**, 3069-3077 (2004).
31. Kim,I. *et al.* Polycystin-2 expression is regulated by a PC2-binding domain in the intracellular portion of fibrocystin. *J. Biol. Chem.* **283**, 31559-31566 (2008).
32. Jiang,S.T. *et al.* Defining a link with autosomal-dominant polycystic kidney disease in mice with congenitally low expression of Pkd1. *Am. J. Pathol.* **168**, 205-220 (2006).
33. Nishio,S. *et al.* Pkd1 regulates immortalized proliferation of renal tubular epithelial cells through p53 induction and JNK activation. *J. Clin. Invest* **115**, 910-918 (2005).
34. Lu,W. *et al.* Late onset of renal and hepatic cysts in Pkd1-targeted heterozygotes. *Nat. Genet.* **21**, 160-161 (1999).
35. Pritchard,L. *et al.* A human PKD1 transgene generates functional polycystin-1 in mice and is associated with a cystic phenotype. *Hum. Mol. Genet.* **9**, 2617-2627 (2000).
36. Hassane,S. *et al.* Pathogenic sequence for dissecting aneurysm formation in a hypomorphic polycystic kidney disease 1 mouse model. *Arterioscler. Thromb. Vasc. Biol.* **27**, 2177-2183 (2007).
37. Thivierge,C. *et al.* Overexpression of PKD1 causes polycystic kidney disease. *Mol. Cell Biol.* **26**, 1538-1548 (2006).
38. Kurbegovic,A. *et al.* Pkd1 transgenic mice: adult model of polycystic kidney disease with extrarenal and renal phenotypes. *Hum. Mol. Genet.* **19**, 1174-1189 (2010).
39. Park,E.Y. *et al.* Cyst formation in kidney via B-Raf signaling in the PKD2 transgenic mice. *J. Biol. Chem.* **284**, 7214-7222 (2009).
40. Burtey,S. *et al.* Overexpression of PKD2 in the mouse is associated with renal tubulopathy. *Nephrol. Dial. Transplant.* **23**, 1157-1165 (2008).
41. Gallagher,A.R. *et al.* A truncated polycystin-2 protein causes polycystic kidney disease and retinal degeneration in transgenic rats. *J. Am. Soc. Nephrol.* **17**, 2719-2730 (2006).
42. Lantinga-van Leeuwen,I.S. *et al.* Transgenic mice expressing tamoxifen-inducible Cre for somatic gene modification in renal epithelial cells. *Genesis.* **44**, 225-232 (2006).
43. Lantinga-van Leeuwen,I.S. *et al.* Kidney-specific inactivation of the Pkd1 gene induces rapid cyst formation in developing kidneys and a slow onset of disease in adult mice. *Hum. Mol. Genet.* **16**, 3188-3196 (2007).
44. Chatha,R.K. *et al.* Von Hippel-Lindau disease masquerading as autosomal dominant polycystic kidney disease. *Am. J. Kidney Dis.* **37**, 852-858 (2001).
45. Piontek,K., Menezes,L.F., Garcia-Gonzalez,M.A., Huso,D.L., & Germino,G.G. A critical developmental switch defines the kinetics of kidney cyst formation after loss of Pkd1. *Nat. Med.* **13**, 1490-1495 (2007).
46. Takakura,A., Contrino,L., Beck,A.W., & Zhou,J. Pkd1 inactivation induced in adulthood produces focal cystic disease. *J. Am. Soc. Nephrol.* **19**, 2351-2363 (2008).
47. Shibazaki,S. *et al.* Cyst formation and activation of the extracellular regulated kinase pathway after kidney specific inactivation of Pkd1. *Hum. Mol. Genet.* **17**, 1505-1516 (2008).
48. Kim,I. *et al.* Conditional mutation of Pkd2 causes cystogenesis and upregulates beta-catenin. *J. Am. Soc. Nephrol.* **20**, 2556-2569 (2009).
49. Happé,H. *et al.* Toxic tubular injury in kidneys from Pkd1-deletion mice accelerates cystogenesis accompanied by dysregulated planar cell polarity and canonical Wnt signaling pathways. *Hum. Mol. Genet.* **18**, 2532-2542 (2009).
50. Takakura,A. *et al.* Renal injury is a third hit promoting rapid development of adult polycystic kidney disease. *Hum. Mol. Genet.* **18**, 2523-2531 (2009).
51. Patel,V. *et al.* Acute kidney injury and aberrant planar cell polarity induce cyst formation in mice lacking renal cilia. *Hum. Mol. Genet.* **17**, 1578-1590 (2008).
52. Verdeguer,F. *et al.* A mitotic transcriptional switch in polycystic kidney disease. *Nat. Med.* **16**, 106-110 (2010).
53. Zhao,M., Szafranski,P., Hall,C.A., & Goode,S. Basolateral junctions utilize warts signaling to control epithelial-mesenchymal transition and proliferation crucial for migration and invasion of Drosophila ovarian epithelial cells. *Genetics* **178**, 1947-1971 (2008).

54. Silberberg,M., Charron,A.J., Bacallao,R., & Wandinger-Ness,A. Mispolarization of desmosomal proteins and altered intercellular adhesion in autosomal dominant polycystic kidney disease. *Am. J. Physiol Renal Physiol* **288**, F1153-F1163 (2005).
55. Geng,L., Burrow,C.R., Li,H.P., & Wilson,P.D. Modification of the composition of polycystin-1 multiprotein complexes by calcium and tyrosine phosphorylation. *Biochim. Biophys. Acta* **1535**, 21-35 (2000).
56. Watnick,T. & Germino,G. From cilia to cyst. *Nat. Genet.* **34**, 355-356 (2003).
57. Tobin,J.L. & Beales,P.L. Bardet-Biedl syndrome: beyond the cilium. *Pediatr. Nephrol.* **22**, 926-936 (2007).
58. Baala,L. *et al.* Pleiotropic effects of CEP290 (NPHP6) mutations extend to Meckel syndrome. *Am. J. Hum. Genet.* **81**, 170-179 (2007).
59. Delous,M. *et al.* The ciliary gene RPGRIP1L is mutated in cerebello-oculo-renal syndrome (Joubert syndrome type B) and Meckel syndrome. *Nat. Genet.* **39**, 875-881 (2007).
60. Kyttala,M. *et al.* MKS1, encoding a component of the flagellar apparatus basal body proteome, is mutated in Meckel syndrome. *Nat. Genet.* **38**, 155-157 (2006).
61. Roume,J. *et al.* A gene for Meckel syndrome maps to chromosome 11q13. *Am. J. Hum. Genet.* **63**, 1095-1101 (1998).
62. Smith,U.M. *et al.* The transmembrane protein meckelin (MKS3) is mutated in Meckel-Gruber syndrome and the wpk rat. *Nat. Genet.* **38**, 191-196 (2006).
63. Tallila,J., Jakkula,E., Peltonen,L., Salonen,R., & Kestila,M. Identification of CC2D2A as a Meckel syndrome gene adds an important piece to the ciliopathy puzzle. *Am. J. Hum. Genet.* **82**, 1361-1367 (2008).
64. Hildebrandt,F. & Otto,E. Cilia and centrosomes: a unifying pathogenic concept for cystic kidney disease? *Nat. Rev. Genet.* **6**, 928-940 (2005).
65. Otto,E.A. *et al.* Mutations in INVS encoding inversin cause nephronophthisis type 2, linking renal cystic disease to the function of primary cilia and left-right axis determination. *Nat. Genet.* **34**, 413-420 (2003).
66. Ferrante,M.I. *et al.* Convergent extension movements and ciliary function are mediated by ofd1, a zebrafish orthologue of the human oral-facial-digital type 1 syndrome gene. *Hum. Mol. Genet.* **18**, 289-303 (2009).
67. Simons,M. *et al.* Inversin, the gene product mutated in nephronophthisis type II, functions as a molecular switch between Wnt signaling pathways. *Nat. Genet.* **37**, 537-543 (2005).
68. Lal,M. *et al.* Polycystin-1 C-terminal tail associates with beta-catenin and inhibits canonical Wnt signaling. *Hum. Mol. Genet.* **17**, 3105-3117 (2008).
69. Song,X. *et al.* Systems biology of autosomal dominant polycystic kidney disease (ADPKD): computational identification of gene expression pathways and integrated regulatory networks. *Hum. Mol. Genet.* **18**, 2328-2343 (2009).
70. Qian,C.N. *et al.* Cystic renal neoplasia following conditional inactivation of apc in mouse renal tubular epithelium. *J. Biol. Chem.* **280**, 3938-3945 (2005).
71. Guirao,B. *et al.* Coupling between hydrodynamic forces and planar cell polarity orients mammalian motile cilia. *Nat. Cell Biol.* **12**, 341-350 (2010).
72. Mitchell,B., Jacobs,R., Li,J., Chien,S., & Kintner,C. A positive feedback mechanism governs the polarity and motion of motile cilia. *Nature* **447**, 97-101 (2007).
73. Park,T.J., Mitchell,B.J., Abitua,P.B., Kintner,C., & Wallingford,J.B. Dishevelled controls apical docking and planar polarization of basal bodies in ciliated epithelial cells. *Nat. Genet.*(2008).
74. Borovina,A., Superina,S., Voskas,D., & Ciruna,B. Vangl2 directs the posterior tilting and asymmetric localization of motile primary cilia. *Nat. Cell Biol.* **12**, 407-412 (2010).
75. Marshall,W.F. Cilia self-organize in response to planar cell polarity and flow. *Nat. Cell Biol.* **12**, 314-315 (2010).
76. Germino,G.G. Linking cilia to Wnts. *Nat. Genet.* **37**, 455-457 (2005).
77. Fischer,E. *et al.* Defective planar cell polarity in polycystic kidney disease. *Nat. Genet.* **38**, 21-23 (2006).
78. Jonassen,J.A., San Agustin,J., Follit,J.A., & Pazour,G.J. Deletion of IFT20 in the mouse kidney causes misorientation of the mitotic spindle and cystic kidney disease. *J. Cell Biol.* **183**, 377-384 (2008).
79. Karner,C.M. *et al.* Wnt9b signaling regulates planar cell polarity and kidney tubule morphogenesis. *Nat. Genet.* **41**, 793-799 (2009).
80. Li,L. *et al.* Aberrant planar cell polarity induced by urinary tract obstruction. *Am. J. Physiol Renal Physiol* **297**, F1526-F1533 (2009).
81. Luyten,A. *et al.* Aberrant regulation of planar cell polarity in polycystic kidney disease. *J. Am. Soc. Nephrol.* **21**, 1521-1532 (2010).

82. Nishio,S. *et al.* Loss of oriented cell division does not initiate cyst formation. *J. Am. Soc. Nephrol.* **21**, 295-302 (2010).
83. Sepich,D.S., Usmani,M., Pawlicki,S., & Solnica-Krezel,L. Wnt/PCP signaling controls intracellular position of MTOCs during gastrulation convergence and extension movements. *Development* **138**, 543-552 (2011).
84. Jones,C. & Chen,P. Primary cilia in planar cell polarity regulation of the inner ear. *Curr. Top. Dev. Biol.* **85**, 197-224 (2008).
85. Knoblich,J.A. Asymmetric cell division: recent developments and their implications for tumour biology. *Nat. Rev. Mol. Cell Biol.* **11**, 849-860 (2010).
86. Sawa,H. Specification of neurons through asymmetric cell divisions. *Curr. Opin. Neurobiol.* **20**, 44-49 (2010).
87. Muller,H.A. & Wieschaus,E. armadillo, bazooka, and stardust are critical for early stages in formation of the zonula adherens and maintenance of the polarized blastoderm epithelium in Drosophila. *J. Cell Biol.* **134**, 149-163 (1996).
88. Horikoshi,Y. *et al.* Interaction between PAR-3 and the aPKC-PAR-6 complex is indispensable for apical domain development of epithelial cells. *J. Cell Sci.* **122**, 1595-1606 (2009).
89. Macara,I.G. Parsing the polarity code. *Nat. Rev. Mol. Cell Biol.* **5**, 220-231 (2004).
90. Suzuki,A. & Ohno,S. The PAR-aPKC system: lessons in polarity. *J. Cell Sci.* **119**, 979-987 (2006).
91. Hao,Y. *et al.* Par3 controls epithelial spindle orientation by aPKC-mediated phosphorylation of apical pins. *Curr. Biol.* **20**, 1809-1818 (2010).
92. den,E.N., Buttery,C.V., Maddugoda,M.P., Ren,G., & Yap,A.S. Cadherin adhesion receptors orient the mitotic spindle during symmetric cell division in mammalian epithelia. *Mol. Biol. Cell* **20**, 3740-3750 (2009).
93. Inaba,M., Yuan,H., Salzmann,V., Fuller,M.T., & Yamashita,Y.M. E-cadherin is required for centrosome and spindle orientation in Drosophila male germline stem cells. *PLoS. One.* **5**, e12473 (2010).
94. Toyoshima,F. & Nishida,E. Spindle orientation in animal cell mitosis: roles of integrin in the control of spindle axis. *J. Cell Physiol* **213**, 407-411 (2007).
95. Thery,M. *et al.* The extracellular matrix guides the orientation of the cell division axis. *Nat. Cell Biol.* **7**, 947-953 (2005).
96. Yamaguchi,T. *et al.* Cyclic AMP activates B-Raf and ERK in cyst epithelial cells from autosomal-dominant polycystic kidneys. *Kidney Int.* **63**, 1983-1994 (2003).
97. Arnould,T. *et al.* The polycystic kidney disease 1 gene product mediates protein kinase C alpha-dependent and c-Jun N-terminal kinase-dependent activation of the transcription factor AP-1. *J. Biol. Chem.* **273**, 6013-6018 (1998).
98. Bhunia,A.K. *et al.* PKD1 induces p21(waf1) and regulation of the cell cycle via direct activation of the JAK-STAT signaling pathway in a process requiring PKD2. *Cell* **109**, 157-168 (2002).
99. Boca,M. *et al.* Polycystin-1 induces resistance to apoptosis through the phosphatidylinositol 3-kinase/Akt signaling pathway. *J. Am. Soc. Nephrol.* **17**, 637-647 (2006).
100. Shillingford,J.M. *et al.* The mTOR pathway is regulated by polycystin-1, and its inhibition reverses renal cystogenesis in polycystic kidney disease. *Proc. Natl. Acad. Sci. U. S. A* **103**, 5466-5471 (2006).
101. Hassane,S. *et al.* Elevated TGFbeta-Smad signalling in experimental Pkd1 models and human patients with polycystic kidney disease. *J. Pathol.* **222**, 21-31 (2010).
102. Badouel,C., Garg,A., & McNeill,H. Herding Hippos: regulating growth in flies and man. *Curr. Opin. Cell Biol.* **21**, 837-843 (2009).
103. Happé,H. *et al.* Altered Hippo signalling in polycystic kidney disease. *J. Pathol.* **224**, 133-142 (2011).
104. Skouloudaki,K. *et al.* Scribble participates in Hippo signaling and is required for normal zebrafish pronephros development. *Proc. Natl. Acad. Sci. U. S. A* **106**, 8579-8584 (2009).
105. Tian,Y. *et al.* TAZ promotes PC2 degradation through a SCFbeta-Trcp E3 ligase complex. *Mol. Cell Biol.* **27**, 6383-6395 (2007).
106. Hossain,Z. *et al.* Glomerulocystic kidney disease in mice with a targeted inactivation of Wwtr1. *Proc. Natl. Acad. Sci. U. S. A* **104**, 1631-1636 (2007).
107. Makita,R. *et al.* Multiple renal cysts, urinary concentration defects, and pulmonary emphysematous changes in mice lacking TAZ. *Am. J. Physiol Renal Physiol* **294**, F542-F553 (2008).
108. Edgar,B.A. From cell structure to transcription: Hippo forges a new path. *Cell* **124**, 267-273 (2006).
109. Kang,H.S., Beak,J.Y., Kim,Y.S., Herbert,R., & Jetten,A.M. Glis3 is associated with primary cilia and Wwtr1/TAZ and implicated in polycystic kidney disease. *Mol. Cell Biol.* **29**, 2556-2569 (2009).

110. Komuro,A., Nagai,M., Navin,N.E., & Sudol,M. WW domain-containing protein YAP associates with ErbB-4 and acts as a co-transcriptional activator for the carboxyl-terminal fragment of ErbB-4 that translocates to the nucleus. *J. Biol. Chem.* **278**, 33334-33341 (2003).
111. Varelas,X. *et al.* The Hippo pathway regulates Wnt/beta-catenin signaling. *Dev. Cell* **18**, 579-591 (2010).
112. Lawrence,P.A., Struhl,G., & Casal,J. Do the protocadherins Fat and Dachsous link up to determine both planar cell polarity and the dimensions of organs? *Nat. Cell Biol.* **10**, 1379-1382 (2008).
113. Cai,J. *et al.* The Hippo signaling pathway restricts the oncogenic potential of an intestinal regeneration program. *Genes Dev.* **24**, 2383-2388 (2010).

3

Toxic tubular injury in kidneys from *Pkd1*-deletion mice accelerates cystogenesis accompanied by dysregulated planar cell polarity and canonical Wnt signaling pathways

Hester Happé[1], Wouter N. Leonhard[1], Annemieke van der Wal[2], Bob van de Water[3], Irma S. Lantinga-van Leeuwen[1], Martijn H. Breuning[1], Emile de Heer[2], Dorien J.M. Peters[1]

[1]Departments of Human Genetics and [2]Pathology, Leiden University Medical Center, 2300 RC Leiden, The Netherlands
[3]Division of Toxicology, Leiden Amsterdam Center for Drug Research, 2300 RA Leiden University, Leiden, The Netherlands

Hum Mol Genet 2009; 18: 2532-2542.

Abstract

Autosomal Dominant Polycystic Kidney Disease (ADPKD) is characterized by large fluid-filled cysts and progressive deterioration of renal function necessitating renal replacement therapy.
Previously we generated a tamoxifen-inducible, kidney epithelium-specific *Pkd1*-deletion mouse model and showed that inactivation of the *Pkd1* gene induces rapid cyst formation in developing kidneys and a slow onset of disease in adult mice.
Therefore, we hypothesized that injury-induced tubular epithelial cell proliferation may accelerate cyst formation in the kidneys of adult *Pkd1*-deletion mice.
Mice were treated with the nephrotoxicant DCVC after *Pkd1*-gene inactivation, which indeed accelerated cyst formation significantly. After the increased proliferation during tissue regeneration, proliferation decreased to basal levels in *Pkd1*-deletion mice just as in DCVC-treated controls. However, in severe cystic kidneys, 10-14 weeks after injury, proliferation increased again. This biphasic response suggests that unrestricted cell proliferation after injury is not the underlying mechanism for cyst formation. Aberrant Planar Cell Polarity (PCP) signaling and increased canonical Wnt signaling are suggested to be involved in cyst formation. Indeed we show here that in *Pkd1* conditional deletion mice expression of the PCP component Four-jointed (*Fjx1*) is decreased while its expression is required during tissue regeneration. In addition, we show that altered centrosome position and activation of canonical Wnt signaling are early effects of *Pkd1*-gene disruption. This suggests that additional stimuli or events are required to trigger the process of cyst formation. We propose that during tissue repair the integrity of the newly formed *Pkd1*-deficient cells is modified rendering them susceptible to subsequent cyst formation.

Introduction

Autosomal Dominant Polycystic Kidney Disease (ADPKD) is characterized by progressive deterioration of kidney function due to the formation of fluid-filled cysts. Around the second decade in general only a few cysts can be detected by ultrasonography, while at middle age renal function declines and thousands of cysts are usually being found. ADPKD has an incidence of 1 in 400 to 1 in 1000 in Caucasians and is in fact a systemic disease with cyst formation as the major hallmark. Extra-renal manifestations are hypertension, formation of aneurysms and formation of cysts in liver and pancreas[1]. In most patients ADPKD is caused by either a mutation in the *PKD1* gene, encoding the protein polycystin-1 (PC1; 85% of clinical cases), or a mutation in the *PKD2* gene, encoding polycystin-2 (PC2; 15% of clinical cases)[2-4].

The exact roles of PC1 and PC2 in cyst formation or other disease manifestations are not clear yet. It is known that in kidneys the primary defect occurs in the epithelium and that a balanced expression level of these proteins is critical to maintain renal epithelial architecture. In renal epithelial cells deregulated *PKD1/2* gene expression, either by dose reduction or by complete gene inactivation through somatic mutations, initiates cystogenesis[5-7]. Both, PC1 and PC2 are expressed in several cellular compartments. The proteins form different multimeric protein complexes in different subcellular locations and they regulate several signaling pathways that together control essential cellular functions such as proliferation, apoptosis, adhesion and differentiation[8, 9]. As all these activities are highly co-coordinated, disruption of any of these processes can lead to cyst formation as shown by a variety of mouse models (e.g. *bcl2* knock-out, *c-myc* over expression, β-catenin mutants, *Fat4* knock-out)[10-13].

We recently generated an inducible *Pkd1*-deletion mouse model in which we can induce *Pkd1*-deletion specifically in renal epithelial cells by administration of tamoxifen. These mice carry a tamoxifen inducible-KspCad–Cre as well as $Pkd1^{lox2\text{-}11,del2\text{-}11}$ or $Pkd1^{lox2\text{-}11,lox2\text{-}11}$ alleles[14, 15]. Upon administration of tamoxifen, the *Pkd1*-gene is deleted and renal cysts are being formed. Interestingly, adult mice (3-5 months) in which the deletion was induced, showed a relatively mild cystic phenotype after 3-5 months, while gene-disruption in newborn mice (post-natal day 4) resulted in massive cyst formation after 1 month. Similar data were reported for other models[16-18]. At neonatal stages kidney development is not yet completed. The kidneys might be more susceptible for *Pkd1*-gene inactivation, given the developmental switch in gene expression between days PN12 and 14[16]. In addition, cell proliferation takes place to elongate the nephron and therefore, we hypothesize that proliferation may accelerate cyst formation in (adult) ADPKD[15].

It has been proposed that tubular lengthening during renal development requires oriented cell division, which is the result of a correctly positioned orientation of the nuclear spindle axis. The Planar Cell Polarity (PCP) pathway controls oriented cell division and is disturbed in non-orthologous models for PKD[19, 20]. This is one of the pathways mediated by Wnt signaling, since the intracellular response to Wnt depends on the signaling cascade activated in the responding cell.

Cells can activate either the non-canonical pathway that controls PCP, or the canonical pathway that modulates gene expression to control cellular differentiation and proliferation. A molecular switch between these pathways requires the involvement of the protein inversin[21].
Also tissue regeneration after injury requires massive cell proliferation and proper differentiation. Therefore, we studied the effects of treatment with a nephrotoxic compound on cyst formation and proliferation in an adult inducible *Pkd1*-deletion model. Indeed, renal injury accelerated cyst formation but did not result in unrestricted cell proliferation. Furthermore, we show that in *Pkd1*-deletion mice tissue regeneration is accompanied by reduced expression of the PCP gene Four-jointed (*Fjx1*), together with increased expression of targets from the canonical Wnt signaling. In addition, we measured a deviation of the position of centrosomes in mutant compared to control mice. Overall these data suggest that the integrity of the newly formed cells is altered.

Results

Rate of cyst formation correlates with cell proliferation at the time of gene disruption
We previously showed that a substantial number of proliferating Ki-67 positive renal epithelial cells could be observed in newborn wild-type mice, while in adult mice Ki-67 positive nuclei were hardly found [15]. We hypothesized that the proliferation status of the tissue may contribute to the observed pathogenic differences between the adult and newborn tamoxifen-treated conditional deletion mice. In the mean time, we also generated mice with gene disruption at 5.5 weeks post-natal (PN40). These young-adult mice showed a more progressive phenotype compared to adult mice with gene disruption at 3 months, but less progressive compared to gene disruption at neonatal stages (not shown). Indeed, the proliferation index at 5.5 weeks is intermediate to newborn and adult stages: 1.5% ± 0.57 (n=6) while the mean proliferation index (PI) in kidneys of young mice (postnatal week 1) is 6.8% ± 1.50 (n=3) and in adult mice (>3 months) the mean PI is around 0.2% ±0.22 (n=3) (Fig. 1).

Renal epithelial injury accelerates cyst formation in adult conditional *Pkd1*-deletion mice
Tissue regeneration upon injury is accompanied by increased cell proliferation. To determine whether injury-induced proliferation accelerates cyst formation, adult *Cre; Pkd1*$^{del2\text{-}11,lox}$ mice were treated with the nephrotoxic compound 1,2-dichlorovinyl-cysteine (DCVC) (cKO+DCVC) or vehicle (cKO-DCVC) (22,23). As control *Pkd1*$^{del2\text{-}11,wt}$ and *Pkd1*$^{del2\text{-}11,lox}$ mice were treated with DCVC (control+DCVC). Blood urea (BU) concentrations were measured to monitor renal function and mice were sacrificed at BU levels exceeding 20 mmol/L (Fig. 2 A and supplementary Fig. S1). Cre-mediated recombination efficiency was 40%-50% in all cKOs as determined by extension MLPA (eMLPA).

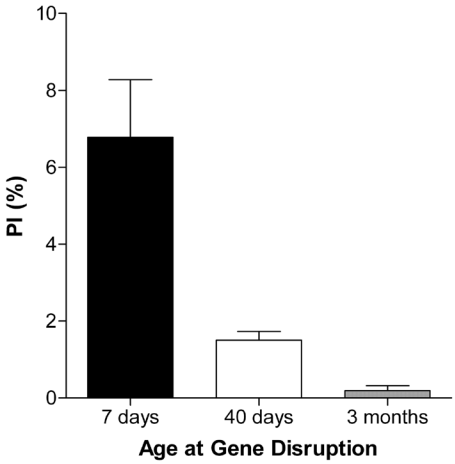


Figure 1. Renal epithelial cell proliferation in mice at different ages. Epithelial cell proliferation in the renal cortex of wild-type mice at different ages, post-natal day 7, day 40 and 3 months corresponding approximately to the ages at which gene disruption was induced by three days tamoxifen-treatment in conditional knock-out mice (neonatal (PN4), young adults (PN40) and adult mice of 3 months).

At 40hrs after treatment all DCVC treated mice showed increased BU concentrations, indicative for renal injury. After two weeks, BU levels were normalized to baseline. After 10-14 weeks blood urea levels increased again only in cKO+DCVC and all groups were sacrificed. Kidneys of cKO+DCVC mice showed a severe cystic phenotype (Fig. 3 C) while non-treated cKO mice showed only mildly dilated tubules (Fig. 3 E) and occasionally a limited area with focal cysts after 10 to 15 weeks. The majority of cysts is from proximal tubular origin, the nephron segment that is most injured by DCVC treatment (Fig. 3 F)[22, 23]. At 2 weeks after injury only very mild tubular dilatation was observed in cKO+DCVC. This became more prominent at 5 weeks after injury, although dilatations were still mild (Fig. 3 A and 3 B respectively).

Controls+DCVC showed no cysts or signs of tubular dilatation after 10 weeks (Fig. 3 D), or even after 6 months (not shown). Concomitantly, the renal cystic index was significantly increased in cKO+DCVC mice compared to both control groups, cKO-DCVC and controls+DCVC (Fig. 2 B). The kidney to bodyweight ratio (KW/BW), another marker for disease severity, is also markedly elevated in cKO+DCVC mice at 10-15 weeks (Fig. 2 C).

From these data we conclude that renal injury accelerates cysts formation in adult *Pkd1*-deletion mice.

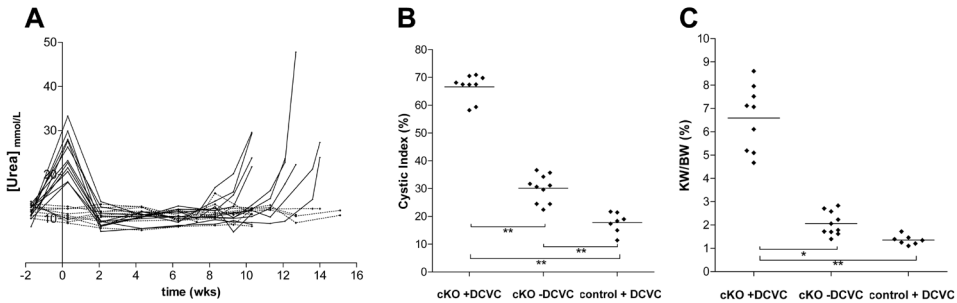


Figure 2. Progression of PKD monitored by Blood Urea (BU) concentrations, KW/BW-ratios and cystic index. (A) BU concentration (mmol/L) in time for cKO+DCVC (solid lines) and cKO–DCVC (dotted lines), plotted for individual mice. (B) Cystic Index (%) and (C) KW/BW-ratios (%). Cystic index is presented as percentage of lumen in tissue. Cystic index and KW/BW-ratios are presented for individual mice with line representing the mean (* P<0.01; ** P<0.001).
Occurrence of severe cystic kidneys was analyzed using a Mantel-Haenszel test, with sever cystic kidneys being defined by a cystic index and kidney to bodyweight ratio exceeding 40% and 4% respectively. Formation of cystic kidneys was accelerated significantly in DCVC treated *Pkd1* deletion mice compared to non-treated deletion mice (P<0.05).

Proliferation normalizes to base line levels after tissue regeneration in *Pkd1*-deletion mice

To study the levels of epithelial cell proliferation at different stages upon renal injury, we determined proliferation indexes in tubular epithelial cells of the renal cortex, the cortico-medullary region and the medulla, using the proliferation marker Ki-67 (Fig. 4).

One week after injury the proliferation indexes were increased in cKO+DCVC and controls+DCVC compared to untreated mutants, and the levels were higher in cortex and cortico-medullary region in cKO+DCVC (Fig. 4 A and 4 B). After the initial repair phase, proliferation returned to the same level as in cKO–DCVC, reaching baseline levels at 2-5 weeks. This pattern is most clearly seen in the cortico-medullary region and cortex, which are mostly injured by DCVC treatment (Fig. 4) (22,23). In severe cystic kidneys of cKO+DCVC at 10 weeks, proliferation was dramatically increased again. This biphasic response, in which proliferation is increased during repair, but returns to basal levels before increasing again, was not observed in cKO–DCVC and controls+DCVC, which do not develop renal cysts at 10-14 weeks after injury.

These data suggest that cyst formation after injury is not the result of unrestricted cell proliferation induced by tissue repair.

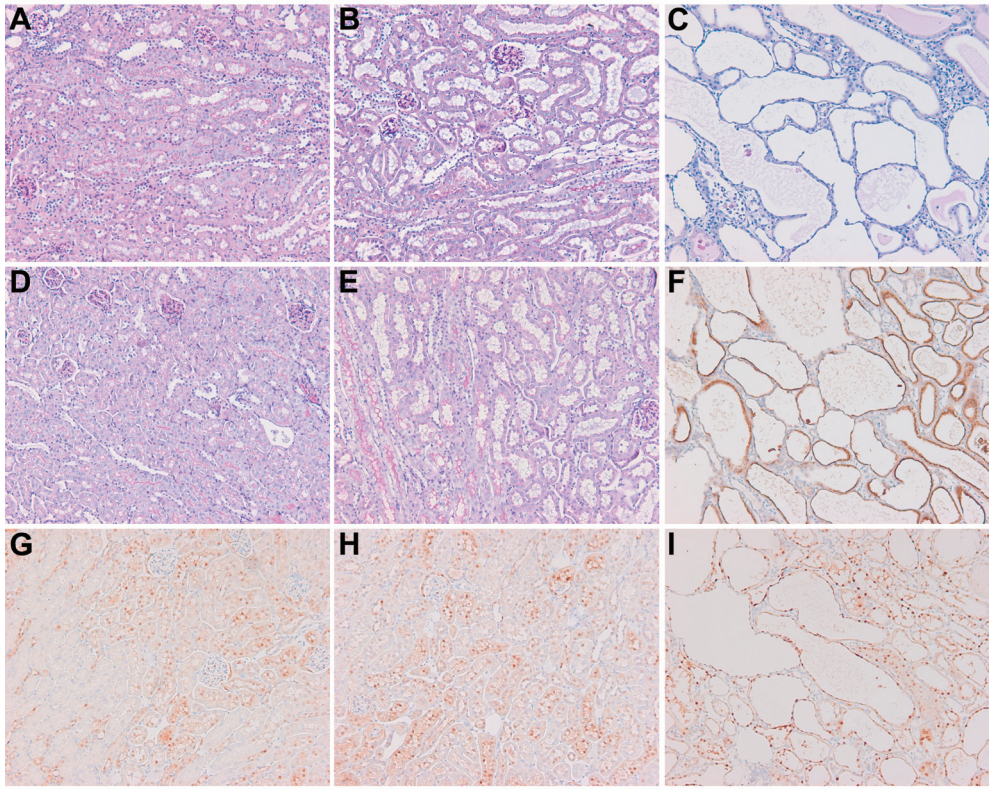


Figure 3. Cyst formation in *Pkd1*-deletion mice. Renal sections of cKO+DCVC mice stained with PAS at (A) 2, (B) 5 and (C) 10 weeks after treatment. (D) At 10 weeks controls+DCVC show no signs of tubular dilation or cystogenesis, while (E) cKO-DCVC only show mild dilatations. (F) The first renal cysts in cKO+DCVC originate from proximal tubules and are positive for megalin. Cyclin D1 nuclear staining is present in cKO-DCVC (G), but seems more intense in cKO+DCVC (H) at 5 weeks and (I) cKO+DCVC at 10 weeks after injury.

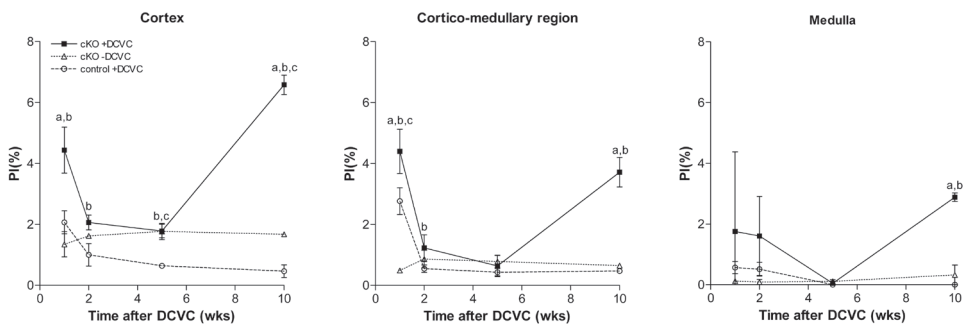


Figure 4. Proliferation indexes after injury in *Pkd1* deletion mice. Renal sections were stained with Ki-67 and PI was determined in (A) cortex, (B) cortico-medullary region and (C) medulla at 1, 2, 5 and 10 weeks after injury. PIs in each group are presented as mean ± SD. Significant differences between cKO+DCVC (closed squares, solid lines) and cKO-DCVC (open triangles, dotted lines) are indicated by a, between cKO+DCVC and control+DCVC (open circles, dashed lines) by b, and between cKO–DCVC and control+DCVC by c with $P<0.05$.

Planar cell polarity gene *Fjx1* is differentially expressed upon renal injury in precystic *Pkd1*-deletion mice

Since proliferation reached baseline levels after tissue regeneration, but the DCVC-treated mutants form cysts much earlier than untreated mutants, we investigated whether the expression of genes involved in oriented cell division/planar cell polarity during tissue repair, recovery and at precystic and cystic stages was altered. Therefore, we studied mRNA expression of Four-jointed (*Fjx1*), Moesin (*Msn*) and Inscuteable (*Insc*) at different time-points. These genes were selected since they showed differential expression upon microarray analysis of cKO mice in which the *Pkd1*-gene was disrupted at post-natal day 40 (PN40). At 2 months upon gene disruption (PN40+2m), which is at precystic stages with mild tubular dilatations, only a limited number of genes (298/34,000; manuscript in preparation) was differentially expressed including *Fjx1* (down-regulated), *Msn* (up-regulated) and *Insc* (up-regulated). (Supplementary Fig. S2A). For other genes involved in PCP, expression was too low (*Fat4, Prickle1*), or did not show differential expression (Dachsous (*Dchs1), Prickle2, Vangl* and *Celsr* (Flamingo)).

Importantly, expression of *Fjx1* a key regulator of PCP was also reduced during the repair process at 1 and 2 weeks in cKO+DCVC, while expression was increased in controls+DCVC (Fig. 5 A). This difference persisted until 5 weeks after injury. At 10 weeks, in severe cystic kidneys, expression of *Fjx1* was significant increased compared cKO–DCVC and control+DCVC. The expression of *Insc* en *Msn* was not significantly different in the different groups, although expression was slightly elevated at 5 weeks for *Insc* and significantly at 10 weeks for *Insc* and *Msn*.

Canonical Wnt targets are differentially expressed upon renal injury in *Pkd1*-deletion mice.

Since it is expected that altered PCP is associated with increased canonical Wnt signaling, we analyzed mRNA expression of several canonical Wnt targets and regulators at different time-points upon renal injury. The genes selected showed differential expression on microarrays at precystic stages of cKO mice with *Pkd1*-gene disruption at post-natal day 40. Expression of these genes is increased, except for Notum and Secreted Frizzled related protein 1 (*Sfrp1*), which show strongly reduced mRNA-levels (Supplementary Fig. S2B). Both genes are canonical Wnt targets as well as negative regulators of Wnt signaling, suggesting that they are subject to complex regulation[24, 25]. For eight other canonical Wnt targets sufficient signal was detected on the arrays but expression was not significantly altered (not shown).

In the DCVC-treated animals we analyzed expression of Cyclin D1 (*Ccnd1*), Survivin (*Birc5*), Prominin-1 (*Prom-1*) and Notum (*Notum*), which are direct canonical Wnt targets with differential expression on microarrays at precystic stages. In addition, we analyzed expression of *Sfrp1,* an indirect target.

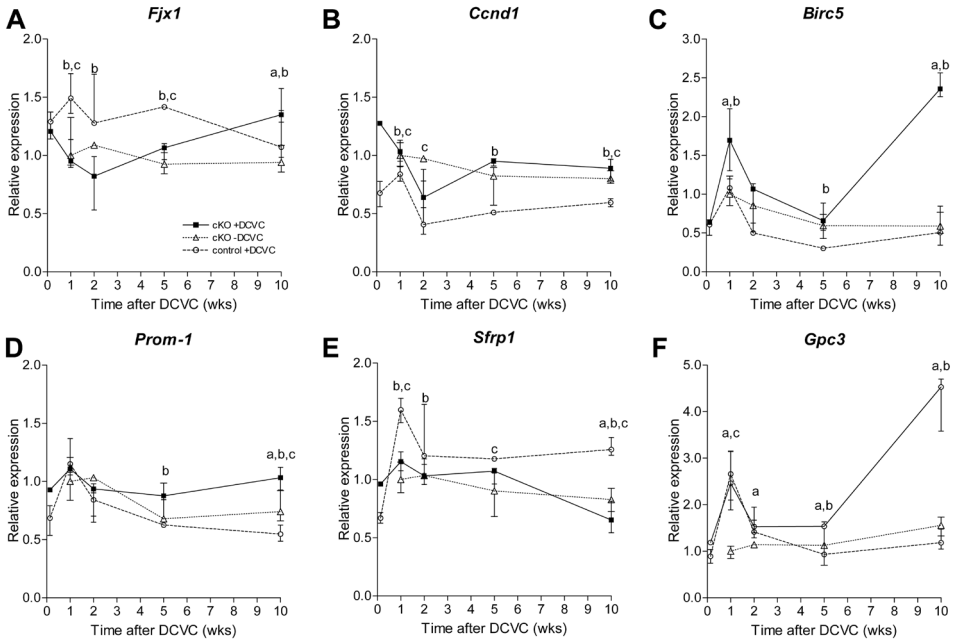


Figure 5. mRNA expression of the PCP component (A) Four-jointed (*Fjx1*), canonical Wnt targets (B) CyclinD1 (*Ccnd1*), (C) Survivin (*Birc5*), (D) Prominin-1 (*Prom-1*), (E) indirect Wnt target and Wnt regulator Secreted Frizzled related protein 1 (*Sfrp1*) and (F) Wnt regulator Glypican-3 (*Gpc3*) analyzed by RT MLPA. Expression was normalized to housekeeping genes. Results are shown as median of expression relative to the expression of cKO-DCVC, 1 week after treatment. Error bars represent interquartile range.
Significant differences with P<0.05 between cKO+DCVC (closed squares, solid lines) and cKO-DCVC (open triangles, dotted lines) are indicated by a, between cKO+DCVC and control+DCVC (open circles, dashed lines) by b and between cKO-DCVC and control+DCVC by c.

In general, expression of all these genes, except the negative regulators, peaked at 1 week upon DCVC. However, at precystic stages mRNA levels were higher in cKO+DCVC compared to controls+DCVC as shown for Cyclin D1, Survivin and Prominin-1 (Fig. 5 B-D). At 1 and 2 weeks the relative expression was not always significantly increased, but at 5 weeks it was. Also in cystic kidneys, at 10 weeks, mRNA levels were significantly elevated.

For most genes expression was also (significantly) elevated in cKO-DCVC mice compared to controls+DCVC, which is in agreement with increased expression seen on the microarrays of PN40+2m mice. Our data indicate that *Pkd1*-gene disruption induces canonical Wnt signaling already at very early, precystic stages.

The expression pattern for Cyclin D1 mRNA was confirmed by immunohistochemical staining for the Cyclin D1 protein. At 1 week after DCVC treatment strong nuclear accumulation of Cyclin D1 could be observed in many nuclei in mutants and controls (Fig. 3 G-I). After the initial increase of Cyclin D1 staining, the intensity decreased and at 5 weeks an increase in number and intensity of

positive nuclei could be observed (Fig. 3 H, I). This was always higher in cKO+DCVC compared to controls+DCVC. Also in cKO–DCVC, Cyclin D1 staining increased over time.
The expression of the two negative regulators of Wnt signaling, *Sfrp1* (Fig. 5 E) and *Notum* (not shown) was significantly lower in cKO+DCVC compared to controls with DCVC. Notum can cleave Glypican-3, a canonical Wnt activator and converts this proteoglycan from being a Wnt activator to a Wnt inhibitor. The expression of the inhibitor Notum was reduced in cKO+DCVC, and Glypican-3 (*Gpc3*; Fig. 5 F) mRNA levels were substantially elevated.
From these data we conclude that upon *Pkd1*-gene disruption planar cell polarity signaling is altered and canonical Wnt signaling is increased.

***Pkd1*-deletion affects centrosome position**

Mitotic spindle orientation has been used as a read-out system for aberrant PCP in kidney development[19, 20]. In the injury model aberrant PCP signaling has to be determined after repair of the injured tissue but in precystic stages. However, in these adult mice cell proliferation is very low and only a few nuclear spindles can be observed. Since components of the primary cilia/basal body/centrosome complex also contribute to formation of the nuclear spindles, we studied centrosome position in interphase cells as described by Jonassen et al[26].
Centrosome position was measured in proximal tubules in the cortico-medullary region at 2 weeks after DCVC treatment. In absence of *Pkd1* the normal bias towards a neutral centrosome position, close to the center of the apical surface of the cell, was lost (Fig. 6). This resulted in a significant different distribution of angles defining centrosome position in cKO+DCVC ($p<0.0001$) and cKO-DCVC ($p<0.05$) compared to control+DCVC. As can be appreciated from figure 6 this effect is stronger in cKO+DCVC, although this did not reach statistical significance.
These results indicate that already early after *Pkd1* inactivation centrosome position is altered.

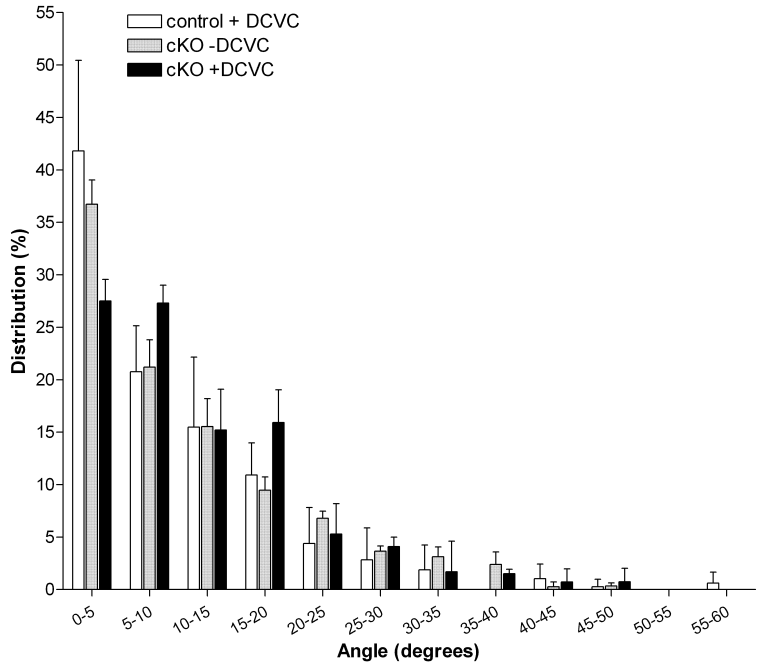


Figure 6. Distribution of centrosome position in *Pkd1*-deletion mice. The position of the centrosome was determined by measuring the angle between a line through the centre of the nucleus perpendicular to the basement membrane and a line through the centrosome towards this point at the basement membrane. Distribution of angles in cKOs was significantly different from controls+DCVC for cKO+DCVC ($p<0.001$) and for cKO-DCVC ($p<0.05$).

Discussion

ADPKD is an adult onset disease characterized by the formation of many fluid-filled cysts in both kidneys with advancing age. When the level of *Pkd1* or *Pkd2* drops below a critical threshold in renal epithelial cells, either by stochastic variation or because of somatic mutations, the differentiation status of the cells alters resulting in increased cell proliferation, extracellular matrix synthesis and altered fluid transport. Previously, we showed that when we knock-out the *Pkd1* gene in newborn mice rapid formation of cysts occurs, while in adult mice there is a lag time of a few weeks between the moment of gene disruption and the onset of increased epithelial cell proliferation and cyst formation[15]. Therefore we hypothesized that the proliferative status of the renal tissue at the time of gene disruption is important for the rate at which cysts are formed after *Pkd1* conditional deletion. In addition, a different gene expression profile in neonatal and adult kidneys may contribute to these phenomena as well[16].

Our data show that *Pkd1*-gene disruption at 5.5 weeks post-natal (PN40) leads to a disease progression rate intermediate to that of neonatal and adult mice. At this stage mice show levels of proliferation between neonatal and adult mice and are beyond the developmental switch in renal gene expression (PN12-14). We also show that DCVC-induced renal epithelial injury significantly accelerates the progression of renal cyst formation. The majority of the cysts was derived from the proximal tubules at the inner cortex, which is the nephron segment that is the main target of injury by this nephrotoxicant[22, 23]. A similar result has recently been shown for a conditional knockout model of the ciliary transport component Kif3a, which develops more progressive renal cystic disease upon ischemic injury[20].

Renal epithelial injury is followed by a repair phase that includes proliferation to restore the tubular epithelial architecture. Importantly, in DCVC-induced *Pkd1*-deletion mice proliferation decreases to basal levels after repair at 2 and 5 weeks, similar to DCVC-induced controls. From this we can conclude that also in the context of the renal tissue, absence of *Pkd1*-expression does not lead to unrestrained epithelial cell proliferation. These results are corroborating previous reports showing that cystic epithelial cells of *Pkd1* null mice do not grow in nude mice[27]. In *Pkd1*-deletion mice cell proliferation upon renal injury showed a biphasic response, e.g. after the initial peak in the repair phase, renal epithelial cell proliferation increased again during cyst formation at 10-14 weeks.

Although cell proliferation during tissue regeneration is controlled in DCVC-treated mutants, these mice form cysts much earlier than untreated mutants. Similar to embryogenesis and renal development, tissue repair reactions require properly regulated cell proliferation to restore the epithelial architecture. Defects in oriented cell division were observed during tubular elongation in renal development in non-orthologous animal models for PKD[19, 20]. In addition, loss of the planar cell polarity (PCP) gene *Fat4* leads to renal cysts formation[13]. Altogether, these data suggest a potential role for aberrant PCP or oriented cell division, two closely linked pathways to which function only a few mammalian genes have been assigned as yet, in cystogenesis. Here, we investigated whether defects in PCP during tissue regeneration could be involved in accelerated cyst formation as observed in adult *Pkd1*-deletion mice. In adult precystic kidneys the number of proliferating nuclei with a detectable nuclear spindle is too low to measure[20]. Therefore, we studied centrosome position as described by Jonassen *et al.*[26], who showed that the intraflagellar transport protein IFT20 plays a role in controlling Wnt signaling. Furthermore, it is required for proper positioning of the centrosomes in nondividing cells and for correct orientation of the mitotic spindles in dividing cells. We analyzed the position of centrosomes after repair of injury, but at a precystic stage. As expected, in the majority of cells of control mice (+DCVC) centrosomes are positioned close to the center of the apical membrane. In mutants with and without DCVC, however, a significantly different pattern in distribution of centrosome position was observed. From these data we conclude that improper positioning of centrosomes is an early event upon *Pkd1*-gene disruption. Jonassen *et al.*[26] suggested that in renal epithelial cells the cilium may

provide an external cue to position the mother centrosome, thereby coordinating the plane of cell division of an individual cell with neighboring tubular cells. Whether the effect of *Pkd1*-gene disruption on centrosome localization is a result of polycystin-1 requirement in normal ciliary structure and function, or through interaction with Wnt signaling components, or both, requires further research.

Altered PCP-signaling was further studied by gene expression analysis. Microarray based gene expression profiling in precystic kidneys of conditional *Pkd1*-deletion mice (PN40+2m) revealed differential expression of the PCP-related genes *Fjx1*, *Insc* and *Msn*, and expression of these genes was studied during tissue regeneration. Although the subcellular localization of the encoded proteins is probably also important, the expression pattern of *Fjx1* is particularly interesting. Four-jointed is a Golgi-associated kinase that phosphorylates the extracellular domains of Fat and Dachsous[28]. In the first week after DCVC-treatment *Fjx1* mRNA levels are elevated in control mice suggesting that four-jointed is needed during tissue repair. In *Pkd1*-deletion mutants, however, expression of *Fjx1* goes down suggesting defects in PCP signaling.

PCP is regulated by the non-canonical Wnt pathway. So, defects in PCP signaling could be expected to be accompanied by an increase in canonical Wnt signaling. Indeed, microarray gene expression analysis showed elevated mRNA levels of canonical Wnt targets in precystic stages of conditional *Pkd1*-deletion mice. Moreover, expression of the negative Wnt regulatory genes *Sfrp1* and *Notum* was decreased. After renal injury most of the Wnt targets analyzed showed a similar biphasic response for gene expression as observed for proliferation, with higher levels in the precystic stage in DCVC-treated mutants than in DCVC-treated controls. Cyclin D1 expression, however, did not show the second increase in gene expression, e.g. mRNA levels were not higher in cystic kidneys than in untreated mutants. Regulation of this gene and some other Wnt targets is complex implicating several parallel signaling pathways with positive and negative feedback loops.

Since also in untreated *Pkd1*-deletion mice centrosome position and expression of canonical Wnt targets are altered, we conclude that these are early responses to *Pkd1*-gene disruption. We speculate that these early alterations create a permissive condition for accelerating cyst formation and that additional factor(s) are required. Abnormal integrity of the newly formed cells, resulting from the absence of *Pkd1* expression during repair, might be such a factor. The polycystins, form multimeric protein complexes at the cell membrane and function in cell–cell and cell–matrix interactions, mechanosensation and signal transduction[8, 29-32]. It is likely that polycystins are required during repair for the proper formation of these protein complexes. Without *Pkd1*, cellular structure, geometry and cohesion will be modified. In agreement with this hypothesis polycystin-1/-2 levels are elevated after ischemic injury[33-35]. Without renal injury, gradually, cell renewal will result in *Pkd1*-deficient cells with strongly disturbed cellular integrity that are more sensitive to triggers for subsequent cyst formation.

Abnormal Wnt signaling has been implicated in the pathogenesis of polycystic kidney disease; ciliary defects affect Wnt signaling, over-expression of *Pkd1* is accompanied by nuclear localization of β-catenin, constitutively active β-catenin induces cyst formation[12, 21, 36]. Recent data also suggest that the C-terminal tail of PC1 may have a direct role in modulating Wnt signaling by inhibiting the interaction between β-catenin and the T-cell factor (TCF)[37]. This study also demonstrated activation of the canonical Wnt signaling pathway in cysts of different sizes, isolated from ADPKD patient tissues. Our data indicate that already at precystic stages canonical Wnt signaling is activated. In ADPKD, activation of canonical Wnt signaling seems to be rather subtle since we did not observe nuclear localization of β-catenin in *Pkd1*-deletion mice at any stage (data not shown) and as we reported previously we could not detect nuclear accumulation of non-phosphorylated β-catenin in cyst lining epithelium in end-stage ADPKD-kidneys[38]. This is different from various forms of cancer where core components of canonical Wnt signaling are constitutively activated, leading to patho-physiological levels of active β-catenin, while PC1 only seems to modulate the canonical Wnt pathway[39].

Formally, we can not exclude that the early changes in gene expression in our mouse model are without biological significance and that stronger Wnt signaling observed in advanced stages of PKD is the result of secondary events during cyst formation. However, Lal *et al*.[37] suggested that PC1 expression is necessary to inhibit basal Wnt signaling, probably by an interaction of the carboxy-terminal 200 amino acids cleavage product of polycystin-1 with β-catenin.

In conclusion, nephrotoxic injury dramatically accelerates polycystic kidney disease in adult *Pkd1*-deletion mice. Proliferation after injury, first decreases to basal levels, indicating that accelerated cyst formation is not the result of unrestricted cell proliferation. Altered centrosome position and activation of canonical Wnt signaling are early effects of *Pkd1* gene disruption but additional stimuli or events are required to trigger the process of cyst formation.

Materials & Methods

Experimental animals and study design

The inducible *Pkd1*-deletion mice (tam-*KspCad-CreER*^{T2}*;Pkd1*$^{del2\text{-}11/lox2\text{-}11}$) and tamoxifen treatment have been described previously[14, 15]. The *Pkd1* gene was inactivated in adult mice (approximately 11 weeks), by oral administration of tamoxifen (5mg/day, 3 consecutive days). Renal injury was induced 6 days later by i.p. administration of 15 mg/kg DCVC or vehicle[40](40). *Cre;Pkd1*^{del,wt}, *Pkd1*^{del,wt} and *Pkd1*^{del,lox} mice all received DCVC.

Blood samples were obtained from the tail vein at indicated time points with lithium-heparin coated capillary tubes (Roche Diagnostics). Blood urea concentrations were determined using the Reflotron Plus (Roche Diagnostics). Mice were sacrificed at previous determined time points, or when blood urea concentrations exceeded 20 mmol/L (indicating severe renal failure). After sacrifice, kidney to bodyweight ratio was determined for each animal.

Recombination efficiency was determined by extension MLPA (eMLPA) analysis as recently described by Leonhard *et al.*[41]

Local animal experimental committee of the Leiden University Medical Center and the Commission Biotechnology in Animals of the Dutch Ministry of Agriculture approved the performed experiments.

mRNA expression analysis

For gene expression analysis, Reverse Transcriptase Multiplex Ligation-dependent Probe Amplification (RT-MLPA) reactions were performed as described previously[42]. Briefly, kidneys of mice sacrificed at indicated time points were homogenized and total RNA was isolated. From an aliquot of 60-200 ng total RNA, cDNA was synthesized. On this cDNA two separate hybridization reactions were performed.

To each sample MLPA probe mix (two oligonucleotides per probe) and SALSA MLPA buffer were added (MRC-Holland), and samples were incubated at 95°C for 1 min followed by incubation at 60°C for 4 hours. Ligation of annealed oligonucleotides was performed at 54°C for 10-15 min. followed by ligase inactivation at 98°C for 5 min and ligation products were amplified by PCR using Salsa*Taq* (MRC-Holland) and FAM or HEX-labeled primers. The amplified samples were mixed with Hi-Di Formamide containing GeneScan-500 ROX size standard (Applied Biosystems), heated for five minutes at 95°C, and run on a 3730 DNA analyzer (Applied Biosystems). Data were analyzed using GeneScan analysis 3.5 and Microsoft Excel software. Expression of the housekeeping genes *Ywhaz* (tyrosine 3-monooxygenase/tryptophan 5-monooxygenase activation protein, zeta polypeptide) and *Hprt* (hypoxanthine phosphoribosyl transferase) served as reference for gene expression.

Peak ratios of target gene and housekeeping genes were calculated and results of the different groups were normalized to the median of the control+DCVC mice at t= 1 wk), which has been set to 1. Sequences and details of probes, primers and competitors are available upon request.

Quantitative gene expression analysis for *Msn* was performed on a 7900HT Fast Real-Time PCR System (Applied Biosystems) using SYBR Green technology with 2x SybrGreen mastermix (Applied Biosystems) according to manufacturers' protocol. *HPRT* was used as housekeeping gene. Primer sequences are available upon request.

(Immuno-)histological analysis

Formalin fixed, paraffin embedded kidney sections (4 µm) were analyzed using standard haematoxylin and eosin (HE) staining, periodic acid Schiff (PAS) staining or were used for immunohistochemistry. Sections were subjected to heat mediated antigen retrieval procedure (10mM citrate buffer pH 6.0 for anti-Ki-67, anti-cyclinD1, 10mM/1mM TRIS/EDTA pH 9.0 for anti-γ-tubulin and anti-collagenIV). After blocking of endogenous peroxidase activity for 15 minutes in 0.1% H_2O_2 in water, sections were incubated with primary antibodies diluted in 1% BSA in PBS. Following incubation with secondary antibody, immune reactions were revealed

using diaminobenzidine as a chromogen and counterstained with haematoxylin, dehydrated, and mounted. Slides for immuno-fluorescence were mounted with vectashield containing DAPI after secondary antibody incubation.

Antibodies

Primary antibodies: rabbit polyclonal anti-megalin (1:500, Pathology LUMC, Leiden, the Netherlands[43]), goat polyclonal anti-uromodulin (1:500, Organon Teknika-Cappel, Turnhout, Belgium), rabbit polyclonal anti-aquaporin-2 (1:4000 Calbiochem, Amsterdam, The Netherlands), polyclonal anti-Ki-67 (1:3000, Nova Castra), rabbit monoclonal anti-cyclin D1 (1:200 clone, 92G2, Cell Signaling), rabbit polyclonal anti-collagen IV IgG1 (1:500, Abcam) and mouse monoclonal anti-γ-tubulin IgG1 (1:750, clone GTU-88 Sigma-Aldrich). Secondary antibodies: anti-rabbit envision HRP (DakoCytomation, Glostrup, Denmark), rabbit-anti-goat HRP (1:300), goat-anti-rabbit IgG Alexa546 and goat- anti-mouse IgG1 Alexa 488 (both 1:200, Invitrogen).

Proliferative index (PI)

The PI was assessed as previously described[15]. Briefly, the percentage of Ki-67-positive renal epithelial cells was determined in three segments of the kidney. Between 1600 and 2200 tubular epithelial nuclei per section were counted in cortex (C) and cortico-medullary junction (CM) and 350 to 600 per section in medulla (M). Only clearly definable nuclei with heavy/or granular staining were identified as Ki-67 positive.

Morphometric Analysis

PAS stained transverse kidney sections were used for determination of cystic index. Cystic index was defined as the area percentage of lumen over the total image area. Three to five images were obtained from cortex and cortico-medullary region. For both renal areas mean cystic index was calculated, after which total cystic index was calculated as the mean of both areas. Areas were determined using Image J software (public domain software, NIH, USA).

For centrosome orientation Z-stacks were acquired using a Leica DM500B microscope with a Leica DM DFC 350 FX camera using Leica Application Suite 1.8.0 build1346. Analyzed images are maximum projections of 25-30 Z-images taken 0.24 μm apart. Centrosome positions in transverse sectioned proximal tubules at 2 weeks after injury were determined essentially as described by Jonassen *et al.* using Image J software[26]. In brief, the position of the centrosome was determined by measuring the angle between a line through the centre of the nucleus perpendicular to the basement membrane and a line through the centrosome towards this point at the basement membrane. Collagen IV staining was used to indicate the basement membrane (supplementary Fig. S3). In total 950 angles were measured blindly in 3 cKO+DCVC, 3 cKO-DCVC and 6 controls+DCVC.

Statistical analysis

Statistical comparisons between groups concerning the development of cystic kidneys within 15 weeks were performed with the Mantel-Haenszel test in which severe cystic kidneys are defined by a combination of kidney- to bodyweight ratio, and renal cystic index at the indicated time point.

Differences between groups in cystic index, KW/BW and mRNA expression were assessed using one-way ANOVA.

The Kolomogorov-Smirnov Z test was used to determine differences in angle distribution between groups. In addition a Mann Whitney test was performed to test whether differences between groups were significant.

A P-value <0.05 was considered statistically significant.

Acknowledgements

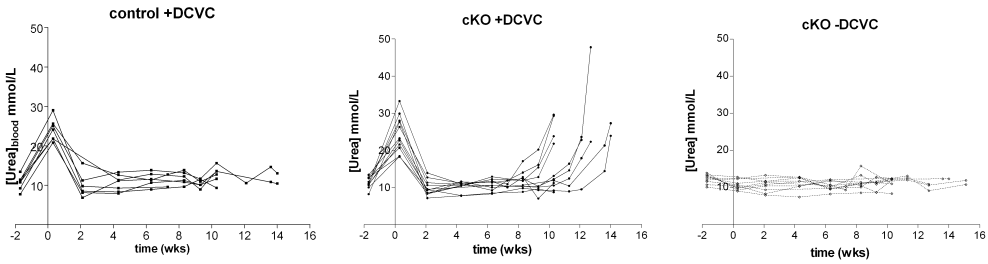
We thank Peter-Bram 't Hoen for support in microarray data-analysis, the Leiden Genome Technology Center for performing the micro-array experiment, Ron Wolterbeek for statistical support. This research was supported by grants from the Dutch Kidney Foundation (NSN C05-2132) and the Polycystic Kidney Disease Research Foundation (175G08a).

References

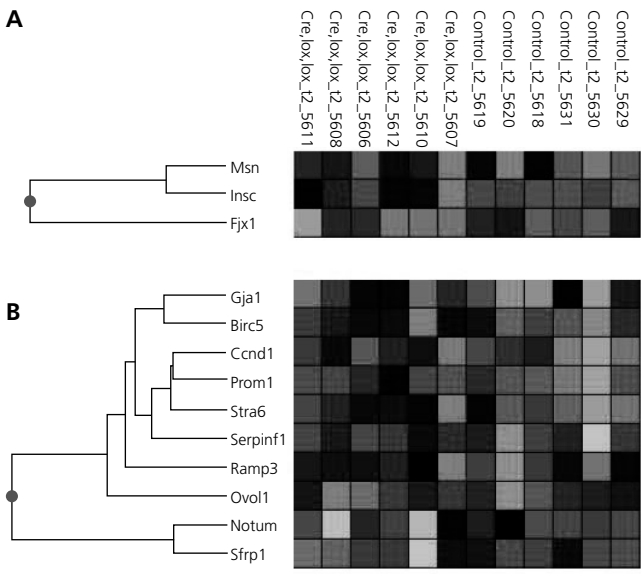
1. Gabow,P.A. Autosomal dominant polycystic kidney disease--more than a renal disease. *Am. J. Kidney Dis.* **16**, 403-413 (1990).
2. Peters,D.J. & Sandkuijl,L.A. Genetic heterogeneity of polycystic kidney disease in Europe. *Contrib. Nephrol.* **97**, 128-139 (1992).
3. The European Polycystic Kidney Disease Consortium. The polycystic kidney disease 1 gene encodes a 14 kb transcript and lies within a duplicated region on chromosome 16. *Cell* **77**, 881-894 (1994).
4. Mochizuki,T. *et al.* PKD2, a gene for polycystic kidney disease that encodes an integral membrane protein. *Science* **272**, 1339-1342 (1996).
5. Qian,F., Watnick,T.J., Onuchic,L.F., & Germino,G.G. The molecular basis of focal cyst formation in human autosomal dominant polycystic kidney disease type I. *Cell* **87**, 979-987 (1996).
6. Wu,G. *et al.* Somatic inactivation of Pkd2 results in polycystic kidney disease. *Cell* **93**, 177-188 (1998).
7. Lantinga-van Leeuwen,I.S. *et al.* Lowering of Pkd1 expression is sufficient to cause polycystic kidney disease. *Hum. Mol. Genet.* **13**, 3069-3077 (2004).
8. Wilson,P.D. Polycystic kidney disease. *N. Engl. J. Med.* **350**, 151-164 (2004).
9. Nauli,S.M. *et al.* Polycystins 1 and 2 mediate mechanosensation in the primary cilium of kidney cells. *Nat. Genet.* **33**, 129-137 (2003).
10. Sorenson,C.M., Padanilam,B.J., & Hammerman,M.R. Abnormal postpartum renal development and cystogenesis in the bcl-2 (-/-) mouse. *Am. J. Physiol* **271**, F184-F193 (1996).
11. Trudel,M., D'Agati,V., & Costantini,F. C-myc as an inducer of polycystic kidney disease in transgenic mice. *Kidney Int.* **39**, 665-671 (1991).
12. Saadi-Kheddouci,S. *et al.* Early development of polycystic kidney disease in transgenic mice expressing an activated mutant of the beta-catenin gene. *Oncogene* **20**, 5972-5981 (2001).
13. Saburi,S. *et al.* Loss of Fat4 disrupts PCP signaling and oriented cell division and leads to cystic kidney disease. *Nat. Genet.* **40**, 1010-1015 (2008).
14. Lantinga-van Leeuwen,I.S. *et al.* Transgenic mice expressing tamoxifen-inducible Cre for somatic gene modification in renal epithelial cells. *Genesis.* **44**, 225-232 (2006).
15. Lantinga-van Leeuwen,I.S. *et al.* Kidney-specific inactivation of the Pkd1 gene induces rapid cyst formation in developing kidneys and a slow onset of disease in adult mice. *Hum. Mol. Genet.* **16**, 3188-3196 (2007).
16. Piontek,K., Menezes,L.F., Garcia-Gonzalez,M.A., Huso,D.L., & Germino,G.G. A critical developmental switch defines the kinetics of kidney cyst formation after loss of Pkd1. *Nat. Med.* **13**, 1490-1495 (2007).
17. Shibazaki,S. *et al.* Cyst formation and activation of the extracellular regulated kinase pathway after kidney specific inactivation of Pkd1. *Hum. Mol. Genet.* **17**, 1505-1516 (2008).
18. Takakura,A., Contrino,L., Beck,A.W., & Zhou,J. Pkd1 inactivation induced in adulthood produces focal cystic disease. *J. Am. Soc. Nephrol.* **19**, 2351-2363 (2008).
19. Fischer,E. *et al.* Defective planar cell polarity in polycystic kidney disease. *Nat. Genet.* **38**, 21-23 (2006).
20. Patel,V. *et al.* Acute kidney injury and aberrant planar cell polarity induce cyst formation in mice lacking renal cilia. *Hum. Mol. Genet.* **17**, 1578-1590 (2008).
21. Simons,M. *et al.* Inversin, the gene product mutated in nephronophthisis type II, functions as a molecular switch between Wnt signaling pathways. *Nat. Genet.* **37**, 537-543 (2005).
22. Lock,E.A. Studies on the mechanism of nephrotoxicity and nephrocarcinogenicity of halogenated alkenes. *Crit Rev. Toxicol.* **19**, 23-42 (1988).
23. Lash,L.H., Elfarra,A.A., & Anders,M.W. Renal cysteine conjugate beta-lyase. Bioactivation of nephrotoxic cysteine S-conjugates in mitochondrial outer membrane. *J. Biol. Chem.* **261**, 5930-5935 (1986).
24. Kawano,Y. & Kypta,R. Secreted antagonists of the Wnt signalling pathway. *J. Cell Sci.* **116**, 2627-2634 (2003).
25. Traister,A., Shi,W., & Filmus,J. Mammalian Notum induces the release of glypicans and other GPI-anchored proteins from the cell surface. *Biochem. J.* **410**, 503-511 (2008).
26. Jonassen,J.A., San Agustin,J., Follit,J.A., & Pazour,G.J. Deletion of IFT20 in the mouse kidney causes misorientation of the mitotic spindle and cystic kidney disease. *J. Cell Biol.* **183**, 377-384 (2008).
27. Nishio,S. *et al.* Pkd1 regulates immortalized proliferation of renal tubular epithelial cells through p53 induction and JNK activation. *J. Clin. Invest* **115**, 910-918 (2005).

28. Ishikawa,H.O., Takeuchi,H., Haltiwanger,R.S., & Irvine,K.D. Four-jointed is a Golgi kinase that phosphorylates a subset of cadherin domains. *Science* **321**, 401-404 (2008).
29. Scheffers,M.S. *et al.* Polycystin-1, the product of the polycystic kidney disease 1 gene, co-localizes with desmosomes in MDCK cells. *Hum. Mol. Genet.* **9**, 2743-2750 (2000).
30. Roitbak,T. *et al.* A polycystin-1 multiprotein complex is disrupted in polycystic kidney disease cells. *Mol. Biol. Cell* **15**, 1334-1346 (2004).
31. Yu,A.S., Kanzawa,S.A., Usorov,A., Lantinga-van Leeuwen,I.S., & Peters,D.J. Tight junction composition is altered in the epithelium of polycystic kidneys. *J. Pathol.* **216**, 120-128 (2008).
32. Wilson,P.D., Geng,L., Li,X., & Burrow,C.R. The PKD1 gene product, "polycystin-1," is a tyrosine-phosphorylated protein that colocalizes with alpha2beta1-integrin in focal clusters in adherent renal epithelia. *Lab Invest* **79**, 1311-1323 (1999).
33. Ibraghimov-Beskrovnaya,O. *et al.* Polycystin: in vitro synthesis, in vivo tissue expression, and subcellular localization identifies a large membrane-associated protein. *Proc. Natl. Acad. Sci. U. S. A* **94**, 6397-6402 (1997).
34. Zhao,Y., Haylor,J.L., & Ong,A.C. Polycystin-2 expression is increased following experimental ischaemic renal injury. *Nephrol. Dial. Transplant.* **17**, 2138-2144 (2002).
35. Obermuller,N. *et al.* Altered expression pattern of polycystin-2 in acute and chronic renal tubular diseases. *J. Am. Soc. Nephrol.* **13**, 1855-1864 (2002).
36. Thivierge,C. *et al.* Overexpression of PKD1 causes polycystic kidney disease. *Mol. Cell Biol.* **26**, 1538-1548 (2006).
37. Lal,M. *et al.* Polycystin-1 C-terminal tail associates with beta-catenin and inhibits canonical Wnt signaling. *Hum. Mol. Genet.* **17**, 3105-3117 (2008).
38. Le,N.H. *et al.* Aberrant polycystin-1 expression results in modification of activator protein-1 activity, whereas Wnt signaling remains unaffected. *J. Biol. Chem.* **279**, 27472-27481 (2004).
39. Nusse,R. Wnt signaling in disease and in development. *Cell Res.* **15**, 28-32 (2005).
40. van de Water,B., Nagelkerke,J.F., & Stevens,J.L. Dephosphorylation of focal adhesion kinase (FAK) and loss of focal contacts precede caspase-mediated cleavage of FAK during apoptosis in renal epithelial cells. *J. Biol. Chem.* **274**, 13328-13337 (1999).
41. Leonhard,W.N., Roelfsema,J.H., Lantinga-van Leeuwen,I.S., Breuning,M.H., & Peters,D.J. Quantification of Cre-mediated recombination by a novel strategy reveals a stable extra-chromosomal deletion-circle in mice. *BMC. Biotechnol.* **8**, 18 (2008).
42. Eldering,E. *et al.* Expression profiling via novel multiplex assay allows rapid assessment of gene regulation in defined signalling pathways. *Nucleic Acids Res.* **31**, e153 (2003).
43. Christensen,E.I. *et al.* Segmental distribution of the endocytosis receptor gp330 in renal proximal tubules. *Eur. J. Cell Biol.* **66**, 349-364 (1995).

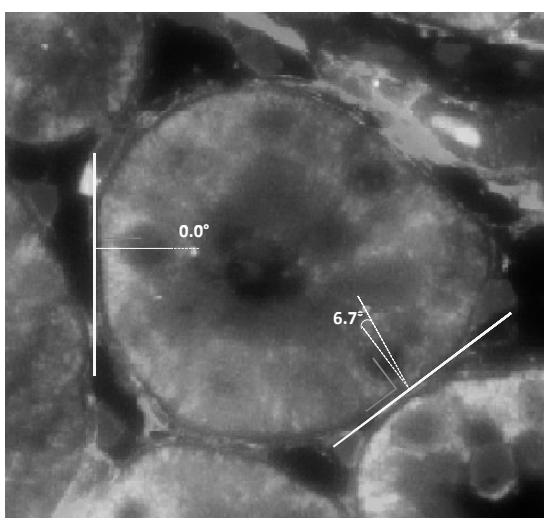
Supplemental figures



Supplementary Figure S1. Blood Urea concentrations of control+DCVC, cKO+DCVC and cKO-DCVC.



Supplementary Figure S2. Differential expression of planar cell polarity genes and canonical Wnt targets in *Pkd1*-deletion mice.
Heat map of (A) 3 PCP genes and of (B) 10 canonical Wnt targets showing differential expression at precystic stage (two months after gene disruption at PN40) compared to control mice. At this time-point 298 /34,000 genes (Illumina Sentrix BeadChips Mouse-6_v1_1) were identified to show differential expression after multiple test correction. Unsupervised hierarchical clustering showed that mice grouped into tamoxifen treated inducible *Pkd1*-deletion mice and untreated mice according to similarities in expression patterns. From these 298 genes, the PCP-genes and Wnt targets were selected and the same clustering had been applied. Red: increased expression, green: reduced expression.



Supplementary Figure S3. The position of the centrosome was determined by measuring the angle between a line through the centre of the nucleus perpendicular to the basement membrane and a line through the centrosome towards this point at the basement membrane. Collagen IV staining was used to indicate the basement membrane shown in red, nuclei are shown in blue and γ-tubulin staining for centrosomes in green. Autofluorescence is also detected in the same channel as γ-tubulin.

4

Morphometric analysis of centrosome position in tissues

Hester Happé[1,2], Emile de Heer[2] and Dorien J.M. Peters[1]

[1]Department of Human Genetics and, [2]Pathology, Leiden University Medical Center, 2300 RC Leiden, The Netherlands

Methods Mol Biol. 2012; 839:249-55.

Abstract

Planar cell polarity (PCP) is the polarization of cells within the plane of an epithelial cell layer. PCP is important in many tissues in different processes. In the kidney, it is hypothesized to be important in acquiring and maintaining correct tubular diameter. Aberrant PCP has been shown to be involved in polycystic kidney disease. Therefore, research in this field requires a method to study PCP. As PCP and outward-in signaling via the cilia are interconnected, the position of the centrosome, the base of the cilium can be used as a read-out system for PCP. Here, we provide a method in which the position of the centrosome is measured as read-out for PCP.

Introduction

Monolayers of epithelial cells exhibit, in addition to apical-basal polarity, also planar cell polarity. Planar cell polarity (PCP) is the coordinated polarization of cells in the plane of a tissue, thereby referring to asymmetries within the plane of the epithelial cell layer. PCP is required for many cellular processes. For example, it is thought to play an important role in acquiring and maintaining correct tubular morphology during renal development as well as during repair after epithelial injury. Aberrant PCP can cause cyst formation and is altered in polycystic kidney disease.[1-5]

PCP and (primary) cilia exert a mutual interaction in maintaining cellular functions.

The PCP pathway plays a role in regulating the position and orientation of cilia. However, when cilia orient to flow direction, orientation of cilia can also regulate PCP. Cilia consist of a microtubule-based axoneme covered by a specialized plasma membrane that extends from the cell surface into the extracellular space. The basal body/centrosome forms the base of the cilium. The position of the centrosome indicates the position of the cilium and deviation of the normal position in the apical membrane may indicate altered PCP.

Another frequently used read-out, to study aberrant PCP is a measurement of the orientation of the nuclear spindle, with the aim to measure alterations in oriented cell division. This analysis can only be done in proliferative tissue when many dividing cells are present, to obtain a sufficient number of measurable cells in anaphase.

Measuring centrosome position in tissues to indicate altered PCP was first described by Jonassen *et al*.[5] We modified the protocol to study centrosome localization in a model for polycystic kidney disease. We showed that at pre-cystic stages renal tubular epithelial cells display a significantly different distribution of centrosome position as compared to control mice.[4] In the majority of renal epithelial cells of control mice, centrosomes are positioned close to the center of the apical membrane. In mutants, however, a significantly different pattern was observed.

The following protocol describes the morphometric analysis of centrosome position in renal tubular epithelial cells in formalin-fixed paraffin-embed renal tissue sections that is applicable to nonproliferative tissue.

Materials

Immunofluorescence

1. Superfrost®Plus microscope slides.
2. Xylene
3. Ethanol, anhydrous denatured, histological grade (100% and 95% and 70%)
4. Deionized water (dH2O)
5. Buffer for heat-mediated antigen retrieval 10/1 mM TRIS/EDTA, pH 9.0.
   To prepare 1L add 1.21 g Trizma® base ($C_4H_{11}NO_3$) and 0.372 g EDTA ($C_{10}H_{14}N_2O_8Na_2 \bullet 2H_2O$) to 950 ml dH_2O. Adjust pH to 9.0, then adjust final volume to 1000 ml with dH2O. Store at 4°C.
6. Phosphate buffered saline (PBS)
   To prepare 1L 10X stock: add 80 g sodium chloride (NaCl), 2 g potassium chloride (KCl), 14.4 g sodium phosphate, dibasic (Na_2HPO_4), and 2.4 g potassium phosphate, monobasic (KH_2PO_4) to 1 L dH_2O. Adjust pH to 7.4. (adjust to pH 7.4 with HCl if necessary) Prepare working solution by dilution of one part with nine parts of water.
7. Antibody dilution buffer: 1% (w/v) bovine serum albumin (BSA) fraction V in PBS.
8. Normal goat serum (NGS).
9. Primary antibody: rabbit polyclonal anti-collagen IV IgG (Abcam)
10. Primary antibody: mouse monoclonal anti-g-tubulin IgG1 (clone GTU-88, Sigma-Aldrich)
11. Secondary antibody: goat-anti-rabbit IgG Alexa546 (Invitrogen)
12. Secondary antibody: goat-anti-mouse IgG1 Alexa 488 (Invitrogen)
13. Vectashield containing DAPI

Image acquisition and morphometric analysis

1. Immersion oil
2. Leica DM500B microscope with a Leica DM DFC 350 FX camera using Leica Application Suite 1.8.0
3. Image J software (public domain software, NIH, USA; http://rsb.info.nih.gov/ij/).

Methods

To measure the position of the centrosome, sections will be stained with γ-tubulin to indicate the centrosome, collagen IV to indicate the basement membrane, and DAPI for the nuclei. The position of the centrosome is measured by the angle defined by the line through the center of the nucleus perpendicular to the basement membrane and a line through the centrosome toward the intersection of the first line at the basement membrane. (*see* **Figure 1**)

Regarding PCP, localization of the centrosome can be affected in two directions. In renal tubules, centrosome position can be changed parallel to the longitudinal axis of the tubule or perpendicular to it. Therefore, only true longitudinal or transversal tubular cross sections should be measured. Otherwise, measurements will be the result of the vector of both directions. As deviations may occur only parallel to the longitudinal axis of the tubule or only perpendicular to it, one should chose to measure deviations only in one direction, or to keep measurements for the two directions separate. Pooling data of measurements in two directions could result in a loss of information. When deviations in the longitudinal direction are considered, it is important to keep track of the orientation of the tubules in such a way that for all pictures it is clear what is the proximal and what is the distal side.

Here, we only considered deviations in of centrosome position perpendicular to the tubular axis.

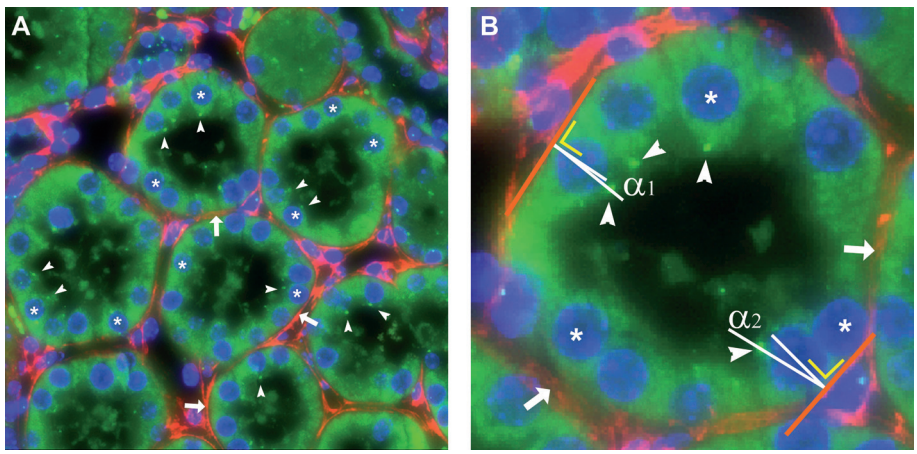


Figure 1. Measurement of centrosome position in renal tubular epithelial cells. Kidney cortex section stained for γ-tubulin (*green*), type IV collagen (*red*), and DAPI-stained nuclei (*blue*). Examples of centrosomes, nuclei, and basal membranes are indicated by arrowheads, asterisks and arrows respectively. (**A**) Image of renal tubules with adjusted color balance. (**B**) The position of the centrosome was determined by measuring the angle between a line through the centre of the nucleus perpendicular to the basement membrane and a line through the centrosome toward this point at the basement membrane. Collagen IV staining was used to visualize the basement membranes in red, nuclei are shown in blue and γ-tubulin staining for centrosomes in green. Autofluorescence is detected in the same channel as γ-tubulin. Centrosome angles are indicated by α_1 and α_2.

Immunofluorescence

Do not allow slides to dry at any time after step 1 during this procedure. Drying of the sections will result in high background staining. All incubation steps should be performed in incubation boxes with wetted (filter) paper on the bottom avoiding evaporation of the incubation liquid and drying of the sections. Ideally, glass slides should not directly lie on the wet paper.

1. Collect formalin-fixed paraffin-embedded kidney sections (4μm) on Superfrost®Plus glass slides and dry o/n at 37°C.
2. Deparaffination/Rehydration

a. Incubate sections in three washes of xylene for 5 minutes each.
b. Incubate sections in two washes of 100% ethanol for 5 minutes each.
c. Incubate sections in two washes of 95% ethanol for 5 minutes each.
d. Incubate sections in two washes of 70% ethanol for 5 minutes each.
e. Wash sections twice in dH2O for 5 minutes each.

3. Carefully boil slides for 10 min in 10/1 mM TRIS/EDTA using a microwave oven, and allow cooling down for 20 min (*see* **Note 1 and 2**)
4. Put circles around sections using DAKO-Pen to make sure the antibody solution stays on the section.
5. Preincubate with 50 μl 5% (v/v) NGS in antibody dilution buffer for 30 minutes at room temperature. (*see* **Note 3**)
6. Discard blocking solution by tapping the glass slide on a tissue and wipe off the rest of the liquid (of course do not touch the section itself)
7. Prepare a primary antibody mixture containing rabbit polyclonal anti-collagen IV IgG1 diluted 1:500 and mouse monoclonal anti-γ-tubulin IgG1 diluted 1:750 in antibody dilution buffer.
8. Incubate with 50 μl of the primary antibody mixture o/n at 4°C with. Discard primary antibody solution.
9. Rinse slides 3 times for 5 minutes with PBS.
10. Remove as much PBS from the glass slides as possible.
11. Prepare secondary antibody solution: antibody dilution buffer containing goat-anti-rabbit IgG Alexa546 (1:200) and goat-anti-mouse IgG1 Alexa 488 (1:200). (Keep in the dark)
12. Incubate sections with 50 μl of the secondary antibody solution for 1hr at room temperature. Keep the slides from now on away from light as much as possible to avoid loss of signal from the Alexa Dyes.
13. Wash 3x 5 min with PBS.
14. Remove as much of the PBS as possible with filter paper without touching the section and air dry the section for a few minutes.
15. Mount slides with Vectashield containing DAPI

Image acquisition and morphometric analysis

1. The slides are viewed using fluorescent microscopy. Excitation at 556 nm induces fluorescence of the Alexa 546 dye at 573 nm (orange emission) for the collagen IV, while excitation at 495 nm induces fluorescence of the Alexa 488 dye at 519 nm (green emission) for γ-tubulin, marker for centrosomes. Excitation at 345 nm induces DAPI fluorescence at 458 (blue emission) for nuclei.

2. Make Z-stacks, of 25–30 Z-images taken 0.24 mm apart, of the area in the section you are interested in using 63X oil-immersion lens with immersion oil. (*see* **Note 4 and 5**)
3. Take 25-35 different pictures of the area of interest, in order to measure appropriate numbers of centrosome angles.
4. Convert the Z-stack to a maximum projection.
5. Import images into Image J and adjust the color balance in order to make the centrosomes clearly visible. (Figure 1A shows an example of a maximum projection with adjusted color balance).
6. Enlarge the picture if needed.
7. Select the tool for measuring angles in Image J.
8. Measuring the angle between a line through the center of the nucleus perpendicular to the basement membrane and a line through the centrosome towards this point at the basement membrane. Collagen IV staining was used to indicate the basement membrane (*see* figure 1B).

   Crl+M will put your measurement in a results screen. You can save this results file and open it in Excel.

   In Image J you have to "drag and drop" these two lines, by clicking at three points in the picture immediately after one another, you cannot adjust one of the two lines afterward. To reduce the effect of natural occurring variance and measuring errors, many angles have to be measured, 200-300 angles per group (3 kidneys per group). It is also wise to do a blind analysis.
   Only measure centrosomes which you are sure that they belong to the same cell for which you are drawing a line through its nucleus. (*see* **Note 6**)

9. When analyzing measurements and performing statistics it is most clear and informative to look at the distribution pattern of the centrosome angles. Differences in distribution can be tested with the Kolomogorov–Smirnov Z-test.

Notes

1. The antigen retrieval (AR) method is dependent on the specific antibodies, double staining is only possible when both antibodies give sufficient result with the same antigen retrieval method. Only one type of AR can be applied. We have found these antibodies to both give good signal using TRIS/EDTA antigen retrieval.

2. First let buffer cook in microwave at high power, put slides in a rack in the buffer, and maintain and subboiling temperature in microwave oven (at lower power).
3. Using a volume of 50µl is usually enough to cover the section, use more when having large sections.
4. In order to get as much centrosomes in focus in one picture as possible, it is preferable to use a microscope that is able to make Z-stacks, followed by a maximum projection of this Z-stack. It is possible to use a microscope without this function, however, the amount of clearly visible centrosomes will be lower as they are small and not all in the same plane of focus.
5. We acquired images of areas within the inner cortex of the kidney, containing transversally sectioned proximal tubules. You can use the collagen IV staining as well as auto-fluorescence as a guide for the location in the kidney.
6. If you are measuring longitudinal cross sections of tubules, make sure you know what is proximal and what is distal and to assign a plus or minus sign to the direction of the angle. Image J will not do this, it measures absolute angles.

Acknowledgments
We thank A.M. van der Wal and F. Prins for technical assistance.

References

1. Fischer,E. *et al.* Defective planar cell polarity in polycystic kidney disease. *Nat. Genet.* **38**, 21-23 (2006).
2. Patel,V. *et al.* Acute kidney injury and aberrant planar cell polarity induce cyst formation in mice lacking renal cilia. *Hum. Mol. Genet.* **17**, 1578-1590 (2008).
3. Saburi,S. *et al.* Loss of Fat4 disrupts PCP signaling and oriented cell division and leads to cystic kidney disease. *Nat. Genet.* **40**, 1010-1015 (2008).
4. Happé,H. *et al.* Toxic tubular injury in kidneys from Pkd1-deletion mice accelerates cystogenesis accompanied by dysregulated planar cell polarity and canonical Wnt signaling pathways. *Hum. Mol. Genet.* **18**, 2532-2542 (2009).
5. Jonassen,J.A., San Agustin,J., Follit,J.A., & Pazour,G.J. Deletion of IFT20 in the mouse kidney causes misorientation of the mitotic spindle and cystic kidney disease. *J. Cell Biol.* **183**, 377-384 (2008).

5

Altered Hippo signaling in polycystic kidney disease

Hester Happé[1], Annemieke M. van der Wal[2], Wouter N. Leonhard[1], Steven J. Kunnen[1], Martijn H. Breuning[1], Emile de Heer[2] and Dorien J.M. Peters[1]

[1]Department of Human Genetics and, [2]Pathology, Leiden University Medical Center, 2300 RC Leiden, The Netherlands

J Pathol 2011; 224: 133-142.

Abstract

Autosomal Dominant Polycystic Kidney Disease (ADPKD) is characterized by progressive deterioration of renal function and formation of cysts, and is an important cause of end stage renal disease. Previously we showed that tubular epithelial injury accelerates cyst formation in inducible *Pkd1*-deletion mice. In these mice expression of the Planar Cell Polarity (PCP) component Four-jointed (*Fjx1*) is decreased during epithelial repair, while in control mice *Fjx1*-expression is increased and may be required during tissue regeneration. In cystic kidneys, however, *Fjx1* expression is also increased.

Besides a PCP component, Four-jointed is also implicated in the Hippo-signaling pathway. This pathway is involved in organ size control by regulating proliferation and apoptosis. The role of Hippo signaling, together with the opposing expression pattern of *Fjx1* during epithelial repair and at cystic stages, triggered us to investigate the activity of the Hippo pathway during these processes. Therefore, we examined its final effector molecule, the transcriptional co-activator Yes-associated protein (YAP) and observed that during tissue repair, YAP expression was not different between *Pkd1*-deletion mice and controls, i.e. during tissue regeneration YAP expression was increased and predominantly localized in the cytoplasm but normalized after tissue repair. At a later stage however, in cystic epithelia and epithelia of dilated tubules, strong nuclear YAP accumulation was observed, accompanied by up-regulation of the YAP transcriptional targets *Birc-3*, *Ctgf*, *InhbA* and *Fjx1*. Altered activity of the Hippo pathway was confirmed in renal tissues from human ADPKD and ARPKD patients, as well as in cystic renal tumors. Our data strengthen the concept that during epithelial repair Four-jointed is involved in PCP signaling, while in cystic kidneys it is related to Hippo-signaling and cyst growth.

Introduction

ADPKD is a systemic disease with cystogenesis as its major hallmark. Extra-renal manifestations are hypertension, cerebral aneurysms, and cysts in liver and pancreas.[1] In young adults only a few cysts can be detected ultrasonographically, whereas at middle age renal function declines and almost all normal renal parenchyma has been replaced by thousands of cysts and fibrotic tissue.
In most patients, ADPKD is caused by either a mutation in the *PKD1* gene, encoding the protein polycystin-1 (PC1), or a mutation in the *PKD2* gene, encoding polycystin-2 (PC2).[2-4] It is known that, in kidneys, the primary defect occurs in the epithelium and that a balanced expression level of these proteins is critical to maintain renal epithelial architecture. In renal epithelial cells deregulated *PKD1/2*-gene expression either by gene dose reduction, or by complete gene inactivation through somatic mutations, initiates cystogenesis.[5-7] Both PC1 and PC2 are expressed in several cellular compartments and form different multimeric protein complexes, in which they modulate several signaling pathways that in concert, control essential cellular functions such as proliferation, apoptosis, cell adhesion and differentiation.[8, 9] Disruption of any of these processes can lead to cyst formation, as demonstrated by a variety of mouse models.[10-14] Previously we generated an inducible *Pkd1*-deletion mouse model in which renal epithelial specific *Pkd1* deletion can be induced by the administration of tamoxifen. Recently we showed that tubular epithelial injury accelerates cyst formation in the adult induced *Pkd1*-deletion mice. This was not the result of uncontrolled cell proliferation, but probably due to altered integrity of the newly formed cells, rendering them more susceptible for cyst formation.[15] In that study we also showed that aberrant canonical Wnt and planar cell polarity (PCP) signaling as well are early changes after *Pkd1* deletion. During the repair phase of tubular epithelial injury, when PCP signaling is needed, renal mRNA expression of the PCP-pathway component Four-jointed (Fjx1), was increased in controls, but not in kidneys of the *Pkd1*-deletion mice. Here, the expression of *Fjx1* decreased after *Pkd1*-gene disruption and persisted at relatively low levels at pre-cystic stages. However, later on, in cystic kidneys *Fjx1* expression dramatically increased.
It has previously been shown that *Fjx1* is not only involved in PCP signaling but is also a regulator of the Hippo pathway, via a complex and currently not completely understood mechanism.[16] The Hippo pathway has extensively been studied in *Drosophila*, where it is involved in controlling cell proliferation and apoptosis.[17-19] In addition, an important role for the Hippo pathway has been suggested in the regulation of organ and tissue size control. Hippo pathway mutants show dramatic alterations in e.g. wing size.[17-20] The pathway is named after the core pathway component, the kinase Hippo. Via several phosphorylation steps eventually, the non-DNA binding transcriptional co-activator Yorkie (Yki) is phosphorylated and retained in the cytoplasm. This prevents Yki target genes from being transcribed. The core components of the *Drosophila* Hippo pathway are well conserved and also function as tumor suppressors in mammals in addition to regulating growth in terms of organ size control.[21]

The abovementioned functions of the Hippo pathway, and the increased expression of *Fjx1* in cystic kidneys, led us to hypothesize that altered Hippo signaling might also be involved in cyst growth. Therefore we studied the nuclear localization of the final effector molecule of the Hippo pathway, the Yki mammalian ortholog YAP, as well as expression of its down-stream target genes. We show that cysts display strong nuclear staining for YAP, while it is absent in pre-cystic tubules. We also show that the expression of a number of suspected mammalian YAP targets is up-regulated in cystic kidneys of *Pkd1*-mutant mouse models. During tissue-repair and at pre-cystic stages, however, Hippo-signaling was not differentially activated in *Pkd1*-mutants although *Fjx1* expression was reduced. In addition, we provide evidence that activation of the Hippo pathway is altered during cyst growth in human ADPKD and autosomal recessive polycystic kidney disease, ARPKD, as well as in cyst growth in renal cancer. Our data suggest a role for aberrant Hippo signaling as a mechanism for cyst growth in polycystic kidney disease.

Materials and Methods

Mice

The inducible conditional *Pkd1*-deletion (cKO) mice (tam-KspCad-CreERT2;*Pkd1*$^{del2\text{-}11/lox2\text{-}11}$) and tamoxifen treatment have been described previously. [22, 23] For the injury experiments, cKO mice with gene disruption at adult age (3 months) and controls were used. Renal tubular epithelial injury was induced using 15mg/kg 1,2-dichlorovinyl-cysteine (DCVC) i.p.[15] *Cre;Pkd1*$^{del2\text{-}11,lox}$ mice were treated with DCVC (cKO+DCVC) or vehicle (cKO-DCVC); as controls, *Pkd1*$^{del2\text{-}11,wt}$ and *Pkd1*$^{del2\text{-}11,lox}$ mice were treated with DCVC (control+DCVC).

In the PN40 series of cKO mice, the *Pkd1* gene was disrupted by tamoxifen administration at 3 consecutive days around day 40. Animals were sacrificed at 1, 2, 3 and 4 months upon tamoxifen treatment. Tissues were used for DNA- and mRNA-isolation or formalin-fixed for immunohistochemistry. Recombination efficiency was determined by eMLPA analysis according to Leonhard *et al.*[24]

The hypomorphic mouse model was described earlier by our group. [6] Mice were on a C57BL/6J genetic background. Control and cystic kidneys were isolated from 3-4 week old mice.

The local ethical animal experimental committee of the Leiden University Medical Center (LUMC) and the Commission Biotechnology in Animals of the Dutch Ministry of Agriculture approved the experiments performed.

Human Tissue Samples of Normal, Cystic Kidneys and Renal Tumors

Renal tissues from ADPKD patients with end stage renal failure and controls were fixed in 40mM phosphate buffered 4% formaldehyde at room temperature for at least 24 hours, dehydrated and paraffin embedded. Control tissues were isolated from donor kidneys intended for

transplantation, but found not suitable for technical reasons. In addition normal appearing areas in renal tissue from renal tumor patients were evaluated. In total 4 control samples, 5 ADPKD kidneys (4 with known mutations in, or positive linkage to, *PKD1*), 2 fetal ARPKD kidneys and 5 patients with renal cancer were analyzed. Two were diagnosed with clear cell renal cell carcinoma (CCRCC), 2 with papillary renal cell carcinoma (PRCC) and 1 with renal mixed epithelial stromal tumor (MEST).[25] All human tissue samples were obtained following procedures approved by the LUMC medical ethical committee (institutional review board).

Immunohistochemistry

Formalin-fixed, paraffin-embedded kidney sections (4 µm) were stained with rabbit-anti-YAP antibodies (#4912, Cell Signaling, Danvers, MA, USA). Segment marker staining was performed on sequential sections using rabbit polyclonal anti-megalin (Pathology LUMC, Leiden, the Netherlands[26]), goat polyclonal anti-Tamm-Horsfall protein (uromodulin, Organon Teknika-Cappel, Turnhout, Belgium), and rabbit polyclonal anti-aquaporin-2 (Calbiochem, Amsterdam, The Netherlands. rabbit envision HRP (Dako, Glostrup, Denmark) or rabbit-anti-goat HRP (Dako) were used as secondary antibodies. Immune reactions were revealed using diaminobenzidine and counterstained with hematoxylin. See supporting information for a more detailed protocol.

Quantification of nuclear YAP in cysts

The percentage of tubules and cysts displaying ≥50% and 25-50% YAP-positive nuclei was calculated in injury-induced cKO and control mice at 5 and 10 weeks after DCVC treatment. Therefore YAP-positive and negative nuclei in tubules and cysts in 3-4 random, non-overlapping fields in the renal cortex of each mouse were counted. The tubular diameter and percentage of YAP nuclei was determined of 10 randomly selected tubules and/or cysts in each field.

Nuclei with strong or apparent nuclear staining were considered positive. The average tubular diameter in control mice was set to 1. The relative tubular diameter (RTD) was calculated for all tubules were divided into 4 groups; tubule (T) with a relative tubular diameter <1.25; dilated tubule (DT), 1.25≤ RTD <1.75; small cysts or cyst (C), 1.75≤RTD<3.5; large cyst RTD ≥ 3.5.

mRNA expression analysis

Kidneys were snap frozen in liquid nitrogen upon isolation and stored at -80°C until further processing. Total RNA was isolated from renal tissue homogenates using TRI-Reagent (Sigma-Aldrich, St. Louis, MO, USA) according to the manufacturers' protocol. cDNA was synthesized with Superscript III (Invitrogen, Paisley, UK). Quantitative gene expression analysis of *Birc-3*, *Ctgf*, *InhbA* and *Yap* was performed on a Light Cycler 480 (Roche Applied Science, Penzberg, Germany) using 2x Sybr-Green master (ROX) (Roche Applied Science) according to manufacturers' protocol. Data were analyzed according to the Pfaffl-method, taking PCR efficiencies into account.[27] The median expression in control+DCVC at 2 wks after DCVC treatment or wild types in case of the

hypomorphic mouse model was set to 1 and expression was normalized to *Hprt* expression. Expression of *Fjx1* was determined as previously described. [15] The detailed protocol can be found in the supporting information.

Statistical analysis

Statistical comparisons between groups concerning the expression of YAP targets were performed using one-way ANOVA with Bonferroni post-testing for cKO mice and controls. For B6 *Pkd1*^{nl,nl} mice and controls, an unpaired t-test or an unpaired Welch's corrected t-test in case of unequal variance was used. P-values <0.05 were considered significant.

Results

YAP expression alters during tissue-repair and cyst growth

We previously showed that adult conditional *Pkd1*-deletion mice (cKO) develop cystic kidneys, upon treatment with the nephrotoxicant 1,2-dichlorovinyl-cysteine (DCVC) while heterozygous *Pkd1*$^{del/+}$-mice or vehicle treated mice do not.[15] Because of the biphasic differential expression pattern of *Fjx1* in this model we propose a role for disturbed Hippo signaling in cyst formation. To validate this hypothesis, YAP expression was analyzed in renal sections of mice sacrificed at 1, 2, 5 and 10 weeks after DCVC-induced injury.

One week after DCVC treatment, epithelial repair is in its final phase. At this stage, increased cytoplasmic YAP was observed in those parts of the proximal tubules the inner cortex, that were most severely damaged by the DCVC, in both cKO as well as controls treated with DCVC, compared with vehicle treated cKOs (fig. 1A-C). The kidney cortex of vehicle treated cKOs only shows nuclear and cytoplasmic staining of YAP in collecting ducts and distal tubules (fig. S1 A-D). Collecting ducts in the medulla also show nuclear staining of YAP.

Two weeks after injury, tissue repair is completed and also the increase in cytoplasmic YAP, observed during epithelial repair, is no longer present, showing no differences compared to non-injured renal tissue (fig. 1D). The same expression pattern was also observed at 5 weeks after injury. However, 10 weeks after injury, when kidneys of DCVC treated cKOs show many cysts of proximal tubular origin[15] (fig. S1 F), strong nuclear accumulation of YAP is observed in cystic tubular epithelial cells (fig. 1E and fig. S1 E). In contrast, nuclear accumulation of YAP is only weak or absent in proximal tubules of vehicle treated cKO (fig. 1F) or DCVC treated controls (fig. S1 A-D), which show no cysts (controls) or only mildly dilated tubules (vehicle treated cKO's).

mRNA expression analysis in cystic kidneys of injury-induced cKO animals 10 weeks after injury, as well as 3 week old *Pkd1*^{nl,nl} mice, did not show significant differences in *Yap* expression levels compared with controls (data not shown).

Nuclear YAP is absent in pre-cystic kidneys but accumulates in cystic epithelia of different *Pkd1*-mutant mouse models

Next we examined the YAP expression in several *Pkd1*-mutant mouse models. cKO mice, in which the *Pkd1* gene was deleted from the renal epithelial cells at approximately 40 days of age, develop polycystic kidneys within 4 months. At 3 months dilated tubules and the first cysts derived from proximal tubules are observed. 4 months after the gene deletion cysts derived from all nephron segments are presents but the largest cyst are of proximal tubular origin. In these mice nuclear YAP is virtually absent in proximal tubular epithelial cells at pre-cystic stages while distal tubules and collecting ducts show nuclear and cytoplasmic YAP (fig. 1G), similar to wild-type animals. However, in cystic epithelia, strong nuclear localization of YAP was observed, although also a minority of the cysts was negative for nuclear YAP (fig. 1H).

Another model, the *Pkd1*^{nl,nl} mice, have reduced levels of *Pkd1* in all cells and show massive cystic kidneys 3 weeks after birth. The majority of these cysts originate from distal tubules or collecting ducts.[6] Also in cystic kidneys of these mice, nuclear YAP is present in cyst-lining epithelia of cysts derived from all segments including proximal tubules, although not in all cysts (fig. 1J-L). Age-matched wild type mice (fig. 1I), show the same phenotype as control kidneys shown in fig. 1F and S1A.

Cystic epithelia in human renal ADPKD, ARPKD and tumor tissues also show nuclear YAP

To extend the observation made in mouse models to the pathology in patients, we stained renal tissues from ADPKD patients and control kidneys for YAP. In a substantial number of cysts, strong nuclear YAP accumulation was observed in the cyst-lining cells (fig. 1M), although cysts without nuclear YAP were present as well. Nuclear YAP was also seen in fibroblasts in fibrotic tissue in cystic ADPKD renal tissue (not shown). No nuclear YAP was present in proximal tubular epithelia of human renal control tissues, while distal tubules and collecting ducts do show some nuclear YAP expression (fig. S2).

Since nuclear translocation of YAP might be a more common mechanism in cyst formation, we also examined cystic kidneys from autosomal recessive polycystic kidney disease (ARPKD) patients, as well as cysts associated with different types of renal tumors.

Similar to renal cysts in ADPKD, cystic epithelia in ARPKD renal tissues also show prominent nuclear localization of YAP (fig. 1N). However, very large cysts with extremely flattened epithelia do not show nuclear YAP accumulation.

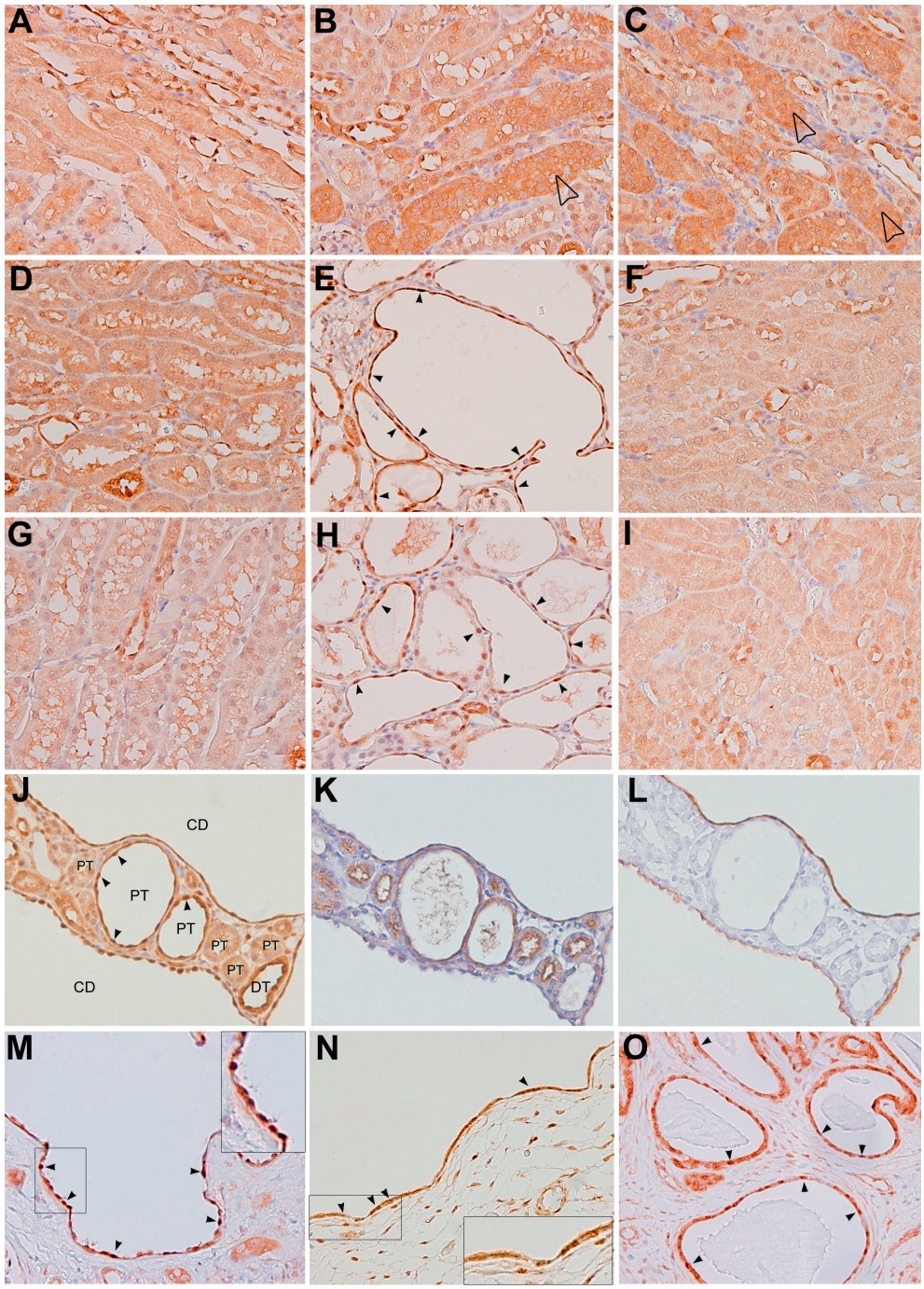
Furthermore, in cysts associated with CCRCC, PRCC and renal MEST, nuclear YAP was observed as well (fig. 1O and S1E-F). As in ADPKD renal tissue, nuclear YAP is also observed in fibroblasts in fibrotic tissue in ARPKD kidneys (fig. 1N) and renal tumors (not shown).

Staining of sequential sections with nephron segment markers, revealed that in ADPKD, ARPKD and renal tumor tissue most cysts already lost their marker. However, in both ADPKD and ARPKD, cysts, originating from distal tubules, collecting ducts, as well as proximal tubules (fig. S3A-D),

displaying nuclear YAP, are observed. CCRCC and PRCC are derived from proximal tubular epithelia while cysts in renal MEST originate from proximal tubular epithelia, distal tubule and loop of Henle (thin segment).[28-30]

In summary, robust nuclear accumulation of YAP is present in cystic epithelia derived from different segments of the nephron in various *Pkd1*-mutant mouse models, but not in pre-cystic and in control tissues. Accumulation of nuclear YAP was also observed in human ADPKD and ARPKD cystic epithelia, as well as in cysts associated with renal tumors, indicating that altered Hippo signaling is a common feature in cyst growth.

Figure 1: YAP expression in renal tissues. A-C shows YAP expression in inducible *Pkd1-deletion* mice (cKO) 1 week after DCVC treatment; (A) cKO–DCVC, (B) cKO+DCVC and (C) control+DCVC. D shows cKO+DCVC 2 weeks after DCVC treatment, E and F display respectively cKO+DCVC and cKO-DCVC 10 weeks after DCVC treatment. G and H show (G) non-cystic tubules and (H) cystic tubules in an inducible *Pkd1*-deletion mouse 3 months after gene disruption (at 40 days). I shows staining for YAP in 3 week old $Pkd1^{wt,wt}$ and J-L in $Pkd1^{nl,nl}$ mice. K and L stained for (I,J) YAP (K) megalin and (L) aquaporin 2. PT; proximal tubule as judged by anti-megalin staining, DT; distal tubule as judged by anti-Tamm Horsfall protein staining (not shown), CD; collecting duct as judged by anti-aquaporin 2 staining.
M, N and O show human renal tissue of (M) ADPKD, (N) ARPKD and (O) mixed epithelial and stromal renal tumor. Open arrowheads indicate increased cytoplasmic staining of YAP; closed arrowheads indicate examples of nuclear YAP staining. Original magnification 20x.


A
B
C
D
E
F
G
H
I
J
CD
PT
PT
PT
PT
PT
PT
CD
DT
K
L
M
N
O

Dilated tubules and cysts show increased numbers of nuclei with nuclear YAP

To confirm the findings observed with immunohistochemistry described above, nuclear staining of YAP was quantified in the injury-induced cKO mice at 5 and 10 weeks after nephrotoxic injury, as this model develops cysts predominantly from proximal tubular origin. The percentage of tubules, dilated tubules cysts and large cysts containing >50% and 25-50% of YAP positive nuclei was calculated. Tubules and cysts derived from distal tubules or collecting duct, as judged by the cytoplasmic YAP staining, were excluded from the analysis.

Table 1 shows that 70% of the cysts from kidneys at 10 weeks after injury show ≥50% YAP-positive nuclei where only 10% of the tubules in time-matched controls show ≥50% YAP- positive nuclei. The percentage of large cysts with ≥50% YAP-positive nuclei is lower than in cysts (i.e. 58%).

In addition, the analysis revealed that in dilated tubules and tubules in cystic kidneys, the number of YAP positive nuclei is already increased (60% and 65% respectively) compared to tubules in control kidneys. However, it must be noted that these tubules, although showing a normal tubular diameter, show aberrant morphology, including enlargement of the tubular lumen and disappearance of brush border. Tubules in pre-cystic, injury-induced kidneys do not show this marked increase in YAP positive nuclei.

In summary, in injury-induced cKO mice morphologic aberrant tubules, dilated tubules and cysts show increased percentages of YAP positive nuclei.

Table 1: Quantification of nuclear YAP in tubules and cysts of injury-induced cKO mice

Group	Time after DCVC	Type	n	% of tubules and cysts with	
				≥50% positive nuclei	≥25< 50% positive nuclei
control + DCVC (n=2)	5 weeks	T	46	0	2
		DT	1	0	0
cKO + DCVC (n=3)	5 weeks	T	41	2	10
		DT	37	14	8
		C	2	0	100
Control +DCVC (n=3)	10 weeks	T	68	10	12
		DT	3	33	33
cKO +DCVC (n=3)	10 weeks	T	34	65	27
		DT	55	60	45
		C	30	70	13
		LC	12	58	17

T; tubule, <1.25 times normal tubular diameter, DT; dilated tubule, ≥1.25 < 1.75 times normal tubular diameter, C;cyst, ≥1.75 < 2.5 times normal tubular diameter, LC; large cyst ≥2.5 times normal tubular diameter.

Up-regulation of transcriptional targets of YAP

YAP is a transcriptional co-activator which can drive the expression of target genes. A number of Yki target genes have been identified in *Drosophila*. In mammals however, the targets of YAP are barely known. We investigated the expression of several "suspected" YAP targets that were chosen according to homology with *Drosophila* Yki target genes, or because of previous reports. We analyzed the expression of baculoviral IAP repeat-containing-3 (*Birc-3;* also known as *cIAP-1* and *cIAP-2*), inhibin beta-A (*InhbA)* and connective tissue growth factor *(Ctgf)* in the injury-induced adult *Pkd1*-deletion mice and the hypomorphic *Pkd1*^{nl,nl} mice. *Birc-3* is the homologue of *dIAP1,* a well established Yki target. *Ctgf* and *InhbA* have been reported as YAP targets in mice.[31, 32] In cKOs, renal expression of YAP targets was not increased 2 weeks after injury (fig. 2A-C). Even more, *Birc-3* expression is lower in vehicle treated cKOs relative to DCVC treated controls (fig. 2A).

In contrast, *Birc-3* and *InhbA* show significant up-regulation only at cystic stages of injury-induced cKOs compared to DCVC treated controls and vehicle treated cKOs (fig. 2A). Expression of these genes is also markedly increased in cystic kidneys of 3-4 weeks old *Pkd1*^{nl,nl} mice, as well as *Ctgf* which is not increased in cystic kidneys of DCVC treated cKOs (fig. 2C-F).

Besides regulating the Hippo pathway, *Fjx1* is also thought to be a transcriptional target of YAP.[18, 33, 34] We previously reported increased expression of *Fjx1* in cystic kidneys of DCVC treated cKO mice.[15] Also cystic kidneys of *Pkd1* ^{nl,nl} mice show up-regulation of *Fjx1* (data not shown).

In summary, three or four out of four "suspected" transcriptional targets of YAP were up-regulated in cystic kidneys of injury-induced cKO mice or hypomorphic *Pkd1* mutant mice, respectively. Thereby further supporting *Birc-3*, *InhbA* and *Fjx1* as targets of YAP, but also indicating a more complex regulation of *Ctgf* expression.

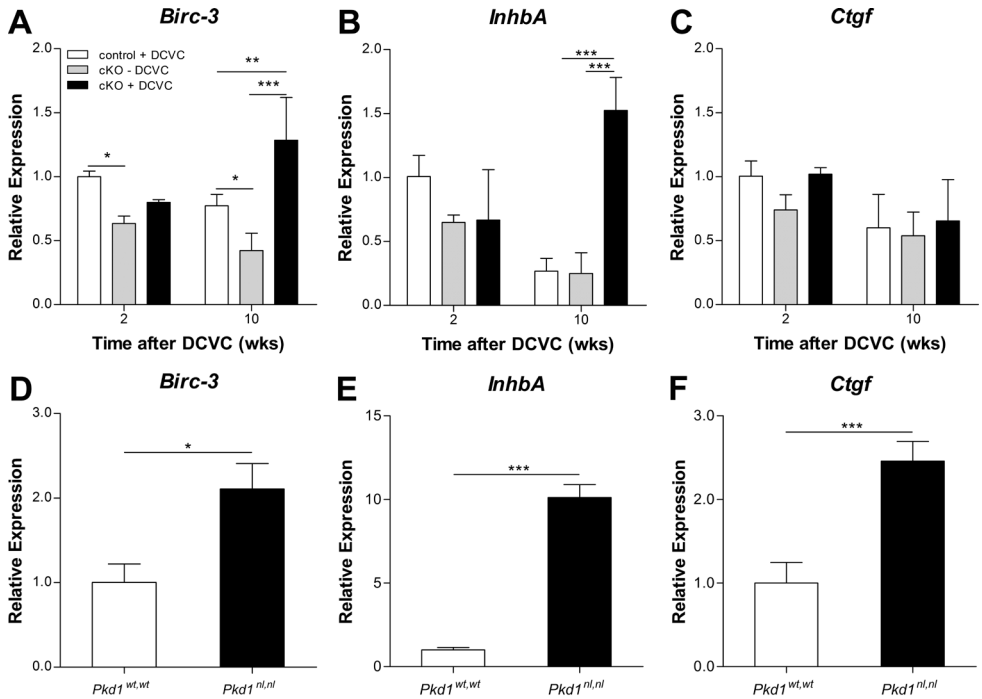


Figure 2: Relative expression of YAP targets in *Pkd1*-mutant mouse models. Expression of *Birc-3*, *InhbA* and *Ctgf* (A through C respectively) in controls treated with DCVC (white bars), and cKO animals treated with vehicle (grey bars) and with DCVC (black bars). Expression levels of controls+DCVC at 2 wks after injury have been set to 1. (D-F) Expression of the same genes in 3-4 weeks old $Pkd1^{nl,nl}$ mice and wild types; expression in wild types has been set to 1. * P< 0.05, **P<0.01, *** P<0.001

Discussion

The Hippo signaling pathway is emerging as an important pathway not only in organ size control but also in cancer. The product of the neurofibromatosis type II tumor suppressor gene (*NF2*), Merlin, is a regulator of the Hippo pathway. In addition, increased YAP expression and nuclear accumulation were shown in multiple types of human cancer. [35-38]

Here, we provide for the first time evidence for altered activation of the Hippo signaling pathway in cyst growth in ADPKD and other cystic diseases. In mouse models for ADPKD nuclear localization of YAP is only observed in cystic epithelia and dilated tubules but not in pre-cystic tubules. Nuclear YAP was detected in cysts derived from all segments. Although normal distal tubules and collecting ducts already show nuclear YAP, it is very likely that the Hippo pathway is also affected in cysts derived from collecting ducts and distal tubules, as $Pkd1^{nl,nl}$ cystic kidneys also show up-regulation of YAP targets.

Increased amounts of YAP-positive nuclei are observed in morphological aberrant tubules, dilated tubules and cysts but not in normal looking pre-cystic tubules. This suggests that aberrant Hippo signaling is not an initiating event in cyst formation but accompanies cyst growth.

Our findings, showing altered Hippo signaling during cyst growth, are in line with previous studies reporting renal cyst formation caused by disturbed Hippo signaling, e.g. deregulation of YAP in Zebrafish results in pro-nephric cyst formation. [39, 40] In addition, mice lacking TAZ (Wwtr1), the YAP ortholog, show renal cystic disease. [40-42] In one of the studies however, increased protein levels of polycystin-2 were reported as a result of TAZ deficiency. [40]

The Hippo pathway is also reported to be involved in the control of cell size. [43] Therefore, altered Hippo signaling may explain the observed hypertrophy of *Pkd1* knock-out cells, in addition to loss of control of the mTOR pathway. [44]

Together with Four-jointed, the PCP proteins Fat and Dachsous not only regulate PCP, but also regulate the Hippo pathway through a complex and not completely understood mechanism. *Fat4* knockout mice develop cystic kidneys and it has been postulated that disturbed PCP is the underlying defect.[13] However, its effect on the Hippo signaling pathway and YAP/TAZ translocation has not been addressed yet. It also remains to be investigated whether in our model increased expression of *Fjx1* in cystic kidneys is causing altered Hippo signaling or is the result of YAP driven transcription.

Nevertheless, our results further strengthen the concept that during epithelial repair Four-jointed is involved in PCP signaling while in cystic kidneys it is related to cyst growth. Decreased expression of *Fjx1* is a direct effect of *Pkd1* inactivation while increased *Fjx1* and YAP target expression can be regarded as an effect of altered signaling during cyst growth, an indirect effect of *Pkd1* inactivation.

Although both under and over-expression of YAP as well as TAZ deficiency, can result in cyst formation, in renal cystic disease it seems to be associated with an increase in nuclear YAP as shown in the different mouse models for ADPKD. This is confirmed by the results in patients with ADPKD and ARPKD, demonstrating nuclear localization of YAP in epithelia in the majority of cysts. This slightly heterogeneous pattern, also observed for a variety of signal transduction components, may be explained by the fact that cystic epithelial cells show bursts in proliferation. [23, 45, 46]

In this study we showed that several postulated targets of YAP are up-regulated in cystic kidneys, which is in agreement with nuclear localization of YAP in cystic epithelia. *Ctgf,* however, is up-regulated in cystic kidneys of hypomorphic *Pkd1* mutant mice which show first signs of fibrosis[47], while cystic kidneys of injury-induced cKO mice show no differential *Ctgf* expression. These data suggest that regulation of *Ctgf* expression is complex.

Transcriptional regulation by YAP is complex; nuclear translocation of YAP can differentially affect transcriptional regulation, depending on cellular context. For example, YAP mostly inhibits apoptosis whereas the YAP-p73 complex shows pro-apoptotic activity. [48] Furthermore, emerging

evidence shows that the availability of transcription factors that can bind to the co-activator YAP/Yki is dependent on tissue, cell type and probably cellular context. [21, 49] Interestingly, YAP/TAZ are transcriptional co-activators for a variety of transcription factors, e.g. TEAD, Glis3, SMAD, ErbB4-CTF, p73, Runx2, many of them implicated in polycystic kidney disease. [17, 21, 50-52] Also modulation of canonical Wnt-signaling, one of the signaling cascades altered in cystic epithelia, by Hippo signaling has been reported recently. [15, 50, 53, 54] By binding Dishevelled, cytoplasmic TAZ inhibits canonical Wnt signaling, while increased nuclear accumulation of TAZ results in increased nuclear β-catenin accumulation and induction of Wnt-target gene expression.[54]

Further research, to gain insight in the binding partners of YAP in different cell types and contexts, is required.

Increased nuclear YAP is not only observed in cystic epithelia in ADPKD, ARPKD but also cystic epithelia in different renal tumors. In these tumors, cystic epithelial expression of nuclear YAP is independent of the VHL status of the tumor. We also observed nuclear YAP in liver cysts derived from bile ducts of hypomorphic *Pkd1* mutant mice (not shown). Therefore, it is tempting to speculate that altered Hippo signaling is a general feature in cystogenesis.

Polycystic kidneys were elegantly called "neoplasia in disguise". [55] Indeed many pathways involved in neoplastic growth are also involved in cyst formation. It is not surprising that a number of drugs developed for the treatment of cancer have shown to be effective in attenuating cyst growth in PKD-mouse models. [56-60] Since altered Hippo signaling plays a role in tumorigenesis, the search for inhibitors of this pathway for cancer treatment can be beneficial for the hunt in the much needed treatment for polycystic kidney disease. [61] The critical role for TAZ/YAP in integrating and modulating signals from different morphogen signaling pathways, including Wnt-, Notch- and TGF-β-signaling further supports the idea that targeting the Hippo pathway could be effective in inhibiting cyst expansion and slowing down progression towards end-stage renal failure in PKD. [47, 53, 54] An interesting future experiment will be to explore whether *in vivo* absence of YAP during cyst growth, indeed, will attenuate cyst expansion.

Acknowledgements

The authors thank Helen McNeill (Toronto) for suggestions. This research was supported by grants from the Dutch Kidney Foundation (NSN C05-2132) and the Polycystic Kidney Disease Research Foundation (175G08a).

Author contributions statement

HH conceived and carried out experiments, analyzed and interpreted data, and generated figures. WNL carried out and analyzed experiments. AMvdW and SJK carried out experiments. HH, EH DJMP and MHB were involved in study design and data interpretation. HH, EH and DJMP were involved in writing the manuscript. All authors had final approval of the submitted manuscript.

References

1. Gabow,P.A. Autosomal dominant polycystic kidney disease--more than a renal disease. *Am. J. Kidney Dis.* **16**, 403-413 (1990).
2. Peters,D.J. & Sandkuijl,L.A. Genetic heterogeneity of polycystic kidney disease in Europe. *Contrib. Nephrol.* **97**, 128-139 (1992).
3. The European Polycystic Kidney Disease Consortium. The polycystic kidney disease 1 gene encodes a 14 kb transcript and lies within a duplicated region on chromosome 16. *Cell* **77**, 881-894 (1994).
4. Mochizuki,T. *et al.* PKD2, a gene for polycystic kidney disease that encodes an integral membrane protein. *Science* **272**, 1339-1342 (1996).
5. Qian,F., Watnick,T.J., Onuchic,L.F., & Germino,G.G. The molecular basis of focal cyst formation in human autosomal dominant polycystic kidney disease type I. *Cell* **87**, 979-987 (1996).
6. Lantinga-van Leeuwen,I.S. *et al.* Lowering of Pkd1 expression is sufficient to cause polycystic kidney disease. *Hum. Mol. Genet.* **13**, 3069-3077 (2004).
7. Torra,R. *et al.* A loss-of-function model for cystogenesis in human autosomal dominant polycystic kidney disease type 2. *Am. J. Hum. Genet.* **65**, 345-352 (1999).
8. Wilson,P.D. Polycystic kidney disease. *N. Engl. J. Med.* **350**, 151-164 (2004).
9. Nauli,S.M. *et al.* Polycystins 1 and 2 mediate mechanosensation in the primary cilium of kidney cells. *Nat. Genet.* **33**, 129-137 (2003).
10. Sorenson,C.M., Padanilam,B.J., & Hammerman,M.R. Abnormal postpartum renal development and cystogenesis in the bcl-2 (-/-) mouse. *Am. J. Physiol* **271**, F184-F193 (1996).
11. Trudel,M., D'Agati,V., & Costantini,F. C-myc as an inducer of polycystic kidney disease in transgenic mice. *Kidney Int.* **39**, 665-671 (1991).
12. Saadi-Kheddouci,S. *et al.* Early development of polycystic kidney disease in transgenic mice expressing an activated mutant of the beta-catenin gene. *Oncogene* **20**, 5972-5981 (2001).
13. Saburi,S. *et al.* Loss of Fat4 disrupts PCP signaling and oriented cell division and leads to cystic kidney disease. *Nat. Genet.* **40**, 1010-1015 (2008).
14. Shannon,M.B., Patton,B.L., Harvey,S.J., & Miner,J.H. A Hypomorphic Mutation in the Mouse Laminin α5 Gene Causes Polycystic Kidney Disease. *J. Am. Soc. Nephrol.* **17**, 1913-1922 (2006).
15. Happé,H. *et al.* Toxic tubular injury in kidneys from Pkd1-deletion mice accelerates cystogenesis accompanied by dysregulated planar cell polarity and canonical Wnt signaling pathways. *Hum. Mol. Genet.* **18**, 2532-2542 (2009).
16. Willecke,M., Hamaratoglu,F., Sansores-Garcia,L., Tao,C., & Halder,G. Boundaries of Dachsous Cadherin activity modulate the Hippo signaling pathway to induce cell proliferation. *Proc. Natl. Acad. Sci. U. S. A* **105**, 14897-14902 (2008).
17. Edgar,B.A. From cell structure to transcription: Hippo forges a new path. *Cell* **124**, 267-273 (2006).
18. Harvey,K. & Tapon,N. The Salvador-Warts-Hippo pathway - an emerging tumour-suppressor network. *Nat. Rev. Cancer* **7**, 182-191 (2007).
19. Pan,D. Hippo signaling in organ size control. *Genes Dev.* **21**, 886-897 (2007).
20. Reddy,B.V. & Irvine,K.D. The Fat and Warts signaling pathways: new insights into their regulation, mechanism and conservation. *Development* **135**, 2827-2838 (2008).
21. Badouel,C., Garg,A., & McNeill,H. Herding Hippos: regulating growth in flies and man. *Curr. Opin. Cell Biol.* **21**, 837-843 (2009).
22. Lantinga-van Leeuwen,I.S. *et al.* Transgenic mice expressing tamoxifen-inducible Cre for somatic gene modification in renal epithelial cells. *Genesis.* **44**, 225-232 (2006).
23. Lantinga-van Leeuwen,I.S. *et al.* Kidney-specific inactivation of the Pkd1 gene induces rapid cyst formation in developing kidneys and a slow onset of disease in adult mice. *Hum. Mol. Genet.* **16**, 3188-3196 (2007).
24. Leonhard,W.N., Roelfsema,J.H., Lantinga-van Leeuwen,I.S., Breuning,M.H., & Peters,D.J. Quantification of Cre-mediated recombination by a novel strategy reveals a stable extra-chromosomal deletion-circle in mice. *BMC. Biotechnol.* **8**, 18 (2008).
25. Zhou,M. *et al.* Adult cystic nephroma and mixed epithelial and stromal tumor of the kidney are the same disease entity: molecular and histologic evidence. *Am. J. Surg. Pathol.* **33**, 72-80 (2009).

26. Christensen,E.I. *et al.* Segmental distribution of the endocytosis receptor gp330 in renal proximal tubules. *Eur. J. Cell Biol.* **66**, 349-364 (1995).
27. Pfaffl,M.W. A new mathematical model for relative quantification in real-time RT-PCR. *Nucleic Acids Res.* **29**, e45 (2001).
28. Pisters,L.L., el-Naggar,A.K., Luo,W., Malpica,A., & Lin,S.H. C-met proto-oncogene expression in benign and malignant human renal tissues. *J. Urol.* **158**, 724-728 (1997).
29. Nagashima,Y. *et al.* Von Hippel-Lindau tumour suppressor gene. Localization of expression by in situ hybridization. *J. Pathol.* **180**, 271-274 (1996).
30. Picken,M.M. & Fresco,R. Mixed epithelial and stromal tumor of the kidney: preliminary immunohistochemical and electron microscopic studies of the epithelial component. *Ultrastruct. Pathol.* **29**, 283-286 (2005).
31. Zhao,B. *et al.* TEAD mediates YAP-dependent gene induction and growth control. *Genes Dev.* **22**, 1962-1971 (2008).
32. Zhang,J., Smolen,G.A., & Haber,D.A. Negative regulation of YAP by LATS1 underscores evolutionary conservation of the Drosophila Hippo pathway. *Cancer Res.* **68**, 2789-2794 (2008).
33. Cho,E. *et al.* Delineation of a Fat tumor suppressor pathway. *Nat. Genet.* **38**, 1142-1150 (2006).
34. Willecke,M. *et al.* The fat cadherin acts through the hippo tumor-suppressor pathway to regulate tissue size. *Curr. Biol.* **16**, 2090-2100 (2006).
35. Zender,L. *et al.* Identification and validation of oncogenes in liver cancer using an integrative oncogenomic approach. *Cell* **125**, 1253-1267 (2006).
36. Dong,J. *et al.* Elucidation of a universal size-control mechanism in Drosophila and mammals. *Cell* **130**, 1120-1133 (2007).
37. Steinhardt,A.A. *et al.* Expression of Yes-associated protein in common solid tumors. *Hum. Pathol.* **39**, 1582-1589 (2008).
38. Hao,Y., Chun,A., Cheung,K., Rashidi,B., & Yang,X. Tumor suppressor LATS1 is a negative regulator of oncogene YAP. *J. Biol. Chem.* **283**, 5496-5509 (2008).
39. Skouloudaki,K. *et al.* Scribble participates in Hippo signaling and is required for normal zebrafish pronephros development. *Proc. Natl. Acad. Sci. U. S. A* **106**, 8579-8584 (2009).
40. Tian,Y. *et al.* TAZ promotes PC2 degradation through a SCFbeta-Trcp E3 ligase complex. *Mol. Cell Biol.* **27**, 6383-6395 (2007).
41. Hossain,Z. *et al.* Glomerulocystic kidney disease in mice with a targeted inactivation of Wwtr1. *Proc. Natl. Acad. Sci. U. S. A* **104**, 1631-1636 (2007).
42. Makita,R. *et al.* Multiple renal cysts, urinary concentration defects, and pulmonary emphysematous changes in mice lacking TAZ. *Am. J. Physiol Renal Physiol* **294**, F542-F553 (2008).
43. Matsui,Y. *et al.* Lats2 is a negative regulator of myocyte size in the heart. *Circ. Res.* **103**, 1309-1318 (2008).
44. Distefano,G. *et al.* Polycystin-1 regulates extracellular signal-regulated kinase-dependent phosphorylation of tuberin to control cell size through mTOR and its downstream effectors S6K and 4EBP1. *Mol. Cell Biol.* **29**, 2359-2371 (2009).
45. Piontek,K., Menezes,L.F., Garcia-Gonzalez,M.A., Huso,D.L., & Germino,G.G. A critical developmental switch defines the kinetics of kidney cyst formation after loss of Pkd1. *Nat. Med.* **13**, 1490-1495 (2007).
46. Takakura,A., Contrino,L., Beck,A.W., & Zhou,J. Pkd1 inactivation induced in adulthood produces focal cystic disease. *J. Am. Soc. Nephrol.* **19**, 2351-2363 (2008).
47. Hassane,S. *et al.* Elevated TGFbeta-Smad signalling in experimental Pkd1 models and human patients with polycystic kidney disease. *J. Pathol.* **222**, 21-31 (2010).
48. Lapi,E. *et al.* PML, YAP, and p73 are components of a proapoptotic autoregulatory feedback loop. *Mol. Cell* **32**, 803-814 (2008).
49. Peng,H.W., Slattery,M., & Mann,R.S. Transcription factor choice in the Hippo signaling pathway: homothorax and yorkie regulation of the microRNA bantam in the progenitor domain of the Drosophila eye imaginal disc. *Genes Dev.* **23**, 2307-2319 (2009).
50. Song,X. *et al.* Systems biology of autosomal dominant polycystic kidney disease (ADPKD): computational identification of gene expression pathways and integrated regulatory networks. *Hum. Mol. Genet.* **18**, 2328-2343 (2009).
51. Kang,H.S., Beak,J.Y., Kim,Y.S., Herbert,R., & Jetten,A.M. Glis3 is associated with primary cilia and Wwtr1/TAZ and implicated in polycystic kidney disease. *Mol. Cell Biol.* **29**, 2556-2569 (2009).

52. Komuro,A., Nagai,M., Navin,N.E., & Sudol,M. WW domain-containing protein YAP associates with ErbB-4 and acts as a co-transcriptional activator for the carboxyl-terminal fragment of ErbB-4 that translocates to the nucleus. *J. Biol. Chem.* **278**, 33334-33341 (2003).
53. Lal,M. *et al.* Polycystin-1 C-terminal tail associates with beta-catenin and inhibits canonical Wnt signaling. *Hum. Mol. Genet.* **17**, 3105-3117 (2008).
54. Varelas,X. *et al.* The Hippo pathway regulates Wnt/beta-catenin signaling. *Dev. Cell* **18**, 579-591 (2010).
55. Grantham,J.J. Polycystic kidney disease: neoplasia in disguise. *Am. J. Kidney Dis.* **15**, 110-116 (1990).
56. Wilson,S.J. *et al.* Inhibition of HER-2(neu/ErbB2) restores normal function and structure to polycystic kidney disease (PKD) epithelia. *Biochim. Biophys. Acta* **1762**, 647-655 (2006).
57. Sweeney,W.E., Jr., von Vigier,R.O., Frost,P., & Avner,E.D. Src inhibition ameliorates polycystic kidney disease. *J. Am. Soc. Nephrol.* **19**, 1331-1341 (2008).
58. Bukanov,N.O., Smith,L.A., Klinger,K.W., Ledbetter,S.R., & Ibraghimov-Beskrovnaya,O. Long-lasting arrest of murine polycystic kidney disease with CDK inhibitor roscovitine. *Nature* **444**, 949-952 (2006).
59. Park,J.Y. *et al.* p21 is decreased in polycystic kidney disease and leads to increased epithelial cell cycle progression: roscovitine augments p21 levels. *BMC. Nephrol.* **8**, 12 (2007).
60. Omori,S. *et al.* Extracellular signal-regulated kinase inhibition slows disease progression in mice with polycystic kidney disease. *J. Am. Soc. Nephrol.* **17**, 1604-1614 (2006).
61. Zhao,B., Li,L., Lei,Q., & Guan,K.L. The Hippo-YAP pathway in organ size control and tumorigenesis: an updated version. *Genes Dev.* **24**, 862-874 (2010).

Supplemental figures

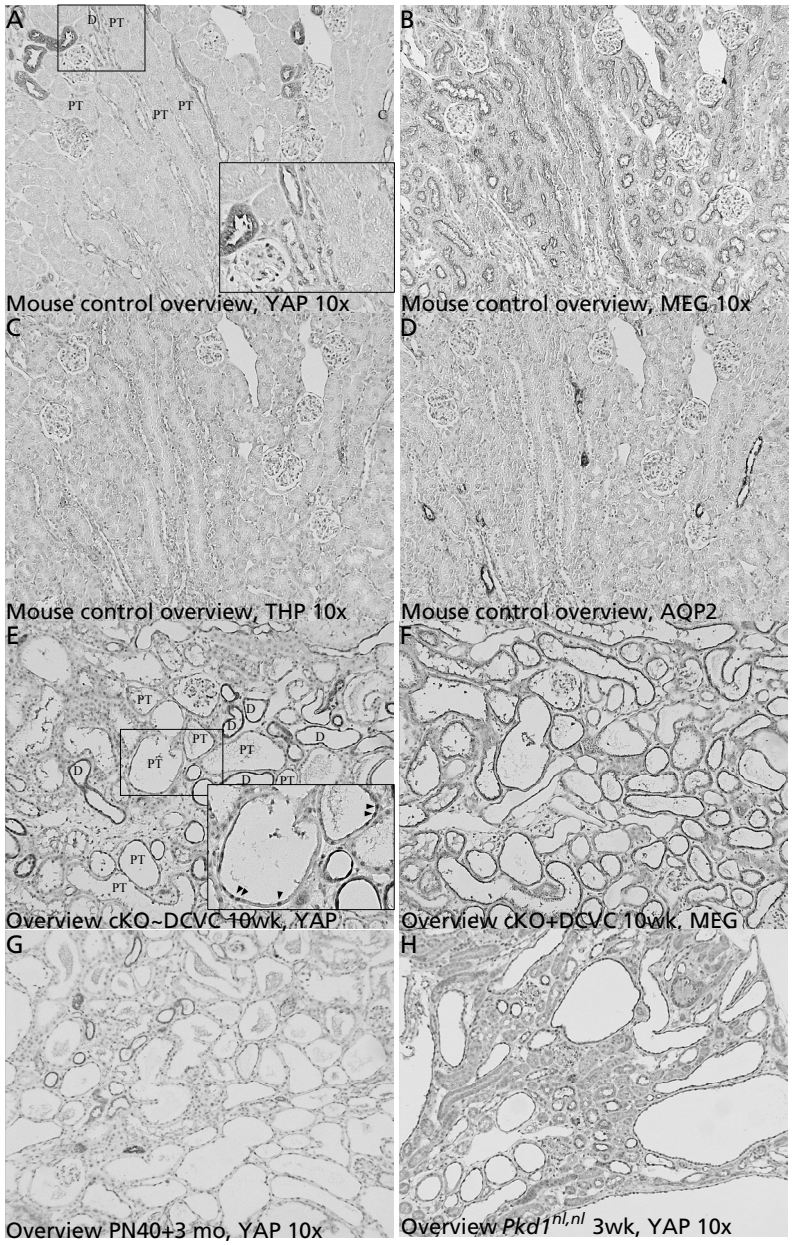


Figure S1: Overview of mouse renal tissues. A-D show control+ DCVC mice 10 weeks after DCVC treatment stained for; (A) YAP, (B) megalin, (C) Tamm-Horsfall protein and (D) aquaporin 2. E and F display an cKO+DCVC 10 weeks after DCVC treatment stained for (E) YAP and (F) megalin. G shows *Pkd1*-deletion mice 3 months after gene disruption at 40 days, stained for YAP, H shows 3 week old *Pkd1* ^{nl,nl} mice, stained for YAP.

PT; proximal tubule as judged by anti-megalin staining, DT; distal tubule as judged by anti-Tamm Horsfall protein staining, CD; collecting duct as judged by anti-aquaporin 2 staining. MEG; megalin, THP; Tamm-Horsfall protein, AQP2; aquaporin 2. Arrowheads show examples of nuclear staining.

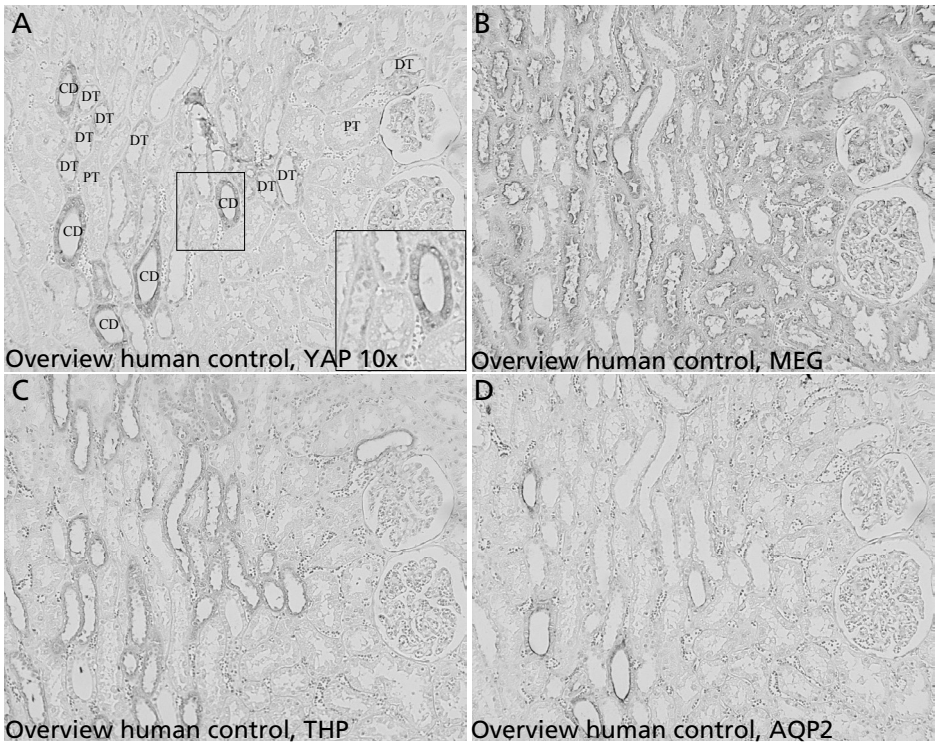


Figure S2: Overview of human renal control tissues. Normal renal tissue; area without irregularities obtained from patient with renal mixed epithelial and stromal tumor, stained for; (A) YAP, (B) megalin and (C) Tamm-Horsfall protein and (D) aquaporin 2. MEG; megalin, THP; Tamm-Horsfall protein, AQP2; aquaporin 2. PT; proximal tubule as judged by anti-megalin staining, DT; distal tubule as judged by anti-Tamm Horsfall protein staining, CD; collecting duct as judged by anti-aquaporin 2 staining.

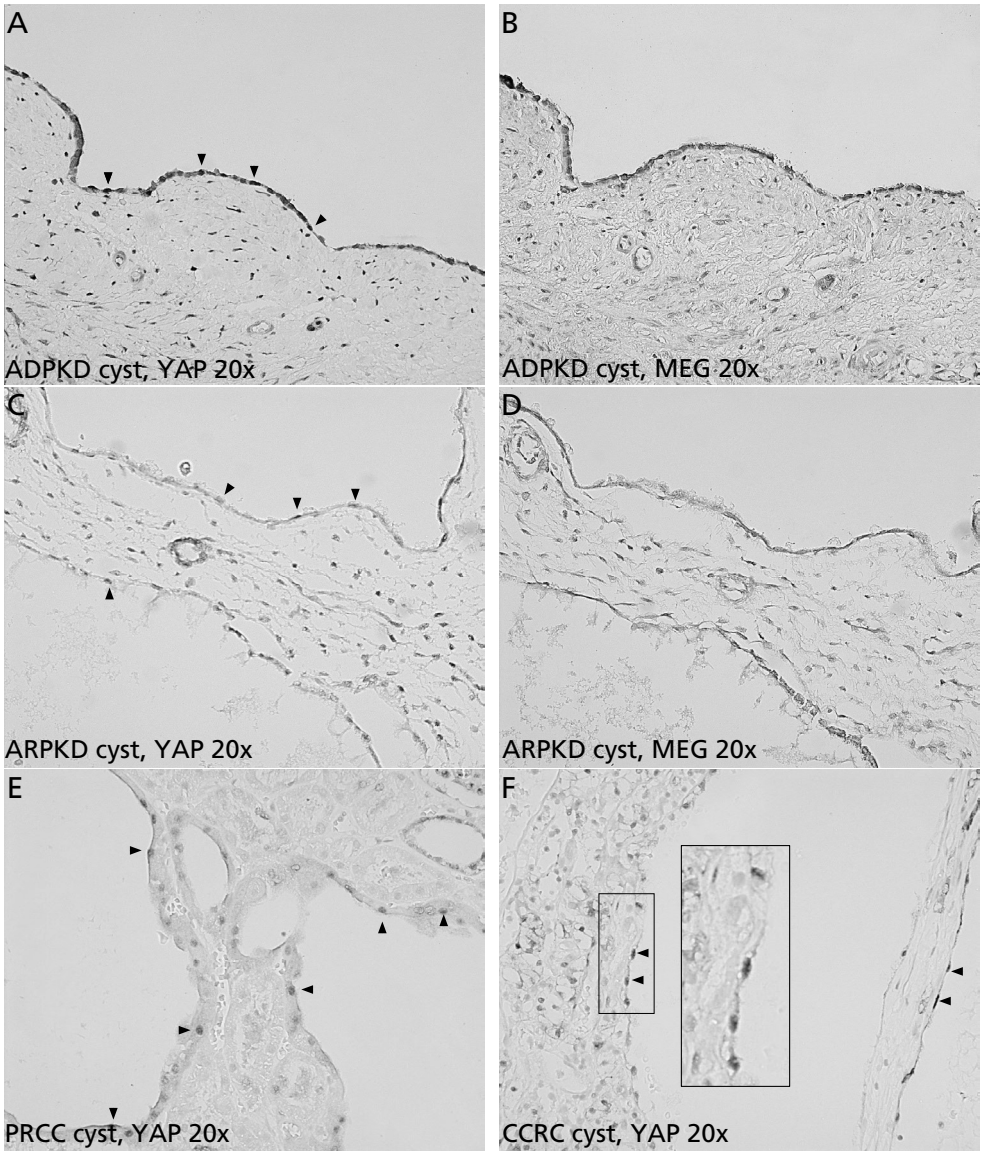


Figure S3: Cysts in human renal tissues. A and B show a cyst in ADPKD renal tissue sequentially stained for (A) YAP and (B) megalin. C and D show a cyst in ARPKD renal tissue sequentially stained for (C) YAP and (D) megalin. E and F show a cyst stained for YAP in a (E) papillary renal cell carcinoma (PRCC) and a (F) clear cell renal cell carcinoma (CCRCC) respectively. MEG; megalin, THP; Tamm-Horsfall protein, AQP2; aquaporin 2. Arrowheads show examples of nuclear staining.

Supplemental Information

mRNA expression analysis

Kidneys were snap frozen in liquid nitrogen upon isolation and stored at -80°C until further processing. Renal tissues were homogenized in PBS containing 1% 2-mercapto-ethanol using a MagNa Lyser Instrument (Roche). Total RNA was isolated from renal tissue homogenates using TRI-Reagent (Sigma-Aldrich) according to the manufacturers' protocol. cDNA was synthesized with Superscript III (Invitrogen). Quantitative gene expression analysis of *Birc-3*, *Ctgf*, *InhbA* and *Yap* was performed on a Light Cycler 480 (Roche Applied Science) using 2x Sybr-Green master (ROX) (Roche Applied Science) according to manufacturers' protocol. Primer sequences are given in table S1. *Hprt* was used as a housekeeping gene. Data were analyzed according to the Pfaffl-method, taking PCR efficiencies into account (Pfaffl,M.W. *Nucleic Acids Res.* **29**, e45 (2001). Expression was calculated relative to the median of control+DCVC at 2 wks after DCVC treatment or wild types in case of the hypomorphic

mouse model, and normalized to *Hprt* expression. Expression of *Fjx1* was determined as previously described (H.Happé *et.al. Hum. Mol. Genet.* **18**, 2532-2542 (2009).

Table S1: Primer sequences for real-time PCR

Gene	Accession	Primer sequence	
Birc-3	NM_007464.3	Fw	agagaggagcagatggagca
		Rv	tttgttcttccggattagtgc
Ctgf	NM_010217.2	Fw	ctgcagactggagaagcaga
		Rv	gatgcacttttgccccttctt
InhbA	NM_008380.1	Fw	tgcagacatgctgtggatct
		Rv	cttaactgtgagccagcaagc
Yap	NM_009534.2	Fw	ttccgatccctttcttaacagt
		Rv	gagggatgctgtagctgctc

Immunohistochemistry

Formalin-fixed, paraffin-embedded kidney sections (4 µm) were used. For YAP staining sections subjected to heat-mediated antigen retrieval procedure (10 mM citrate buffer, pH 6.0). After blocking of endogenous peroxidase activity for 20 min in 0.1% H_2O_2 in water, sections were pre- incubated for 1 hour with 5% normal goat serum. Subsequently sections were incubated over night with rabbit-anti-YAP (#4912, Cell Signaling) diluted 1:50 in 1% BSA in PBS. Segment marker staining was performed on sequential sections of injury-induced cKO and control mice at 10 weeks, of 3 weeks old *Pkd1*^{nl,nl} and wild type mice, and on human renal ADPKD, ARPKD and tumor tissues. To this end rabbit polyclonal anti-megalin (1:500 1h at room temperature, Pathology LUMC, Leiden, the Netherlands (Christensen, E.I. *et al. Eur. J. Cell Biol.* **66**, 349-364 (1995)), goat polyclonal anti-Tamm Horsfall protein (uromodulin, 1:500 1h at room temperature,

Organon Teknika-Cappel, Turnhout, Belgium), and rabbit polyclonal anti-aquaporin-2 (1:4000 o/n at 4°C, Calbiochem, Amsterdam, The Netherlands) diluted in 1% BSA in PBS were used, after to blocking of endogenous peroxidase activity.

Following incubation with rabbit envision HRP (Dako) or rabbit-anti-goat HRP (1:300 Dako), immune reactions were revealed using diaminobenzidine as a chromogen (DAB or Liquid DAB+ substrate chromogen system, DAKO) and counterstained with hematoxylin, dehydrated and mounted.

6

Cyst expansion and regression in a mouse model for polycystic kidney disease

Hester Happé MSc[1], Annemieke M. van der Wal BSc†[2], Daniela C.F. Salvatori PhD[3,4], Wouter N. Leonhard BSc [1], Martijn H. Breuning MD, PhD[5], Emile de Heer PhD[2] and Dorien J.M. Peters PhD[1]

[1]Department of Human Genetics, [2]Department of Pathology, [3]Department of Anatomy and Embryology, [4]Central Animal Facility and [5]Department of Clinical Genetics, Leiden University Medical Center, 2300 RC Leiden, The Netherlands

Kidney International, under revision

Abstract

Autosomal dominant polycystic kidney disease is characterized by progressive cyst formation and fibrosis in the kidneys.

Here we present the orthologous *Pkd1*^{nl,nl} mouse model, with reduced expression of the normal *Pkd1* transcript, on a specific genetic background, i.e. fixed 50%/50% genetic background of C57Bl/6 and 129Ola/Hsd (*B6Ola-Pkd1*^{nl,nl}). In *B6Ola-Pkd1*^{nl,nl} mice, the first cysts developed from mature proximal tubules around birth. Subsequently, larger cysts were visible at day 7, followed by distal tubule and collecting duct cyst formation and progressive cystic enlargement. These mice developed large cystic kidneys within 4 weeks. Interestingly, cyst expansion was followed by renal volume regression due to collapse of cysts. This was accompanied by focal formation of fibrotic areas, increased expression of genes involved in matrix remodeling and subsequently an increase in infiltrating immune cells. Renal function, however, remained stable over time, after an initial increase in blood urea within the first 4 weeks. Mice were able to survive up to a year. Also in kidneys of ADPKD patients collapsed cysts were observed, in addition to massive fibrosis and immune infiltrates.

B6Ola-Pkd1^{nl,nl} mice show regression of cysts and renal volume but no reduction in blood urea levels, implying that renal volume may not be the best predictor of progression to renal failure and end stage renal disease.

Introduction

Autosomal Dominant Polycystic Kidney Disease (ADPKD) is a disease characterized by the formation of large fluid filled cysts in both kidneys that ultimately leads to end stage renal disease and the requirement for renal replacement therapy at the age of 50-60 years. In addition to the renal pathology, extra-renal manifestations can develop, such as cysts in the liver and pancreas, hypertension, cardiac valvular abnormalities, and cerebral aneurysms. [1] Usually, in young adults, only a small number of cysts can be detected, whereas at middle age thousands of cysts surrounded by fibrotic tissue have replaced almost all normal renal parenchyma, leading to a decline in renal function.

In most ADPKD patients, one *PKD1* or *PKD2* allele carries a germ-line mutation while the other allele is normal. Renal cysts are hypothesized to develop after somatic inactivation of the "healthy" allele of *PKD1,* or *PKD2* by a 'second hit' mechanism. [2] In addition, haploinsufficiency, stochastic fluctuations in *PKD1*or *PKD2* gene dosage below a tissue-specific threshold, may suffice to cause cyst formation. [3] A more complex picture was proposed in recent studies reporting several families with incompletely penetrant alleles of *PKD1* inherited at a homozygous state, or together with an inactivating mutation in the other allele. [4-6]

Many mouse and rat models exist for studying early phases of ADPKD, the formation and growth of cysts. However, few models have been described representing the phenotype observed in ADPKD patients with advanced stage disease characterized by cystic tissue, fibrotic areas with inflammation, but also regions with relative normal renal morphology. [7-9] Clearly, animal models closely resembling this phenotype are needed to evaluate accurately the *in vivo* effect of potential therapeutics on ADPKD disease progression in patients.

Previously, the orthologous *Pkd1*^{nl,nl} mouse model with reduced expression of the normal *Pkd1* transcript, had a variable mixed genetic background. [10] These *Pkd1*^{nl,nl} mice were crossed back to full C57BL6/J (B6) and full 129Ola/Hsd (Ola) genetic background. Here we study *Pkd1*^{nl,nl} mice on a 50%/50% genetic background of B6 and Ola, (*B6Ola-Pkd1*^{nl,nl} mice). These mice showed no developmental delay, in contrast to the *B6-Pkd1*^{nl,nl} mice on a full B6 genetic background. [11, 12] Here, we demonstrate that *B6Ola-Pkd1*^{nl,nl} mice showed great similarities with the human renal phenotype regarding fibrosis and inflammation. Interestingly, *B6Ola-Pkd1*^{nl,nl} mice showed an initial increase in renal volume, followed by a partial regression due to collapse of cysts. This was accompanied by the focal formation of fibrotic areas. Similar features were found in human kidneys with ADPKD. These observations have implications for the use of renal volume as sole parameter for the prediction of ADPKD disease progression especially in advanced stages.

Results

B6Ola-Pkd1^{nl,nl} mice show reduced levels of *Pkd1* gene expression and survive without growth retardation

Pkd1^{nl,nl} mice carry a neomycin selection cassette in intron 1, resulting in alternative splicing of the majority of the *Pkd1* transcripts. [10] In *B6Ola Pkd1^{nl,nl}* mice expression levels of the normal *Pkd1* transcript was reduced to 10% compared to 4 week old-wild-type mice (Figure S1A). Although expression of full length *Pkd1* is strongly reduced, a 3'transcript is still produced (Figure S1B). [10]
In wild-type mice normal *Pkd1* expression decreased with age to 20% of the expression at 4 weeks, while normal *Pkd1* expression in mutants remained at the same low level (Figure S1A). *Pkd2* gene expression was significantly reduced in mutants (25-30%) compared to wild-types at the age of 4 and 16 weeks (Figure S1C). As the tuberous sclerosis 2 (*Tsc2*) and *Pkd1* gene are located tail-to-tail, *Tsc2* expression was analyzed. [13] Expression in 4 week old mice was significantly reduced in *B6Ola Pkd1^{nl,nl}* mice, while at older ages expression was not significantly altered (Figure S1D).
In order to determine whether hypomorphic *Pkd1*-mutant mice show grow retardation as previously reported, [10] body weight was monitored. *B6Ola-Pkd1^{nl,nl}* mice, however, showed similar growth curves compared to wild-type littermates, both for males and females (Figure 1A, B). Only after 35 weeks, *B6Ola-Pkd1^{nl,nl}* male mice did not increase in weight, while wild-type males still did. Mice could live up to 52 weeks of age, although from 24 weeks onward occasional dropout of mice was observed (n=3/12 before 32 weeks), and between 43 and 52 weeks 3/4 mice died (at 43, 48 and 50 weeks).

Renal volume declined after 4 weeks without improvement of renal function

At different time-points mice were sacrificed and kidney-to-body weight ratios (2KW/BW) were determined as a measure for renal volume. Figure 1C and D show 2KW/BW and kidney weights respectively. 2KW/BW strongly increased during the first 4 weeks of age (12.6%) due to cystic expansion as shown by renal histology (Figure 1C and 2A). Strikingly, after 4 weeks 2KW/BW started to decline and stabilized after 12 weeks (~2.5%). This phenomenon was confirmed by the cystic index, showing a maximum at 4 weeks (~70%) followed by a decline (~35% at 12 weeks; Figure 1E).
Renal function was impaired at 4 weeks compared to 1 week, as indicated by increased blood urea (BU) levels (Figure 1F). However, BU levels did not decrease significantly as renal volume decreased, indicating no improvement of renal function at later stage.

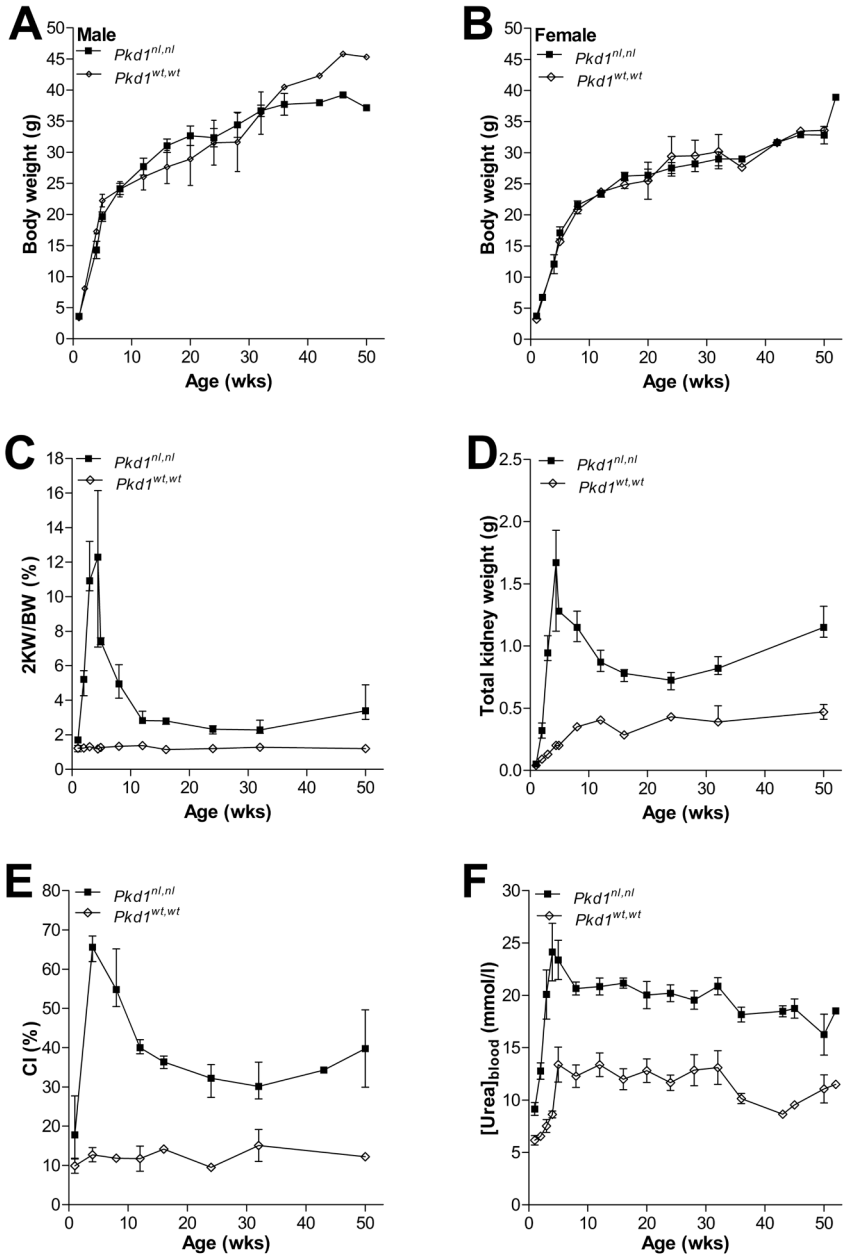


Figure 1. Growth curves, 2KW/BW ratios, cystic indices and blood urea levels in *B6Ola-Pkd1^{nl,nl}* and wild-type mice. Body weight (g) for (A) males and (B) females are indicated in time (mean ± SEM, n=2-7), (C) total kidney weight to body weight ratio (2KW/BW) and (D) total kidney weight (g) at different ages (median and IQR, n=2-7 per age), (E) cystic index represented as area-percentage (median and IQR, n=2-7 per age) and (F) blood urea concentration in time in mmol/l (mean ± SEM, n=5-11 per age). Closed squares; *B6Ola-Pkd1^{nl,nl}* mice, open diamonds; *B6Ola-Pkd1^{wt,wt}*, standard error of the mean (SEM) and interquartile range (IQR).

Cyst formation and origin of cysts

The origin of cyst formation was evaluated at postnatal day 1, 3, 7, 14 and 28 and subsequently at 24 weeks, using nephron segment-specific markers (n=2-3 per age). In newborn mice, at days 1 and 3, many dilated proximal tubules and small cysts positive for megalin were present in the cortex. In addition, although less numerous, dilated aquaporin-2 positive collecting ducts were observed (Figure S2A and C). This indicates that first the majority of cysts arise in proximal tubules in the cortex.

At day 7, more cysts of proximal tubular origin were found in the cortex (Figure 2J). Also the aquaporin-2 positive dilated collecting ducts became more numerous (Figures S2D-F).

At day 14, epithelial cysts occupied the entire cortex and medulla which were mostly derived from collecting ducts (Figure 2K). Although uromodulin positive cysts were also present, many of these cysts showed staining for aquaporin-2 as well. Only few cysts were megalin positive (Figures S2G-I). In addition, normal appearing tubules were still present.

From day 14 onwards the number and size of cysts increased until 21-28 days, while only few normal appearing tubules were present. Four week old *B6Ola-Pkd1*^{nl,nl} mice showed cysts derived from proximal tubules. However, the majority of cysts with marker staining were derived from distal tubules (or loops of Henle) and collecting ducts as indicated by staining for uromodulin and aquaporin-2 (Figure 2L and S2J-L). A small number of cysts were megalin positive, whereas most cysts showed partial, or no marker staining at all.

At later age, when renal volume declined, cysts derived from all segments were still observed. For example, at 24 weeks small cysts and dilated tubules of proximal tubular origin, distal tubular origin/loop of Henle and originating from collecting ducts were seen. Large cysts often had lost expression of segmental markers. In addition, glomerular cysts could be observed from 8 weeks onward.

Renal volume regression is accompanied by collapsing cysts, extensive fibrosis, and inflammation

Histological analysis (Figure 2A) and cystic index (Figure 1E) revealed that the cysts were the largest at 4 weeks. Subsequently, cysts partially regressed, became fibrotic and the kidneys revealed relatively normal tissue (Figure 2B and C).

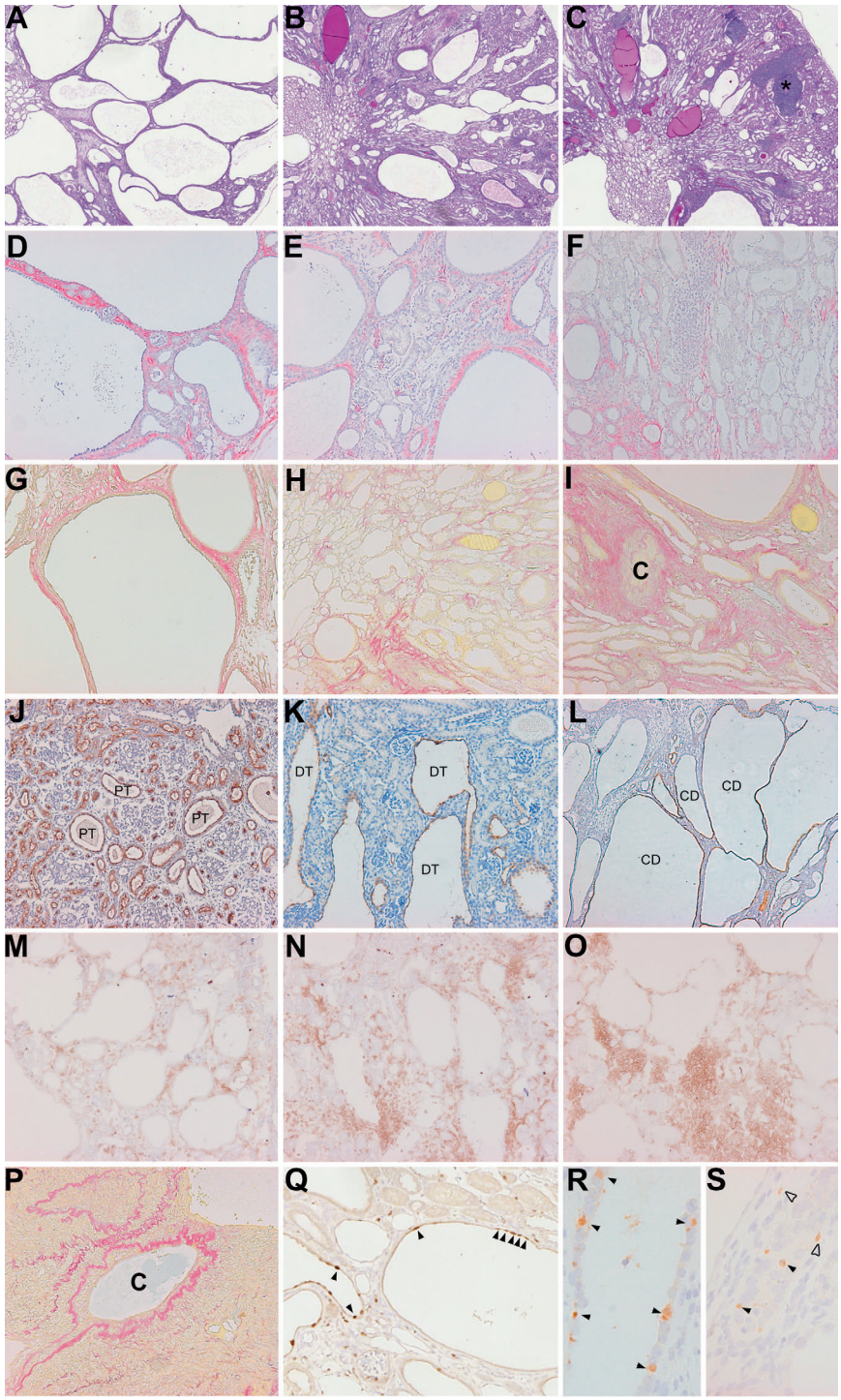
Although wild-type kidneys showed proliferating epithelial cells at the age of 4 weeks, the kidneys of *B6Ola-Pkd1*^{nl,nl} mice showed significantly more proliferating cells as illustrated by the proliferation index (Figure 3A), i.e. multiple Ki-67 positive nuclei and stretches of positive nuclei were present in epithelia of dilated tubules and cysts (Figure 2Q). At 8 weeks of age, proliferation in wild-types was reduced and only occasional Ki-67 positive nuclei were observed. Also in *B6Ola-Pkd1*^{nl,nl} mice proliferation decreased, but remained higher than in wild-types (Figure 3A). From 16 weeks onward (Figure 3A) proliferation seemed to increase again, which was mainly confined to infiltrating immune cells.

While apoptotic nuclei were scarce until three weeks of age, 4 and 8 weeks old *B6Ola-Pkd1*^{nl,nl} mice showed the highest numbers as indicated by the apoptotic index, the percentage of nuclei positive for active caspase-3 (Figure 3B). Apoptosis was observed in cystic epithelia (Figure 2R) as well as in interstitial tissue and non-cystic tubules (Figure 2S). After 8 weeks, numbers of apoptotic nuclei in epithelia and interstitium had decreased, but still outnumbered the apoptotic nuclei in wild-types. From 24 weeks onward, apoptotic nuclei were abundantly present in clusters of inflammatory cells. At all ages, wild-type kidneys showed very limited numbers of apoptotic nuclei (Figure 3B).
The decrease in cystic index, and partial regression of 2KW/BW and CI, was accompanied by "collapse" of cysts and was paralleled by increased fibrosis as shown by SMA and Sirius red staining (Figure 2D to 2I). Areas with collapsed cysts were occupied with fibrotic tissue and remnants of collapsed cysts were visible (Figure 2P and S3A and B). Regression of renal volume was preceded by an increase in SMA positive cells surrounding cysts at 4 weeks (Figure 2D).

Besides fibrosis, increased numbers of inflammatory cells were observed. Already at 4 weeks, small clusters of infiltrating cells were present in cystic kidneys, as indicated by CD45 staining (Figure 2M), while wild-type kidneys only show limited numbers of individual inflammatory cells. In time, in cystic kidneys, these clusters became more numerous and larger (Figure 2N and O), sometimes filling the lumen of the remnant structure of a cyst (Figure 2C and 3A-B).
Careful histological analysis of renal tissue of ADPKD patients also revealed regressing or collapsing cysts, as well as cyst remnants (Figure S3C-E), although the frequency of such abnormalities was relatively low.

Increased expression of genes involved in matrix remodeling in cystic kidneys

Expression of genes involved in matrix remodeling was examined using RT-MLPA (Reverse Transcriptase-Multiplex Ligation-dependent Probe Amplification). A key regulator of extracellular matrix (ECM) remodeling and the fibrotic response is Transforming Growth Factor-β (TGF-β). Expression of down-stream targets such as the plasminogen activator inhibitor-1 (PAI-1 encoded by *Serpine1*) as well as *Mmp2*, *EDA-Fn* and *Col1a1,* encoding matrix metalloproteinase-2, Fibronectin (EDA fragment) and collagen I, is strongly up-regulated in cystic kidneys of *Pkd1*^{nl,nl} mice, peaking at 4 weeks when renal volume was maximal (Figure 4A-D). While expression of PAI-1 is up-regulated, expression of its target, urokinase-type plasminogen activator (*u-PA*), is reduced (not shown). Also the mRNA level of another inhibitor in plasmin synthesis, alpha-2 anti-plasmin (*Serpinf1*), is increased as well (not shown).
In agreement with the expression data, Sirius red staining showed a large increase in ECM deposition from 4 to 8 weeks. After 8 weeks there was a mild increase in ECM deposition, but largely in new foci originating from collapsing cysts. Thus increased ECM deposition is accompanied by the expression of genes involved in ECM remodeling. The expression of these genes followed the same pattern as 2KW/BW ratio and cystic index.


A
B
C
*
D
E
F
G
H
I
C
J
PT
PT
PT
K
DT
DT
DT
L
CD
CD
CD
M
N
O
P
C
Q
R
S

B6Ola *Pkd1*^{nl,nl} mice show extra renal abnormalities

To determine whether *B6Ola-Pkd1*^{nl,nl} mice develop cysts in liver and pancreas, sections of these organs were analyzed. All examined mice showed bile duct ectasia and/or hyperplasia from 4 weeks onwards (n= 32/32; Figure S4), which increased with age. From 12 weeks on, a subset of mice (n=5/7) showed external bile duct dilation. Hepatic fibrosis appeared at 24 weeks in a subset of mice (n=2/5), while at 32 weeks all mice showed hepatic fibrosis (n=5/5). Pancreatic cysts were not observed.

In addition, aortas were isolated from mice aged between 4 and 8 weeks (n=8), and analyzed for the presence of aortic dissecting aneurysms that were previously reported for *Pkd1*^{nl,nl} mice on full C57/BL/6J or mixed genetic background. [11] *B6Ola-Pkd1*^{nl,nl} mice did not show dissecting aortic aneurisms, although in 1 out of 8 *B6Ola-Pkd1*^{nl,nl} mice, segmental granulomatous chronic lesions were present in the arterial wall and peri-arterial regions.

← **Figure 2. Histopathological characteristics of cystic kidneys in *B6Ola-Pkd1*^{nl,nl} mice.** (A-C) PAS staining showing progression of cystic disease in *B6Ola-Pkd1*^{nl,nl} mice at 4, 8, and 24 weeks of age respectively, original magnification 2,5x. (D-F) SMA staining showing myofibroblasts and (G-I) Sirius red staining for collagen as markers for fibrosis at 4 (D,G), 8 (E,H) and 24 (F,I) weeks of age, original magnification 10x. (J-L) Origin of cyst formation, showing dilated tubules and cysts of proximal tubular origin at D7 as indicated by staining for megalin (J), cysts of collecting duct origin at D14 (K) and D28 (L) as indicated by staining for aquaporin-2. Original magnification 10x, 10x and 5x respectively. (M-O) Increased infiltration of inflammatory cells with disease progression as indicated by CD45 staining at 4, 8 and 24 weeks of age respectively, original magnification 10x. (P) Example of collapsing cysts at 24 weeks of age, Sirius red staining, original magnification 10x. (Q) Stretch of, and Ki-67 positive nuclei in cystic epithelium at 4 weeks of age. Original magnification 20x. (R,S) Active caspase-3 staining showing apoptotic nuclei in cystic (R) and non cystic epithelia (S) at 4 weeks of age. Original magnification 40x.
Asterix indicates immune infiltrate filling the lumen of the remnant structure of a cyst. Closed arrowheads indicate examples of positive nuclei in epithelia, while open arrowheads indicate positive nuclei in interstitium. C; collapsing cyst, PT; cyst of proximal tubular origin, DT; cyst of distal tubular origin, CD cyst derived of collecting duct.

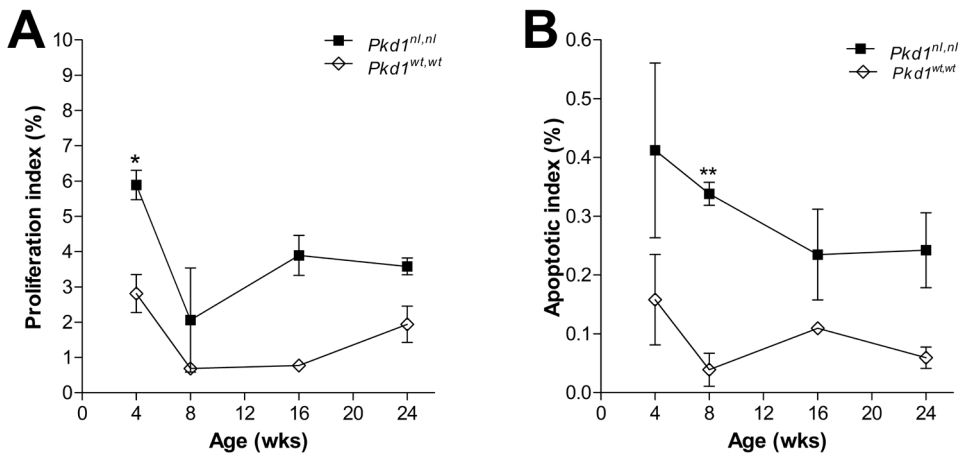


Figure 3. Proliferation index and apoptotic index in time in *B6Ola-Pkd1^{nl,nl}* and wild-type mice.
(A) Proliferation index presented as percentage of Ki-67 positive nuclei over total nuclei. (B) Apoptotic index presented as percentage of active caspase-3 positive nuclei over total nuclei. Results are shown as mean ± SEM. *; P<0.05, **; P<0.01.

Gene expression of potential biomarkers

Neutrophil gelatinase-associated lipocalin (NGAL), sulfated glycoprotein-2 (clusterin) and prostaglandin D2 synthase have been described as potential biomarkers to monitor disease progression in ADPKD. [14-17] The genes encoding for these potential biomarkers, *Lcn2*, *Sgp2* and *Ptgds* respectively, all showed increased mRNA expression levels in *B6Ola Pkd1^{nl,nl}* mice compared to wild-type animals, at all ages. Expression of *Lcn2* and *Sgp2* peaked at 4 weeks and strongly decreased as renal volume regressed (Figure 5 A, B), while *Ptgds* expression did not show such a strong correlation with renal volume (not shown). Also complement component 3 (*C3*), an important player in the innate immunity response, is regarded as a potential biomarker. [18] We found that *C3* expression was highly elevated in cystic kidneys and further increased during disease progression in *B6Ola Pkd1^{nl,nl}* mice (Figure 5C).

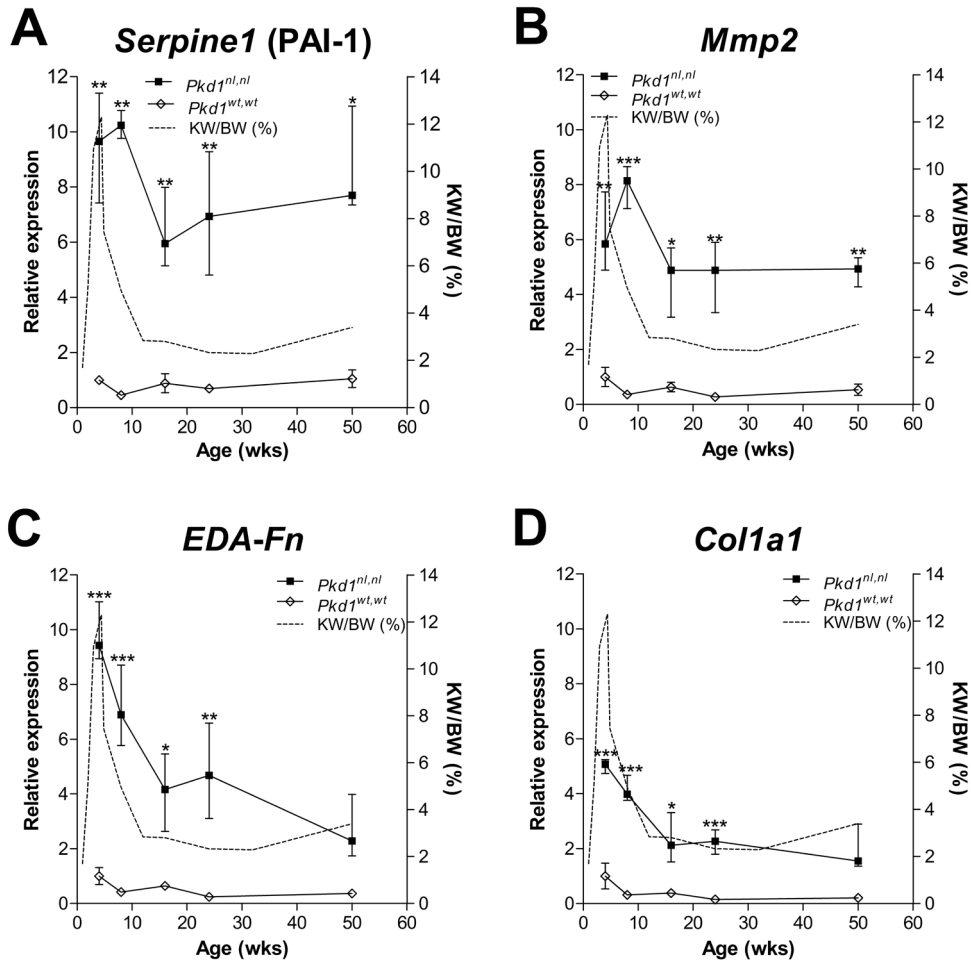


Figure 4. Renal mRNA expression of genes involved in matrix remodeling at different ages. mRNA expression of (A) *Serpine1* (PAI-1) (B) *Mmp2*, (C) *Fn1(EDA)* and (D) *Col1a1* as analyzed by RT-MLPA. Expression was normalized to the housekeeping gene *HPRT*. Results are shown as median expression relative to the expression of wild-type mice at the age of 4 weeks, error bars represent interquartile range (n=2-5). Closed squares; *B6Ola-Pkd1*^{nl,nl} mice, open diamonds; *B6Ola-Pkd1*^{wt,wt}. The dotted line represents 2KW/BW, indicated on right y-axis, showing pattern of renal volume in time. *; P<0.05, **; P<0.01, ***; P<0.001.

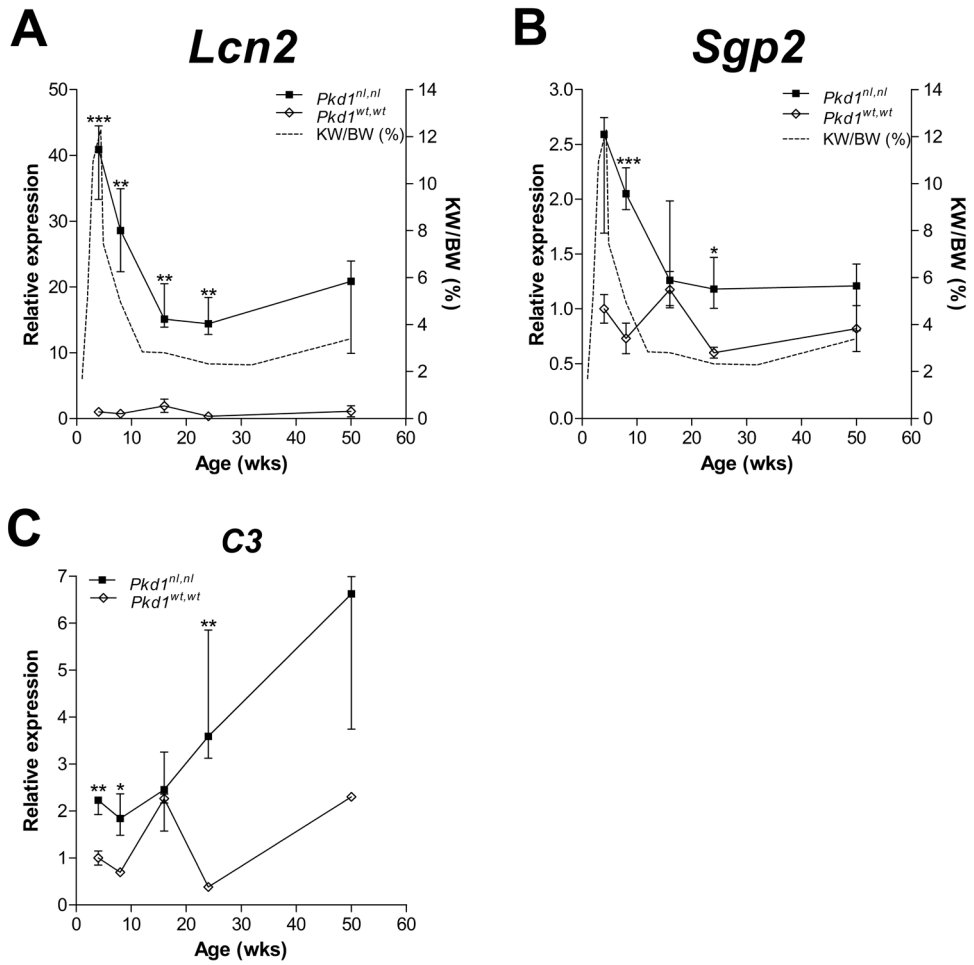


Figure 5. Renal mRNA expression of potential biomarkers for ADPKD disease progression at different ages. mRNA expression of (A) *Lcn2*, (B) *Sgp2*and (C)*C3,* as analyzed by RT-MLPA. Results are shown as median expression relative to the expression of wild-type mice at the age of 4 weeks, error bars represent interquartile range (n=2-5). Closed squares; *B6Ola-Pkd1*^{nl,nl} mice, open diamonds; *B6Ola-Pkd1*^{wt,wt}. The dotted line (in A and B) represents 2KW/BW, indicated on right y-axis, showing pattern of renal volume in time. *; P<0.05, **; P<0.01, ***; P<0.001.

Discussion

The *Pkd1*$^{nl/nl}$ mouse model is an orthologous model for polycystic kidney disease. The severity of the phenotype varies among mice with a mixed genetic background. [10] Here we report that *Pkd1*^{nl,nl} mice on a fixed 50%/50% genetic background of B6 and Ola, develop large cystic kidneys within 4 weeks, but can survive up to a year. All models homozygous for a *Pkd1* inactivating allele, present with severe cystic kidneys around E15 and do not survive embryonic development. [19-23] In contrast, the *B6Ola-Pkd1*^{nl,nl} mice, express low levels of *Pkd1*, are viable, and exhibit grossly normal kidney structure, but with dilated proximal tubules at birth. Although expression of the full length *Pkd1* transcript was strongly reduced, a 3'-transcript is still produced and it cannot be excluded that this may affect renal development and survival. [24] In *B6Ola-Pkd1*^{nl,nl} mice, the first cysts develop from mature proximal tubules around birth. Subsequently, larger cysts were visible at day 7, followed by distal tubule and collecting duct cyst formation and progressive cystic enlargement. At 3-4 weeks of age the majority of cysts were derived from distal tubules or collecting ducts. This is in agreement with our previous findings in 4-7 week old *Pkd1*^{nl,nl} mice on a mixed genetic background [10] and is comparable to cyst formation in *Pkd1*^{nl,nl} mice on full B6 genetic background (Hassane, unpublished). Furthermore, the first cysts observed during embryonic development of *Pkd1*$^{-/-}$ mice were derived from proximal tubules and later on from collecting ducts. [25] However, early cysts in *Pkd1*$^{-/-}$ mice can also be of glomerular origin, while in *B6Ola-Pkd1*^{nl,nl} mice, those cysts were not detected earlier than at 8 weeks. This suggests that low expression of *Pkd1* is able to delay glomerular cyst formation. Although we observe relatively low numbers of proximal tubular cysts, these cysts were not observed in other models with low *Pkd1*-gene expression, i.e. *Pkd1*^{L3,L3} mice and mice in which *Pkd1*-expression was reduced by an artificial microRNA. [26, 27] The use of different proximal tubular epithelium markers may explain the different observations.

In *B6Ola-Pkd1*^{nl,nl} mice, cysts showing expression of aquaporin-2 as well as uromodulin were frequently observed, indicating they may be derived from the transition between distal tubules and collecting ducts, e.g. connecting tubule. Also cysts without expression of any segment-specific maker were observed, reflecting dedifferentiated epithelium, as frequently seen in human ADPKD tissues.

Notably, *B6Ola-Pkd1*^{nl,nl} mice did not show growth retardation. This is in contrast to the severe growth retardation observed in *Pkd1*^{nl,nl} mice on mixed genetic [10] and full B6 genetic background (Hassane, unpublished), as well as in *Pkd1*^{L3,L3} mice. [26] Also dissecting aortic aneurysms, as reported previously for *B6-Pkd1*^{nl,nl} mice, [10, 11] were absent. Differential expression of genes, in the two genetic backgrounds, is likely to affect the phenotype, including aneurysm formation. Interestingly, different sensitivity for angiotensin-induced aneurysm formation was observed previously for the C57Bl/6 and 129 Ola strains. [28, 29] Also ADPKD patients, even in the same family, do not all develop vessel abnormalities, indicating that in addition to inactivation of the *Pkd1* gene, a certain combination of modifying genes must be present to initiate aneurysm formation...

In time, *B6Ola-Pkd1*$^{nl/nl}$ mice showed accumulation of collagen and massive fibrosis, as seen in human cystic kidneys. This is accompanied by strong up-regulation of genes involved in ECM remodeling, including expression of SMAD2/3 targets (*Mmp2, EDA-Fn, Col1a1 and Serpine1*) downstream of the TGF-β signaling pathway. [12] Although TGF-β signaling is an important regulator of fibrosis and matrix remodeling, the pathway is also involved in tissue regeneration. [30] This may explain the high expression of TGF-β targets already during stages characterized by cyst expansion.

Additional signaling pathways known to be involved in ADPKD e.g. canonical Wnt and Hippo signaling were found to be differentially regulated in *B6Ola Pkd1*^{nl,nl} mice. [31-34] Expression of the Wnt-target, *Axin2* was increased while mRNA levels of *Notum*, a negative regulator of Wnt signaling, were decreased in cystic kidneys (Figure S5). In addition, several transcriptional targets of YAP were up-regulated (Figure S6) and also nuclear localization of YAP, the final effector of the Hippo signaling cascade, was observed in cyst lining epithelial cells, although this was less prominent at later ages (not shown).

The regression of renal volume in our mouse model is a striking phenomenon that is also observed in ARPKD patients surviving the neonatal period. [35, 36] This regression, succeeding the development of massive cystic kidneys at 3-4 weeks, was accompanied by "collapse" of cysts that was paralleled by an increase in fibrosis. Collapsing cysts were also observed in human kidneys from ADPKD patients, but with a low frequency. Previously, it was already suggested that apoptosis plays an important role in the pathogenesis of PKD. Apoptosis was found to be abundantly present in cystic as well as non-cystic epithelia in polycystic kidneys of PKD mice and patients and was suggested to contribute to the loss of normal renal tubules. [37] However, conditional *Pkd1*-deletion mice do not show a significant increase in apoptosis. [38, 39] In the *B6Ola-Pkd1*^{nl,nl} mice, apoptosis in cystic epithelia was highest during the period of regression in renal volume, while proliferation markedly decreased. This suggests that apoptosis may not be involved in the formation of cysts, but may play an important role in the progression of the disease and the progressive deterioration of renal function.

Renal volume as clinical end-point used in clinical trials for ADPKD [40, 41] was questioned after disappointing results of clinical trials with mTOR inhibitors. It was suggested that renal volume might not be an ideal end-point in advanced PKD. [42, 43] Indeed we only observed a minor effect on renal volume after low dose sirolimus treatment in the *B6Ola-Pkd1*^{nl,nl} model. [44] In line with our data, regarding renal volume regression, and increased fibrosis and inflammatory infiltrates, another study revealed that the extent of fibrosis and inflammation correlates better with disease progression to renal failure than renal volume. [45]

Models, in which almost all nephrons develop cysts simultaneously in a relative short time span, are useful to study cyst initiation and progression. However, models closely resembling advanced stage human ADPKD are of outmost importance, especially to better predict the effects of new therapeutics.

Recently, several families have been reported with non- or incompletely penetrant alleles of *PKD1* or *PKD2*. [4-6] When these hypomorphic alleles are inherited at a homozygous state, or in *trans* with another mutation, they can cause severe, early onset PKD. Even more, two hypomorphic *PKD1*- or *PKD2*-alleles were identified in patients with an ARPKD-like renal cystic phenotype in families with no history of PKD. [5, 6]

With regard to the characteristic aspects of human ADPKD disease progression, fibrosis and inflammation, [7] the *B6Ola-Pkd1*^{nl,nl} model shows similarity with the human ADPKD renal pathology. But when onset and proportion of nephrons involved, is taken into account, the model particularly resembles patients with two incomplete penetrant alleles of *PKD1* or *PKD2*.

In conclusion, the renal cystic phenotype of *B6Ola-Pkd1*$^{nl/nl}$ mice seems to reflect the phenotype of patients with early onset PKD as result of two hypomorphic mutations. This model shows that regression of cysts and renal volume occurs, implying that renal volume may not be a good predictor of progression to renal failure and end stage renal disease.

Methods

Mice

Pkd1^{nl,nl} mice were generated as previously described. [10] A loxP-flanked neomycin selection cassette was inserted into intron 1 of *Pkd1* by homologous recombination and a third loxP site was inserted into intron 11. Chimeric offspring were backcrossed with full C57BL6/Jico (B6) and 129Ola/Hsd (Ola). Next *Pkd1*^{nl,nl} mice on a 50%/50% genetic background of B6 and Ola, [(C57BL/6Jico x 129Ola/Hsd)F1=*B6Ola-Pkd1*^{nl,nl} mice], were generated. Mice were sacrificed at several ages (n=5 *B6Ola-Pkd1*^{nl,nl}, n=2 wild-types) and kidneys, liver, pancreas were isolated. From mice (n=8) between 4 and 8 weeks aortas were isolated.

Body weight and blood urea concentration were analyzed to monitor growth and renal function respectively. Blood urea concentrations were determined using the Reflotron Plus (Roche Diagnostics).

All experiments with mice were approved by the Animal Care and Use Committee of Leiden University and by the Commission for Biotechnology in Animals of the Dutch Ministry of Agriculture.

Human renal tissues

All human tissue samples were obtained following procedures approved by the LUMC medical ethical committee (institutional review board).

(Immuno)histochemistry

Formalin fixed, paraffin embedded kidney sections (4 μm) were analyzed using periodic acid Schiff (PAS) staining, Sirius Red staining or were used for immunohistochemistry. For staining with Sirius Red, de-paraffinized sections were incubated in 0.2% phosphomolybdic acid hydrate for five minutes and 0.1% Sirius red for 90 minutes. Subsequently sections were incubated for one minute in saturated picric acid and then placed in 70% ethanol, dehydrated and mounted.

Staining for segment specific markers was performed on sequential sections. Proximal tubules were stained using rabbit polyclonal anti-megalin (1:500 LUMC, Leiden, the Netherlands [46]), thick ascending loop of Henle and distal convoluted tubules were stained with goat polyclonal anti-uromodulin protein (uromodulin, 1:500, Organon Teknika-Cappel, Turnhout, Belgium) and collecting ducts were stained using rabbit polyclonal anti-aquaporin-2 (1:4000, Calbiochem, Amsterdam, The Netherlands)

Staining of fibroblasts was performed using mouse monoclonal anti-α-smooth muscle actin (SMA) alkaline phosphatase conjugate (clone 1A4, Sigma-Aldrich, St. Louis MO, USA).

Sections were subjected to heat mediated antigen retrieval procedure (10mM citrate buffer pH 6.0) for staining for polyclonal anti-Ki-67 (1:3000, Nova Castra, Valkenswaard, the Netherlands) and anti-cleaved caspase-3 (1:300, Cell Signaling, Beverly, MA). Immunohistochemistry was performed as described previously. [32]

Acetone fixed, frozen renal sections were stained for infiltrating cells using anti-CD45 (ly5) antibody (clone 30-F11 01111D, Pharmingen, San Diego CA, USA) followed by incubation with rabbit anti-rat Ig/HRP 1:100 in PBS containing 1% normal mouse serum. Antibody complexes were visualized using DAB and counterstained with hematoxylin.

Formalin fixed aortas, from aortic root to the bifurcation of the iliac arteries, were sectioned and sections were mounted serially onto glass slides. Aortic sections were stained with hematoxylin eosin (HE) and resol-fuchsin staining for elastin lamellae.

Morphometric Analysis

Transverse kidney sections were stained with PAS, anti-Ki-67 and anti-active caspase-3 were used for determination of cystic-, proliferation- and apoptotic index respectively. Five to twelve random, non-overlapping, high resolution images per mouse at a magnification of 10X were obtained from the total renal area using a Panoramic Midi digital slide scanner (3DHistech, Budapest, Hungary).

Cystic index was defined as the area percentage of lumen over the total image area. Proliferation and cystic index are defined by the percentage of Ki-67 and caspase-3 positive nuclei, over total amount of hematoxylin positive nuclei. Lumen and total area, as well as numbers positive nuclei were determined using Image J software (public domain software, NIH, USA).

Mean cystic, proliferation, and apoptotic index were calculated for each mouse (>3000 nuclei/mouse; n=2-3 mice), after which mean cystic index per genotype per time point was calculated.

mRNA expression analysis

For gene expression analysis, Reverse Transcriptase Multiplex Ligation-dependent Probe Amplification (RT-MLPA) reactions were performed as described previously. [32] Per time point n=5 *B6Ola-Pkd1*^{nl,nl} mice and n=2 wt mice were analyzed.

Expression of the housekeeping gene *Hprt* (hypoxanthine guanine phosphoribosyl transferase) served as reference for gene expression.

Peak ratios of target gene and housekeeping genes were calculated and results of *B6Ola-Pkd1*^{nl,nl} mice were normalized to the median of 4 week old wild-type mice, which has been set to 1. Two *Pkd1* probe sets were developed, a 5'-*Pkd1* probe set, identifying exon 1-2 of the normal *Pkd1* transcript and the *3'-Pkd1* probe set identifying exon 45-46 and thereby identifying both mutant and normal *Pkd1* transcripts.

Sequences and details of probes, primers and competitors are available upon request.

Statistics

Statistical comparisons between *B6Ola-Pkd1*^{nl,nl} mice and controls concerning proliferation index, apoptotic index and mRNA expression was performed using an unpaired t-test, or unpaired Welch's corrected t-test in case of unequal variance. P-values <0.05 were considered significant.

Acknowledgements

We acknowledge the excellent technical assistance of Saskia Maas for the preparation of the different tissues.

References

1. Gabow,P.A. Autosomal dominant polycystic kidney disease--more than a renal disease. *Am. J. Kidney Dis.* **16**, 403-413 (1990).
2. Qian,F., Watnick,T.J., Onuchic,L.F., & Germino,G.G. The molecular basis of focal cyst formation in human autosomal dominant polycystic kidney disease type I. *Cell* **87**, 979-987 (1996).
3. Ong,A.C. & Harris,P.C. Molecular basis of renal cyst formation--one hit or two? *Lancet* **349**, 1039-1040 (1997).
4. Rossetti,S. *et al.* Incompletely penetrant PKD1 alleles suggest a role for gene dosage in cyst initiation in polycystic kidney disease. *Kidney Int.* **75**, 848-855 (2009).
5. Vujic,M. *et al.* Incompletely penetrant PKD1 alleles mimic the renal manifestations of ARPKD. *J. Am. Soc. Nephrol.* **21**, 1097-1102 (2010).
6. Losekoot,M. *et al.* Neonatal onset autosomal dominant polycystic kidney disease (ADPKD) in a patient homozygous for a PKD2 missense mutation due to uniparental disomy. *Journal of Medical Genetics*(2011).
7. Zeier,M. *et al.* Renal histology in polycystic kidney disease with incipient and advanced renal failure. *Kidney Int.* **42**, 1259-1265 (1992).
8. Okada,H. *et al.* Progressive renal fibrosis in murine polycystic kidney disease: an immunohistochemical observation. *Kidney Int.* **58**, 587-597 (2000).
9. Martinez,J.R. & Grantham,J.J. Polycystic kidney disease: etiology, pathogenesis, and treatment. *Dis. Mon.* **41**, 693-765 (1995).
10. Lantinga-van Leeuwen,I.S. *et al.* Lowering of Pkd1 expression is sufficient to cause polycystic kidney disease. *Hum. Mol. Genet.* **13**, 3069-3077 (2004).
11. Hassane,S. *et al.* Pathogenic sequence for dissecting aneurysm formation in a hypomorphic polycystic kidney disease 1 mouse model. *Arterioscler. Thromb. Vasc. Biol.* **27**, 2177-2183 (2007).
12. Hassane,S. *et al.* Elevated TGFbeta-Smad signalling in experimental Pkd1 models and human patients with polycystic kidney disease. *J. Pathol.* **222**, 21-31 (2010).
13. The European Polycystic Kidney Disease Consortium. The polycystic kidney disease 1 gene encodes a 14 kb transcript and lies within a duplicated region on chromosome 16. *Cell* **77**, 881-894 (1994).
14. Meijer,E. *et al.* Association of urinary biomarkers with disease severity in patients with autosomal dominant polycystic kidney disease: a cross-sectional analysis. *Am. J. Kidney Dis.* **56**, 883-895 (2010).
15. Bolignano,D. *et al.* Neutrophil gelatinase-associated lipocalin in patients with autosomal-dominant polycystic kidney disease. *Am. J. Nephrol.* **27**, 373-378 (2007).
16. Bolignano,D. *et al.* Neutrophil gelatinase-associated lipocalin (NGAL) as a marker of kidney damage. *Am. J. Kidney Dis.* **52**, 595-605 (2008).
17. Lai,X. *et al.* Characterization of the renal cyst fluid proteome in autosomal dominant polycystic kidney disease (ADPKD) patients. *Proteomics. Clin. Appl.* **2**, 1140-1152 (2008).
18. Mrug,M. *et al.* Overexpression of innate immune response genes in a model of recessive polycystic kidney disease. *Kidney Int.* **73**, 63-76 (2008).
19. Boulter,C. *et al.* Cardiovascular, skeletal, and renal defects in mice with a targeted disruption of the Pkd1 gene. *Proc. Natl. Acad. Sci. U. S. A* **98**, 12174-12179 (2001).
20. Kim,K., Drummond,I., Ibraghimov-Beskrovnaya,O., Klinger,K., & Arnaout,M.A. Polycystin 1 is required for the structural integrity of blood vessels. *Proc. Natl. Acad. Sci. U. S. A* **97**, 1731-1736 (2000).
21. Muto,S. *et al.* Pioglitazone improves the phenotype and molecular defects of a targeted Pkd1 mutant. *Hum. Mol. Genet.* **11**, 1731-1742 (2002).
22. Wu,G. *et al.* Cardiac defects and renal failure in mice with targeted mutations in Pkd2. *Nat. Genet.* **24**, 75-78 (2000).
23. Lu,W. *et al.* Comparison of Pkd1-targeted mutants reveals that loss of polycystin-1 causes cystogenesis and bone defects. *Hum. Mol. Genet.* **10**, 2385-2396 (2001).
24. Trudel,M. & Kurbegovic,A. Toward Understanding Pkd1 Cystogenetic Mechanism. *J. Am. Soc. Nephrol.* **22**, 59A (2011).
25. Ahrabi,A.K. *et al.* Glomerular and proximal tubule cysts as early manifestations of Pkd1 deletion. *Nephrol. Dial. Transplant.* **25**, 1067-1078 (2010).

26. Jiang,S.T. *et al.* Defining a link with autosomal-dominant polycystic kidney disease in mice with congenitally low expression of Pkd1. *Am. J. Pathol.* **168**, 205-220 (2006).
27. Wang,E. *et al.* Progressive renal distortion by multiple cysts in transgenic mice expressing artificial microRNAs against Pkd1. *J. Pathol.* **222**, 238-248 (2010).
28. Bourdeau,A. *et al.* Potential role of modifier genes influencing transforming growth factor-beta1 levels in the development of vascular defects in endoglin heterozygous mice with hereditary hemorrhagic telangiectasia. *Am. J. Pathol.* **158**, 2011-2020 (2001).
29. King,V.L., Trivedi,D.B., Gitlin,J.M., & Loftin,C.D. Selective cyclooxygenase-2 inhibition with celecoxib decreases angiotensin II-induced abdominal aortic aneurysm formation in mice. *Arterioscler. Thromb. Vasc. Biol.* **26**, 1137-1143 (2006).
30. Geng,H. *et al.* Inhibition of autoregulated TGFbeta signaling simultaneously enhances proliferation and differentiation of kidney epithelium and promotes repair following renal ischemia. *Am. J. Pathol.* **174**, 1291-1308 (2009).
31. Lin,F. *et al.* Kidney-specific inactivation of the KIF3A subunit of kinesin-II inhibits renal ciliogenesis and produces polycystic kidney disease. *Proc. Natl. Acad. Sci. U. S. A* **100**, 5286-5291 (2003).
32. Happé,H. *et al.* Toxic tubular injury in kidneys from Pkd1-deletion mice accelerates cystogenesis accompanied by dysregulated planar cell polarity and canonical Wnt signaling pathways. *Hum. Mol. Genet.* **18**, 2532-2542 (2009).
33. Song,X. *et al.* Systems biology of autosomal dominant polycystic kidney disease (ADPKD): computational identification of gene expression pathways and integrated regulatory networks. *Hum. Mol. Genet.* **18**, 2328-2343 (2009).
34. Happé,H. *et al.* Altered Hippo signalling in polycystic kidney disease. *J. Pathol.* **224**, 133-142 (2011).
35. Gunay-Aygun,M. *et al.* Correlation of kidney function, volume and imaging findings, and PKHD1 mutations in 73 patients with autosomal recessive polycystic kidney disease. *Clin. J. Am. Soc. Nephrol.* **5**, 972-984 (2010).
36. Bergmann,C. *et al.* Clinical consequences of PKHD1 mutations in 164 patients with autosomal-recessive polycystic kidney disease (ARPKD). *Kidney Int.* **67**, 829-848 (2005).
37. Woo,D. Apoptosis and loss of renal tissue in polycystic kidney diseases. *N. Engl. J. Med.* **333**, 18-25 (1995).
38. Shibazaki,S. *et al.* Cyst formation and activation of the extracellular regulated kinase pathway after kidney specific inactivation of Pkd1. *Hum. Mol. Genet.* **17**, 1505-1516 (2008).
39. Leonhard,W.N. *et al.* Curcumin inhibits cystogenesis by simultaneous interference of multiple signaling pathways: in vivo evidence from a Pkd1-deletion model. *Am. J. Physiol Renal Physiol* **300**, F1193-F1202 (2011).
40. Serra,A.L. *et al.* Sirolimus and kidney growth in autosomal dominant polycystic kidney disease. *N. Engl. J. Med.* **363**, 820-829 (2010).
41. Walz,G. *et al.* Everolimus in patients with autosomal dominant polycystic kidney disease. *N. Engl. J. Med.* **363**, 830-840 (2010).
42. Grantham,J.J. Polycystic kidney disease: neoplasia in disguise. *Am. J. Kidney Dis.* **15**, 110-116 (1990).
43. Watnick,T. & Germino,G.G. mTOR inhibitors in polycystic kidney disease. *N. Engl. J. Med.* **363**, 879-881 (2010).
44. Novalic,Z. *et al.* Dose-Dependent Effects of Sirolimus on mTOR Signaling and Polycystic Kidney Disease. *J. Am. Soc. Nephrol.*(2012).
45. Caroli,A. *et al.* Intermediate Volume on Computed Tomography Imaging Defines a Fibrotic Compartment that Predicts Glomerular Filtration Rate Decline in Autosomal Dominant Polycystic Kidney Disease Patients. *Am. J. Pathol.* **179**, 619-627 (2011).
46. Christensen,E.I. *et al.* Segmental distribution of the endocytosis receptor gp330 in renal proximal tubules. *Eur. J. Cell Biol.* **66**, 349-364 (1995).

Supplemental figures

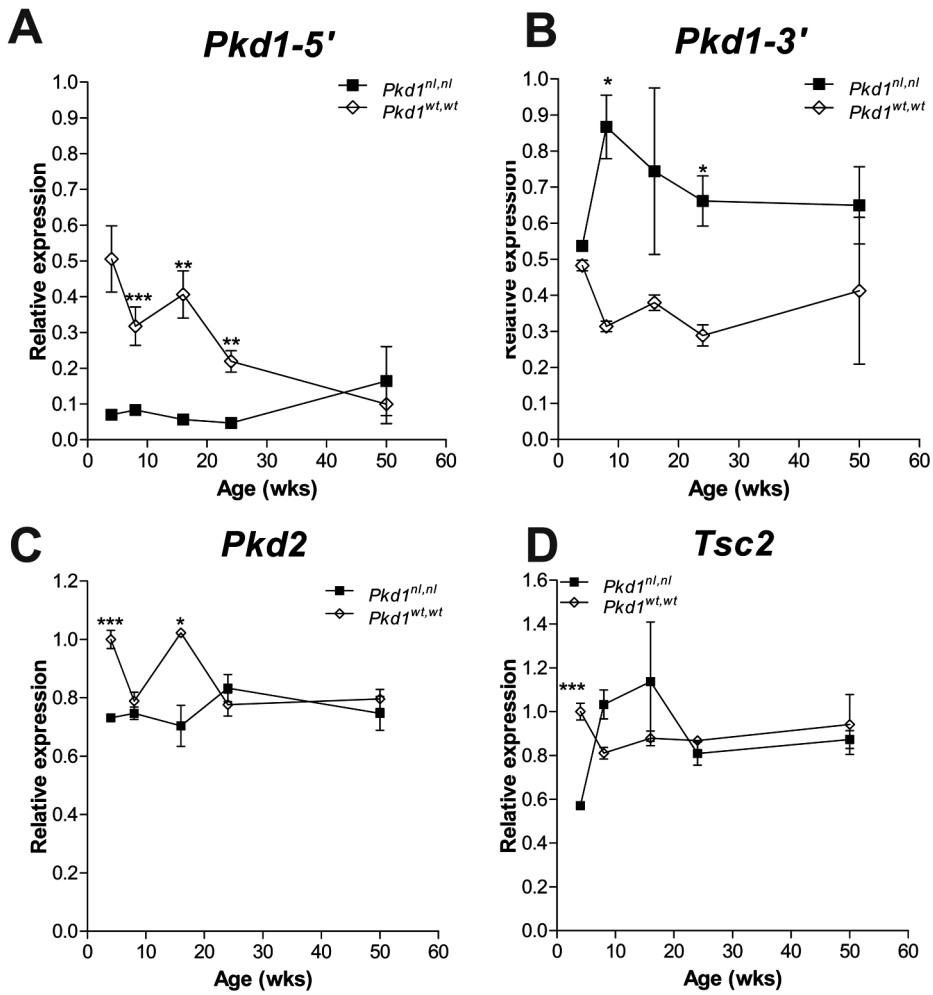


Figure S1: Renal mRNA expression of normal *Pkd1* and *TSC2* transcript in *B6Ola-Pkd1^{nl,nl}* and wild type mice at different ages. (A) Expression of normal *Pkd1-5'* transcript, (B) *Pkd1-3'* transcript, (C)*Pkd2* and *(D) Tsc2*. mRNA expression was analyzed by RT-MLPA. For the *Pkd1* transcripts, results are shown as mean expression ± SEM only normalized to housekeeping genes (A and B). *Pkd2* and *TSC2* expression are shown as median expression relative to the expression of wild type mice at the age of 4 weeks, error bars represent interquartile range. Closed squares; *B6Ola-Pkd1^{nl,nl}* mice, open diamonds; *B6Ola-Pkd1^{wt,wt}*, ***; P<0.001.

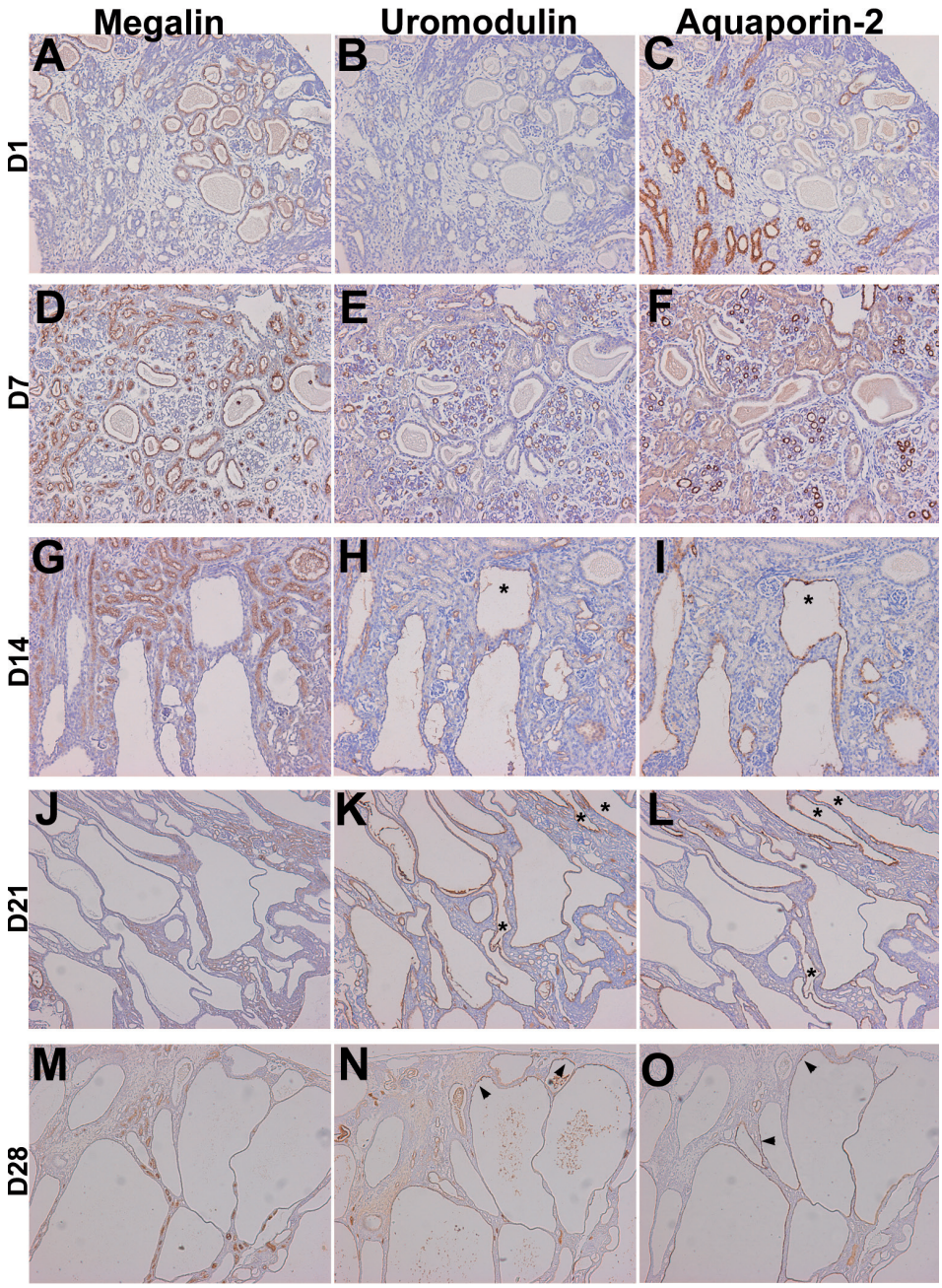


Figure S2: Time course of cyst formation and involvement of different nephron segments. Peroxidase staining of renal sections from (A-C) day 1, (D-F) day 7, (G-I) day 14, (J-L) day 21 and (M-O) day 28. Sequential sections were stained for (A, D, G, J and M) megalin, (B, E, H, K and N) uromodulin and (C, F, I, L and O) aquaporin-2, indicating tubules and cysts from proximal tubular, distal tubular and collecting ductal origin respectively. Asterisks indicate cysts positive for two segmental markers. Arrowheads indicate cysts with partial loss of marker expression, pointing to sites with remaining expression. Original magnification (A-I) 10x, (J-O) 5x.

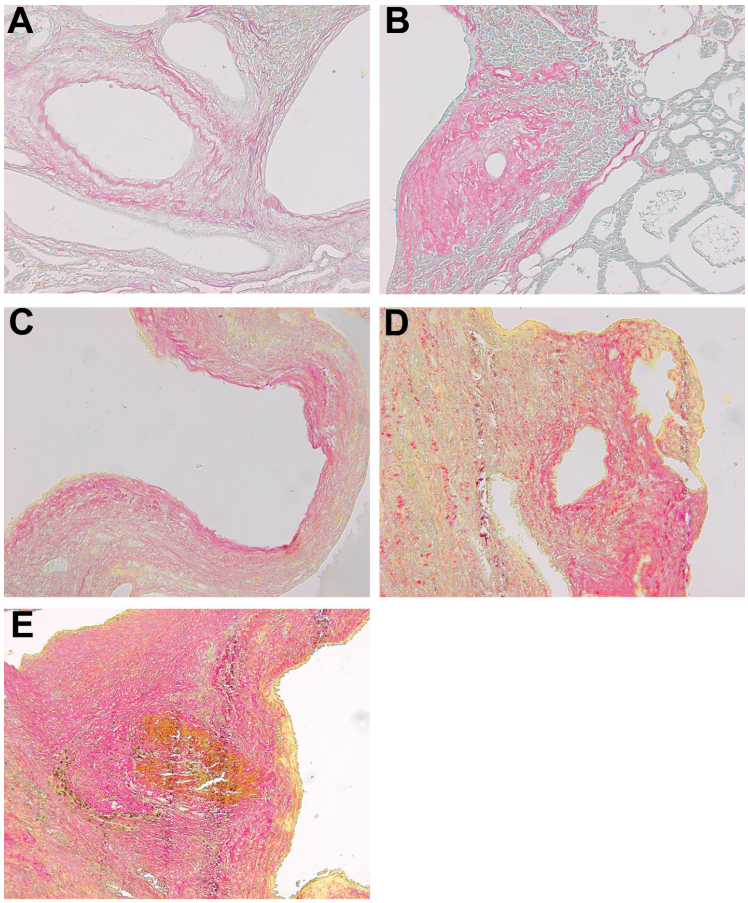


Figure S3: Collapsing cysts in mice and human ADPKD. Collapsing cyst in *B6Ola-Pkd1*^{nl,nl} mice at the age of (A) 16 weeks and (B) 50 weeks and (C-E) human ADPKD. Original magnification 10x (A-D) and 5x (E).

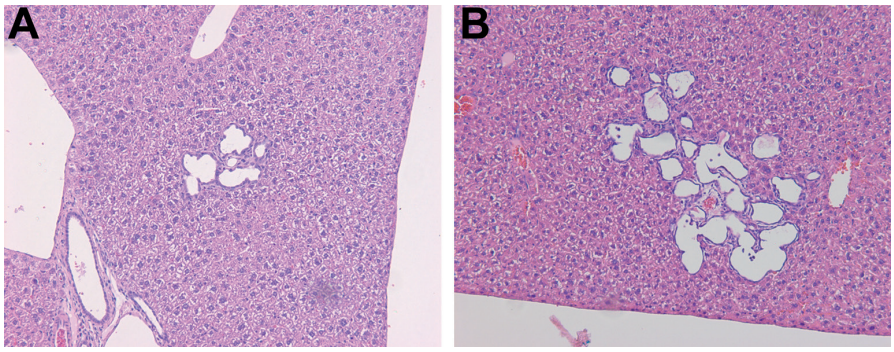


Figure S4: Bile duct ectasia in *B6Ola-Pkd1*^{nl,nl} mice. HE staining *B6Ola-Pkd1*^{nl,nl} livers at the age of (A) 8 weeks and (B) 24 weeks showing bile duct ectasia. Original magnification 10x.

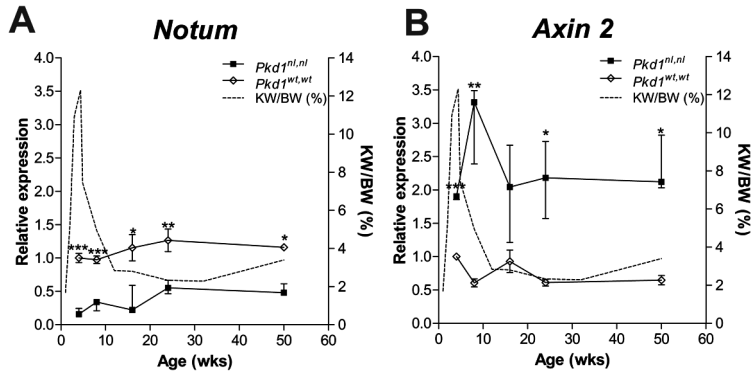


Figure S5: mRNA expression of genes involved in canonical Wnt signaling. mRNA expression of (A) *Notum* and (B) *Axin2*, at different ages as determined by RT-MLPA. Results are shown as median expression relative to the expression of wild type mice at the age of 4 weeks, error bars represent interquartile range. Closed squares; *B6Ola-Pkd1*^{nl,nl} mice, open diamonds; *B6Ola-Pkd1*^{wt,wt}. The dotted line represents KW/BW, indicated on right y-axis, showing pattern of renal volume in time. *; P<0.05, **; P<0.01, ***; P<0.001.

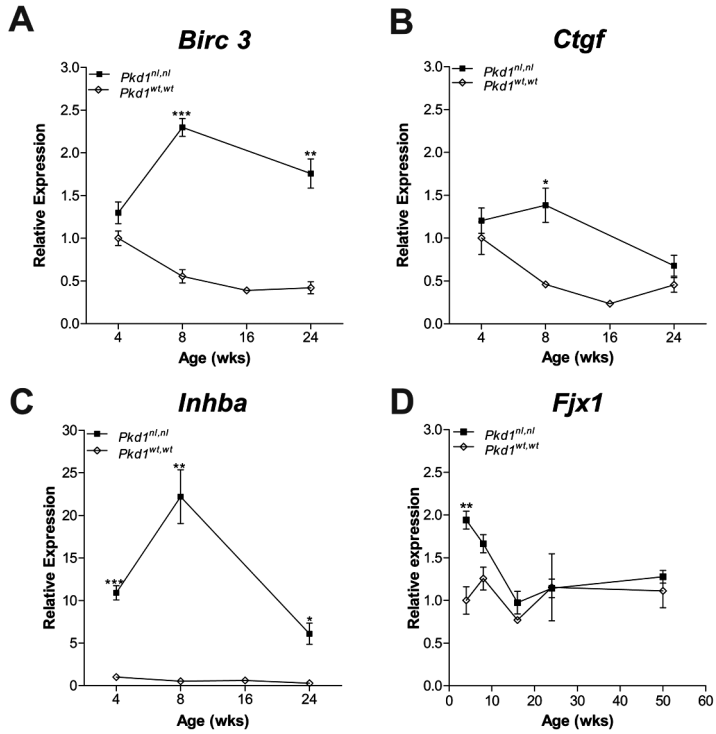


Figure S6: Expression of YAP targets. mRNA expression of YAP targets (A) *Birc3*, (B) *Ctgf* , (C) *Inhba* and (D) *Fjx1* at different ages as determined by real time PCR for *Birc3*, *Ctgf* and *Inhba* and RT-MLPA for *Fjx1*. Results are shown as expression relative to the expression of wild type mice at the age of 4 weeks, (mean ± SEM). Closed squares; *B6Ola-Pkd1*^{nl,nl} mice, open squares; *B6Ola-Pkd1*^{wt,wt}, *; P<0.05, **; P<0.01, ***; P<0.001.

7

Summarizing discussion



Summarizing discussion

Autosomal dominant polycystic kidney disease (ADPKD) is characterized by large fluid-filled cysts and progressive deterioration of renal function necessitating renal replacement therapy. In this thesis different phases of ADPKD were studied. The major findings of this study are incorporated in the schematic representation of the proposed sequence of events in cystogenesis and disease progression shown in figure 1. The initiation phase, with hyper proliferative epithelial cells as a hallmark, is followed by a phase of cyst growth and cyst expansion. Later on, proliferation of cystic epithelia ceases and interstitial fibrosis and inflammation become apparent.

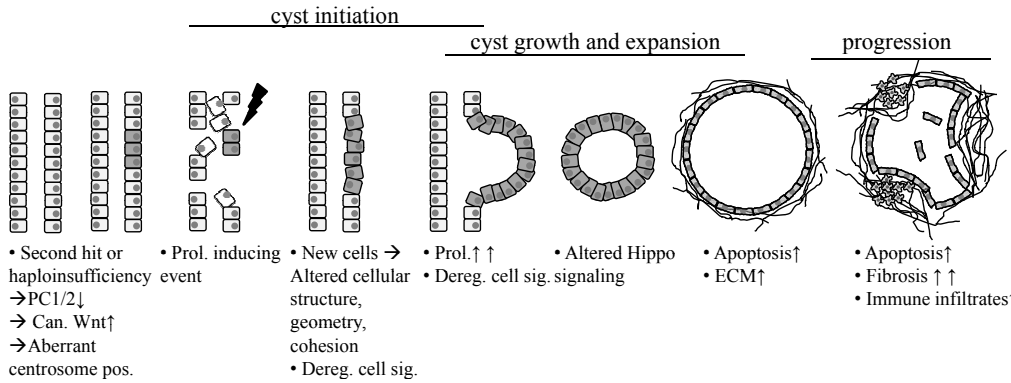


Figure 1. Schematic representation of the proposed sequence of events in cystogenesis and disease progression in ADPKD. All tubular epithelial cells contain one mutated *PKD1* or *PKD2* allele and one unaffected allele. During life, in a subset of cells, protein levels of PC1 and/or PC2 become misbalanced due to a second hit or haploinsufficiency. There are early changes after inactivation of the *PKD1* gene that alone are not sufficient for cyst formation such as up-regulation of canonical Wnt signaling and aberrant centrosome position (indicative of aberrant planar cell polarity).When *PKD1/2*-deficient cells proliferate in response to for example injury, cyst formation is initiated and many signaling pathways become deregulated. The epithelial cells become hyperproliferative and depolarized. Additional signaling pathways such as Hippo signaling become deregulated, thereby contributing to cyst growth and expansion. Subsequently, ECM production around cysts starts to occur and apoptosis is present in cystic epithelia. During the progression phase cysts collapse, fibrotic tissue is formed, and large immune infiltrates start to form.

Cyst initiation

In **chapter 3** the initiation of cyst formation was studied. In contrast to patients with ADPKD, a heterozygous mutation in *Pkd1* does hardly lead to cyst formation in mice. Using a tamoxifen-inducible, kidney epithelium-specific *Pkd1*-deletion mouse model, our group showed that inactivation of the *Pkd1* gene induces rapid cyst formation in developing kidneys and a slow onset of disease in adult mice.[1] Therefore, we hypothesized that the proliferative status of the renal tissue at the time of gene disruption is important for the rate at which cysts are formed after *Pkd1* conditional deletion. In **chapter 3** we investigated this hypothesis and showed that

Pkd1-gene disruption at PN40 leads to a disease progression rate intermediate to that of neonatal and adult mice as expected from the renal proliferation levels, which are intermediate to that of neonatal and adult mice. We also showed that DCVC-induced renal epithelial injury significantly accelerates the progression of renal cyst formation. The data in **chapter 3** confirm our hypothesis that cyst formation after *Pkd1*-gene disruption is dependent on the proliferative status of the renal epithelial cells, as renal epithelial injury is followed by a repair phase that includes proliferation to restore the tubular epithelial architecture (Fig.1)

After the increased proliferation during tissue regeneration, proliferation decreased to basal levels in *Pkd1*-deletion mice just as in DCVC-treated controls. However, in severe cystic kidneys, 10–14 weeks after injury, proliferation increased again. This biphasic response suggests that unrestricted cell proliferation after injury subsequent to *Pkd1*-gene deletion is not the underlying mechanism for cyst formation.

Similar to embryogenesis and renal development, tissue repair reactions require properly regulated cell proliferation to restore epithelial architecture. Defects in oriented cell division were observed during tubular elongation in renal development in non-orthologous animal models for PKD.[2, 3] In addition, loss of the Planar Cell Polarity (PCP) gene *Fat4* leads to renal cysts formation.[4] Altogether; these data suggest a potential role for aberrant PCP or oriented cell division.

In order to investigate whether defects in PCP during tissue regeneration could be involved in accelerated cyst formation as in adult *Pkd1*-deletion mice, we analyzed the position of centrosomes after repair of injury at a pre-cystic stage. The use of centrosome position as a readout system for PCP was discussed in **chapter 2 and 4**.

As expected, in the majority of cells of control mice (+DCVC), centrosomes are positioned close to the center of the apical membrane. In mutants with and without DCVC, however, a significantly different pattern in the distribution of centrosome position was observed. Centrosomes were positioned further away from its normal position in the center of the apical membrane above the middle of the nucleus. From these data, we conclude that improper positioning of centrosomes is an early event after *Pkd1*-gene disruption. Additionally, gene expression of several PCP-related genes was investigated and showed differential expression in pre-cystic kidneys of *Pkd1* conditional knockout mice. The expression pattern of Four-jointed-1 (*Fjx1)* is particularly interesting. Our results suggested that Four-jointed is needed during tissue repair. In *Pkd1*-deletion mutants, however, the expression of *Fjx1* decreased upon *Pkd1*-gene disruption, suggesting defects in PCP signaling. It is believed that when PCP signaling is aberrant, canonical Wnt signaling is activated.[5] Indeed signs of activated canonical Wnt signaling were observed.

Since in untreated *Pkd1*-deletion mice centrosome position and the expression of canonical Wnt targets were also altered, we conclude that these are early responses to *Pkd1*-gene disruption (Fig. 1). We speculate that these early alterations create a permissive condition for accelerating cyst formation and that additional factors are required. Abnormal integrity of the newly formed cells, resulting from the absence of *Pkd1* expression during repair, might be such a factor. It is likely

that polycystins are required during repair for the proper formation of these protein complexes. Without *Pkd1*, cellular structure, geometry and cohesion will be modified (Fig. 1). In agreement with this hypothesis, Silberberg *et al*. showed that polycystins are required for assembling cell-cell contacts.[6] Additionally, polycystin-1/-2 levels are elevated after ischemic injury.[7-9]

Concurrently with the publication of our study, a report was published also showing the accelerating effect of injury on cyst formation in *Pkd1* conditional knockout mice but without investigating planar cell polarity. However, in this study ischemic reperfusion injury was used instead of a nephrotoxic compound. Here, the cyst accelerating event is termed "third hit", where the first hit is the germ line mutation in the first *Pkd1* allele and the second a somatic mutation in the remaining "normal" allele, following the two hit hypothesis. The term "third hit", however, suggests that this hit is also a genetic hit, while it is in fact a modifying factor related to tubular epithelial proliferation. Recently, more papers were published regarding the role PCP signaling in ADPKD, including a study in which cyst formation was found without aberrant PCP signaling in pre-cystic stages and aberrant PCP signaling but without cyst formation.[10-12]

Additionally a recent paper suggested that cyst formation is more likely to be caused by non-canonical Wnt signaling, PCP signaling, than by the related canonical Wnt signaling. Here it was shown that in a *Pkd1* and *Pkd2* model no β-catenin activity was reported after establishment of urinary flow or in cystic epithelia.[13] How this study should be interpreted is unclear and requires further research, since many studies (including ours) showed that increased canonical Wnt signaling is associated with cyst formation. The results of all of these studies show that the puzzle is more complex and results and mechanisms may depend on the models used as was also discussed in **chapter 2.**

Hippo signaling and cyst growth

The Hippo signaling pathway is emerging as an important pathway, not only in organ size control but also in cancer. The product of the neurofibromatosis type II tumor suppressor gene (*NF2*), Merlin, is a regulator of the Hippo pathway. In addition, increased YAP expression and nuclear accumulation were shown in multiple types of human cancer.[14-17] This pathway is subject of investigation in **chapter 5**, as in chapter 3 we showed that during the repair phase of tubular epithelial injury, when PCP signaling is needed, renal mRNA expression of the PCP-pathway component Four-jointed (Fjx1), was increased in controls, but not in kidneys of the *Pkd1*-deletion mice. Here, the expression of *Fjx1* decreased after *Pkd1*-gene disruption and persisted at relatively low levels at pre-cystic stages. Interestingly, later on, in cystic kidneys *Fjx1* expression dramatically increased. The above mentioned roles of the Hippo pathway, together with the opposing expression pattern of *Fjx1* during epithelial repair and at cystic stages, triggered us to investigate the activity of the Hippo pathway during these processes.

In **chapter 5**, we provide for the first time evidence for altered activation of the Hippo signaling pathway in cyst growth in ADPKD and other cystic diseases. In different mouse models for

ADPKD, nuclear localization of YAP is observed only in cystic epithelia and dilated tubules but not in tubules of pre-cystic kidneys. Increased amounts of YAP-positive nuclei are observed in morphological aberrant tubules, dilated tubules, and cysts but not in normal-looking pre-cystic tubules. This suggests that aberrant Hippo signaling is not an initiating event in cyst formation but accompanies progressive cystic growth.

Our findings, showing altered Hippo signaling during cyst growth, are in line with previous studies reporting renal cyst formation caused by disturbed Hippo signaling; for example, deregulation of YAP in zebrafish results in pro-nephric cyst formation.[18, 19] In addition, mice lacking TAZ (Wwtr1), the YAP paralog, show renal cystic disease.[19-21]

The results in **chapter 5** strengthen the concept that during epithelial repair, Four-jointed is involved in PCP signaling, while in cystic kidneys it is related to cyst growth. Decreased expression of *Fjx1* is a direct effect of *Pkd1* inactivation, while increased *Fjx1* and YAP target expression can be regarded as an effect of altered signaling during cyst growth, an indirect effect of *Pkd1* inactivation (Fig. 1).

Although both under- and over-expression of YAP, as well as TAZ deficiency, can result in cyst formation in animal models, in renal cystic disease it seems to be associated with an increase in nuclear YAP, as shown in the different mouse models for ADPKD. This is confirmed by the results in patients with ADPKD and ARPKD, demonstrating nuclear localization of YAP in epithelia in the majority of cysts. In addition, we showed that, nuclear translocation of YAP in cystic epithelia was accompanied by the up-regulation of several postulated targets of YAP in cystic kidneys. Additionally, increased nuclear YAP was observed not only in cystic epithelia in ADPKD and ARPKD, but also in cystic epithelia in different renal tumors and in liver cysts derived from bile ducts of hypomorphic *Pkd1* mutants. It is therefore tempting to speculate that altered Hippo signaling is a general feature in cystogenesis.

Polycystic kidneys have been elegantly called 'neoplasia in disguise'.[22] Indeed, many pathways involved in neoplastic growth are also involved in cyst formation. It is not surprising that a number of drugs developed for the treatment of cancer have been shown to be effective in attenuating cyst growth in PKD mouse models.[23-28] This supports the idea that targeting the Hippo pathway could be effective in inhibiting cyst expansion and slowing down progression towards end-stage renal failure in PKD. An interesting future experiment will be to explore whether *in vivo* absence of YAP during cyst growth indeed attenuates cyst expansion.

Recently YAP and TAZ were found to be transcription factors involved in relaying mechanical signals exerted by ECM rigidity and cell shape. This regulation requires Rho GTPase activity and tension of the actomyosin cytoskeleton, but is independent of the Hippo signaling pathway.[29] Interestingly, *Pkd1* and *Pkd2* are also thought to be involved in mechano-transduction and are known to play a role in arterial pressure sensing.[30] In addition, the Rho GTPase Cdc42 is up-regulated in pre-cystic kidneys of *Pkd1* conditional knockout mice.[10] It would be interesting to investigate whether the role of YAP in cyst growth is dependent on the Hippo signaling cascade with or without crosstalk with PCP signaling through Four-jointed, mechano-transduction, or both.

Disease progression

Chapter 3 and **chapter 5 describe** processes involved in cyst initiation and cyst growth, while **chapter 6** deals with aspects involved in disease progression.

Many mouse and rat models exist for studying the formation and subsequent growth of cysts in polycystic kidney disease. However, few models have been described representing the phenotype observed in ADPKD patients with advanced stage disease. Clearly, animal models with a phenotype that resembles the human pathology are needed to predict accurately the effect of potential therapeutics on disease progression in ADPKD patients.

The *Pkd1*^{nl,nl} mouse model is a model for PKD in which the variation of the phenotype depends on the genetic background. Here we report that on a controlled 50%/50% genetic background of B6 and Ola (*B6Ola*), *Pkd1*^{nl,nl} mice develop large cystic kidneys within 4 weeks and are able to survive up to a year. In contrast, to the models homozygous for a *Pkd1* inactivating allele, *B6Ola-Pkd1*^{nl,nl} mice, express low levels of *Pkd1*, are viable, and exhibit grossly normal kidney structure, but with dilated proximal tubules at birth.[31-35] Although expression of the full length *Pkd1* transcript is strongly reduced, a 3'-transcript is still produced and it cannot be excluded that this may have an effect on renal development and survival.[36]

In *B6Ola-Pkd1*^{nl,nl} mice, tubular dilatation and the first cysts could be observed at post-natal day 1. The first cysts are mostly from proximal tubular origin while later on the majority of cysts appeared to be derived from distal tubules, or collecting ducts.

Interestingly, *B6Ola-Pkd1*^{nl,nl} mice show an initial increase in renal volume, followed by a decrease in renal and cystic volume. The partial regression in renal volume was accompanied by "collapse" of cysts, which was paralleled by an increase in fibrosis and influx of inflammatory cells (Fig. 1). In addition, apoptosis in cystic epithelia was highest during the period of regression in renal volume, suggesting that altered balance between apoptosis and proliferation, favoring apoptosis, may play a role in the regression and "collapse" of cysts.

Previously, it was already suggested that apoptosis plays an important role in the pathogenesis of PKD. Apoptosis was found to be abundantly present in cystic as well as non-cystic epithelia in polycystic kidneys of PKD mouse and patients and was suggested to contribute to the loss of normal renal tubules. Although, apoptosis may not be involved in cystogenesis, it may play an important role in the progression of the disease and the progressive deterioration of renal function.[37] The regression of renal volume in our mouse model is a striking phenomenon that is also observed in ARPKD patients that survive the neonatal period.[38, 39] However, careful investigation of renal tissue of ADPKD patients revealed regressing or collapsing cysts, as well as cyst remnants. It can be expected that in classical forms of ADPKD, the phenomenon of collapsing cysts will not occur extensively.

Renal volume as clinical end-point used in clinical trials for ADPKD[40, 41] was questioned after disappointing results of clinical trials with mTOR inhibitors. It was suggested that renal volume might not be the best end-point in advanced PKD.[22, 42] Indeed we only observed a minor effect

on renal volume after low dose sirolimus treatment in the *B6Ola-Pkd1*^{nl,nl} model.[43] In line with our data, regarding renal volume regression, and increased fibrosis and inflammatory infiltrates, a study revealed that extent of fibrosis and inflammation correlates better with disease progression to renal failure than renal volume.[44] It would be worthwhile investigating the applicability of if this method as clinical end-point in clinical or trials or maybe even in daily clinical practice.

Models, in which almost all nephrons develop cysts simultaneously in a relative short time span, are useful to study cyst initiation and progression. However, models closely resembling advanced stage human ADPK are of outmost importance, especially to better predict the effect of new therapeutics.

With regard to the characteristic aspects of human ADPKD disease progression, fibrosis and inflammation,[45] the *B6Ola-Pkd1*^{nl,nl} model shows great similarity with the human ADPKD renal pathology. Even more, when onset and degree of nephrons involved is taken into account, the model mostly resembles patients with two incomplete penetrant alleles of *PKD1* and *PKD2*, showing a severe early onset renal cystic phenotype.[46-48] It would be interesting to identify the course of the disease renal volume changes in these patients.

The *B6Ola-Pkd1*^{nl,nl} model not only resembles the phenotype of human ADPKD ; it also shows altered activity of canonical Wnt signaling, TGF-β signaling, the mTOR pathway and Hippo signaling, all of them are found to be altered in models for PKD and , importantly, in renal tissue ADPKD patients.[43, 49-52, 52-57]

In conclusion, the renal cystic phenotype of *B6Ola Pkd1*^{nl,nl} mice seems to reflect the phenotype of patients with early onset PKD as result of two hypomorphic mutations. In addition, this model showed that regression of cysts and renal volume occurs, implying that renal volume may not be a good predictor of progression to renal failure and end stage renal disease.

General discussion

In this thesis it was shown that injury induced proliferation is involved in cyst formation. Altered PCP and Wnt signaling create a permissive condition in which requires an additional factor setting cyst formation in motion. Abnormal integrity of the newly formed cells, resulting from the absence of *Pkd1* expression during repair, might be such a factor (Fig. 1). As the base of this aberrant cellular integrity lies within the epithelial repair it would be interesting to investigate the process of repair more carefully, as in our study no differences at the end of repair between controls *Pkd1* heterozygotes and conditional *Pkd1*-deletion mice were observed, while others did for *Pkd1* and *Pkd2* mutant mice with other types of injury.[58, 59] Possibly, differences can be observed in earlier phases, before repair approaches completion.

In ADPKD patients injury induced proliferation may occur as well. The injury causing factors can be of exogenous as well as endogenous origin. Especially when there are already cysts present

surrounded by relatively normal renal parenchyma. These cysts compress the surrounding tissue and are a source for oxidative stress and injury, causing proliferation. When the disease progresses more, inflammatory cells as well as the presence of fibrotic tissue become a source of injury and proliferation. This accelerates the cyst formation in healthy tubules and in its turn provides more sources of injury and proliferation.

Then we showed that the Hippo signaling pathway is also implicated in cyst growth. This pathway is known to be implicated in organ size control, tumorigenesis and recently also tissue regeneration and stem cell self renewal. Although a complex network of signaling pathways is involved in cyst growth, finding treatment for ADPKD may benefit from the great promise that the Hippo-YAP pathway holds as a target for anti-cancer therapy and regenerative medicine.

Finally disease progression was studied and showed that the *B6Ola-Pkd1* mouse model showed regression of renal and cystic volume followed by fibrosis and inflammation. This was not seen in the conditional *Pkd1*-deletion model. In these mice fibrosis is hardly observed probably due to the rapid cyst formation in all most all nephrons synchronously, leading to renal failure. Furthermore, in these mice *Pkd1* deletion is only achieved in renal epithelial cells while in *B6Ola-Pkd1* mice all cells express low levels of *Pkd1*, including fibroblast and inflammatory cells. As altered activation of Cdc42, a protein involved in cell migration, was found to be involved in cystogenesis in *Pkd1* mutant mice[10], it would interesting to investigate the effect of *Pkd1* deletion in fibroblast and inflammatory cells and their role in ADPKD disease progression. In addition, macrophage depletion studies in mice with PKD provide evidence for an accelerating role of macrophages in growth of renal cysts.[60] However, in the *Pkd1* model used only renal epithelial cells were depleted of polycystin-1, while the *Pkd2* model all cells have reduced polycystin-2 expression. As inflammation and interstitial fibrosis, in which macrophages play an important role, are important in ADPKD disease progression, therapies also targeting macrophage recruitment into the kidney may be beneficial in the treatment of ADPKD disease progression.

Due to the similarities with the human ADPKD renal pathology the *B6Ola-Pkd1* mice provide a suitable model to study the effect of potential therapeutic drugs on ADPKD disease progression. In addition this model showed that renal volume is a poor clinical end point as surrogate for disease progression.

Taken together cyst formation, cyst growth and ADPKD disease progression are complex processes regulated by many signaling networks. This not only provides many targets for therapeutic intervention but is also a difficulty at the same time. Aiming for a single therapeutic target will most likely be not successful, and therapeutic intervention in ADPKD requires a multi-target therapy.

References

1. Lantinga-van Leeuwen,I.S. *et al.* Kidney-specific inactivation of the Pkd1 gene induces rapid cyst formation in developing kidneys and a slow onset of disease in adult mice. *Hum. Mol. Genet.* **16**, 3188-3196 (2007).
2. Fischer,E. *et al.* Defective planar cell polarity in polycystic kidney disease. *Nat. Genet.* **38**, 21-23 (2006).
3. Patel,V. *et al.* Acute kidney injury and aberrant planar cell polarity induce cyst formation in mice lacking renal cilia. *Hum. Mol. Genet.* **17**, 1578-1590 (2008).
4. Saburi,S. *et al.* Loss of Fat4 disrupts PCP signaling and oriented cell division and leads to cystic kidney disease. *Nat. Genet.* **40**, 1010-1015 (2008).
5. Simons,M. *et al.* Inversin, the gene product mutated in nephronophthisis type II, functions as a molecular switch between Wnt signaling pathways. *Nat. Genet.* **37**, 537-543 (2005).
6. Silberberg,M., Charron,A.J., Bacallao,R., & Wandinger-Ness,A. Mispolarization of desmosomal proteins and altered intercellular adhesion in autosomal dominant polycystic kidney disease. *Am. J. Physiol Renal Physiol* **288**, F1153-F1163 (2005).
7. Ibraghimov-Beskrovnaya,O. *et al.* Polycystin: in vitro synthesis, in vivo tissue expression, and subcellular localization identifies a large membrane-associated protein. *Proc. Natl. Acad. Sci. U. S. A* **94**, 6397-6402 (1997).
8. Zhao,Y., Haylor,J.L., & Ong,A.C. Polycystin-2 expression is increased following experimental ischaemic renal injury. *Nephrol. Dial. Transplant.* **17**, 2138-2144 (2002).
9. Obermuller,N. *et al.* Altered expression pattern of polycystin-2 in acute and chronic renal tubular diseases. *J. Am. Soc. Nephrol.* **13**, 1855-1864 (2002).
10. Luyten,A. *et al.* Aberrant regulation of planar cell polarity in polycystic kidney disease. *J. Am. Soc. Nephrol.* **21**, 1521-1532 (2010).
11. Nishio,S. *et al.* Loss of oriented cell division does not initiate cyst formation. *J. Am. Soc. Nephrol.* **21**, 295-302 (2010).
12. Li,L. *et al.* Aberrant planar cell polarity induced by urinary tract obstruction. *Am. J. Physiol Renal Physiol* **297**, F1526-F1533 (2009).
13. Miller,M.M. *et al.* T-cell factor/beta-catenin activity is suppressed in two different models of autosomal dominant polycystic kidney disease. *Kidney Int.* **80**, 146-153 (2011).
14. Zender,L. *et al.* Identification and validation of oncogenes in liver cancer using an integrative oncogenomic approach. *Cell* **125**, 1253-1267 (2006).
15. Dong,J. *et al.* Elucidation of a universal size-control mechanism in Drosophila and mammals. *Cell* **130**, 1120-1133 (2007).
16. Steinhardt,A.A. *et al.* Expression of Yes-associated protein in common solid tumors. *Hum. Pathol.* **39**, 1582-1589 (2008).
17. Hao,Y., Chun,A., Cheung,K., Rashidi,B., & Yang,X. Tumor suppressor LATS1 is a negative regulator of oncogene YAP. *J. Biol. Chem.* **283**, 5496-5509 (2008).
18. Skouloudaki,K. *et al.* Scribble participates in Hippo signaling and is required for normal zebrafish pronephros development. *Proc. Natl. Acad. Sci. U. S. A* **106**, 8579-8584 (2009).
19. Tian,Y. *et al.* TAZ promotes PC2 degradation through a SCFbeta-Trcp E3 ligase complex. *Mol. Cell Biol.* **27**, 6383-6395 (2007).
20. Hossain,Z. *et al.* Glomerulocystic kidney disease in mice with a targeted inactivation of Wwtr1. *Proc. Natl. Acad. Sci. U. S. A* **104**, 1631-1636 (2007).
21. Makita,R. *et al.* Multiple renal cysts, urinary concentration defects, and pulmonary emphysematous changes in mice lacking TAZ. *Am. J. Physiol Renal Physiol* **294**, F542-F553 (2008).
22. Grantham,J.J. Polycystic kidney disease: neoplasia in disguise. *Am. J. Kidney Dis.* **15**, 110-116 (1990).
23. Wilson,S.J. *et al.* Inhibition of HER-2(neu/ErbB2) restores normal function and structure to polycystic kidney disease (PKD) epithelia. *Biochim. Biophys. Acta* **1762**, 647-655 (2006).
24. Sweeney,W.E., Jr., von Vigier,R.O., Frost,P., & Avner,E.D. Src inhibition ameliorates polycystic kidney disease. *J. Am. Soc. Nephrol.* **19**, 1331-1341 (2008).
25. Bukanov,N.O., Smith,L.A., Klinger,K.W., Ledbetter,S.R., & Ibraghimov-Beskrovnaya,O. Long-lasting arrest of murine polycystic kidney disease with CDK inhibitor roscovitine. *Nature* **444**, 949-952 (2006).

26. Park,J.Y. *et al.* p21 is decreased in polycystic kidney disease and leads to increased epithelial cell cycle progression: roscovitine augments p21 levels. *BMC. Nephrol.* **8**, 12 (2007).
27. Omori,S. *et al.* Extracellular signal-regulated kinase inhibition slows disease progression in mice with polycystic kidney disease. *J. Am. Soc. Nephrol.* **17**, 1604-1614 (2006).
28. Zhao,B., Li,L., Lei,Q., & Guan,K.L. The Hippo-YAP pathway in organ size control and tumorigenesis: an updated version. *Genes Dev.* **24**, 862-874 (2010).
29. Dupont,S. *et al.* Role of YAP/TAZ in mechanotransduction. *Nature* **474**, 179-183 (2011).
30. Sharif-Naeini,R. *et al.* Polycystin-1 and -2 dosage regulates pressure sensing. *Cell* **139**, 587-596 (2009).
31. Boulter,C. *et al.* Cardiovascular, skeletal, and renal defects in mice with a targeted disruption of the Pkd1 gene. *Proc. Natl. Acad. Sci. U. S. A* **98**, 12174-12179 (2001).
32. Kim,K., Drummond,I., Ibraghimov-Beskrovnaya,O., Klinger,K., & Arnaout,M.A. Polycystin 1 is required for the structural integrity of blood vessels. *Proc. Natl. Acad. Sci. U. S. A* **97**, 1731-1736 (2000).
33. Muto,S. *et al.* Pioglitazone improves the phenotype and molecular defects of a targeted Pkd1 mutant. *Hum. Mol. Genet.* **11**, 1731-1742 (2002).
34. Wu,G. *et al.* Cardiac defects and renal failure in mice with targeted mutations in Pkd2. *Nat. Genet.* **24**, 75-78 (2000).
35. Lu,W. *et al.* Comparison of Pkd1-targeted mutants reveals that loss of polycystin-1 causes cystogenesis and bone defects. *Hum. Mol. Genet.* **10**, 2385-2396 (2001).
36. Trudel,M. & Kurbegovic,A. Toward Understanding Pkd1 Cystogenetic Mechanism. *J. Am. Soc. Nephrol.* **22**, 59A (2011).
37. Woo,D. Apoptosis and loss of renal tissue in polycystic kidney diseases. *N. Engl. J. Med.* **333**, 18-25 (1995).
38. Gunay-Aygun,M. *et al.* Correlation of kidney function, volume and imaging findings, and PKHD1 mutations in 73 patients with autosomal recessive polycystic kidney disease. *Clin. J. Am. Soc. Nephrol.* **5**, 972-984 (2010).
39. Bergmann,C. *et al.* Clinical consequences of PKHD1 mutations in 164 patients with autosomal-recessive polycystic kidney disease (ARPKD). *Kidney Int.* **67**, 829-848 (2005).
40. Serra,A.L. *et al.* Sirolimus and kidney growth in autosomal dominant polycystic kidney disease. *N. Engl. J. Med.* **363**, 820-829 (2010).
41. Walz,G. *et al.* Everolimus in patients with autosomal dominant polycystic kidney disease. *N. Engl. J. Med.* **363**, 830-840 (2010).
42. Watnick,T. & Germino,G.G. mTOR inhibitors in polycystic kidney disease. *N. Engl. J. Med.* **363**, 879-881 (2010).
43. Novalic,Z. *et al.* Dose-dependent effects of sirolimus on mTOR-signaling and PKD in Pkd1-mouse models. *J. Am. Soc. Nephrol.*(2011).
44. Caroli,A. *et al.* Intermediate Volume on Computed Tomography Imaging Defines a Fibrotic Compartment that Predicts Glomerular Filtration Rate Decline in Autosomal Dominant Polycystic Kidney Disease Patients. *Am. J. Pathol.* **179**, 619-627 (2011).
45. Zeier,M. *et al.* Renal histology in polycystic kidney disease with incipient and advanced renal failure. *Kidney Int.* **42**, 1259-1265 (1992).
46. Rossetti,S. *et al.* Incompletely penetrant PKD1 alleles suggest a role for gene dosage in cyst initiation in polycystic kidney disease. *Kidney Int.* **75**, 848-855 (2009).
47. Vujic,M. *et al.* Incompletely penetrant PKD1 alleles mimic the renal manifestations of ARPKD. *J. Am. Soc. Nephrol.* **21**, 1097-1102 (2010).
48. Losekoot,M. *et al.* Neonatal onset autosomal dominant polycystic kidney disease (ADPKD) in a patient homozygous for a PKD2 missense mutation due to uniparental disomy. *Journal of Medical Genetics*(2011).
49. Lin,F. *et al.* Kidney-specific inactivation of the KIF3A subunit of kinesin-II inhibits renal ciliogenesis and produces polycystic kidney disease. *Proc. Natl. Acad. Sci. U. S. A* **100**, 5286-5291 (2003).
50. Happé,H. *et al.* Toxic tubular injury in kidneys from Pkd1-deletion mice accelerates cystogenesis accompanied by dysregulated planar cell polarity and canonical Wnt signaling pathways. *Hum. Mol. Genet.* **18**, 2532-2542 (2009).
51. Hassane,S. *et al.* Elevated TGFbeta-Smad signalling in experimental Pkd1 models and human patients with polycystic kidney disease. *J. Pathol.* **222**, 21-31 (2010).
52. Happé,H. *et al.* Altered Hippo signalling in polycystic kidney disease. *J. Pathol.* **224**, 133-142 (2011).
53. Shillingford,J.M. *et al.* The mTOR pathway is regulated by polycystin-1, and its inhibition reverses renal cystogenesis in polycystic kidney disease. *Proc. Natl. Acad. Sci. U. S. A* **103**, 5466-5471 (2006).

54. Bonnet,C.S. *et al.* Defects in cell polarity underlie TSC and ADPKD-associated cystogenesis. *Hum. Mol. Genet.* **18**, 2166-2176 (2009).
55. Song,X. *et al.* Systems biology of autosomal dominant polycystic kidney disease (ADPKD): computational identification of gene expression pathways and integrated regulatory networks. *Hum. Mol. Genet.* **18**, 2328-2343 (2009).
56. Hartman,T.R. *et al.* The tuberous sclerosis proteins regulate formation of the primary cilium via a rapamycin-insensitive and polycystin 1-independent pathway. *Hum. Mol. Genet.* **18**, 151-163 (2009).
57. Fischer,D.C. *et al.* Activation of the AKT/mTOR pathway in autosomal recessive polycystic kidney disease (ARPKD). *Nephrol. Dial. Transplant.* **24**, 1819-1827 (2009).
58. Bastos,A.P. *et al.* Pkd1 haploinsufficiency increases renal damage and induces microcyst formation following ischemia/reperfusion. *J. Am. Soc. Nephrol.* **20**, 2389-2402 (2009).
59. Prasad,S., McDaid,J.P., Tam,F.W., Haylor,J.L., & Ong,A.C. Pkd2 dosage influences cellular repair responses following ischemia-reperfusion injury. *Am. J. Pathol.* **175**, 1493-1503 (2009).
60. Karihaloo,A. *et al.* Macrophages promote cyst growth in polycystic kidney disease. *J. Am. Soc. Nephrol.* **22**, 1809-1814 (2011).

8

Nederlandse samenvatting voor niet-ingewijden

Nederlandse samenvatting voor niet-ingewijden

Autosomal Dominant Polycystic Kidney Disease (ADPKD) is een van de meest voorkomende erfelijke aandoeningen. Deze ziekte heeft als belangrijkste kenmerk de vorming van met vloeistof gevulde cysten (vochtblazen) in de nieren. Maar ook in de lever en alvleesklier kunnen cysten ontstaan. Vaak hebben patiënten ook last van een hoge bloeddruk en kunnen er zwakke plekken in de bloedvaten optreden. Over een periode van tientallen jaren vormen er zich duizenden met vocht gevulde cysten die de plaats innemen van het gezonde nierweefsel, wat resulteert in een slechter functioneren van de nieren. Uiteindelijk zijn de meeste patiënten tussen hun 50e en 60e levensjaar aangewezen op nierdialyse omdat er niet genoeg gezond nierweefsel over is om alle afvalstoffen uit het bloed te filteren. Op dit moment zijn er nog geen medicijnen beschikbaar om de vorming van de cysten in de nieren te vertragen of te voorkomen en daarmee een volledige uitval van de nierfunctie te voorkomen.
Om medicijnen te kunnen ontwikkelen om deze patiënten te kunnen behandelen is het nodig om het mechanisme te begrijpen wat ten grondslag ligt aan de cystenvorming en het ontwikkelen van volledige uitval van de nierfunctie. Hiervoor is wetenschappelijk onderzoek nodig.
Het doel van mijn promotieonderzoek was om te onderzoeken hoe de cysten in de nier nu ontstaan en welke factoren hier een rol bij spelen. Ook heb ik de groei van cysten bestudeerd en de ontwikkeling bekeken van een nier met cysten die nog voldoende functioneert naar een nier met volledige uitval van de nierfunctie.

ADPKD wordt veroorzaakt door een fout (mutatie) in het *PKD1*- of *PKD2*-gen. Patiënten met ADPKD hebben in hun DNA één foute en één goede kopie van het *PKD1* of *PKD2* gen, terwijl gezonde mensen twee goede kopieën van hun ouders hebben gekregen. De nieren zijn opgebouwd uit nefronen; de functionele eenheden van de nier. Een nefron bestaat uit een filtertje en een nierbuisje dat de urine opvangt. In de nieren van ADPKD patiënten wordt een probleem veroorzaakt door de cellen die de binnenkant van de nierbuisjes bekleden. Om de goede opbouw van de nierbuisjes te behouden zijn er gebalanceerde hoeveelheden nodig van het polycystine-1 (PC1) en 2 (PC2) eiwit. Het recept om deze eiwitten te maken staat beschreven in respectievelijk het *PKD1*- en *PKD2*-gen. Wetenschappelijk onderzoek heeft laten zien dat bij muizen het uitschakelen van één *Pkd1* kopie niet resulteert in de vorming van ernstige cystennieren, terwijl het uitschakelen van beide kopieën de dood voor de geboorte of vlak daarna tot gevolg heeft. Dit heeft geleid tot de hypothese dat in het geval van ADPKD, in een subset van de cellen die de nierbuisjes bekleden, de hoeveelheid van PC1 of PC2 onder een kritische waarde moet dalen om cystenvorming als gevolg te hebben. Dit kan veroorzaakt worden door een mutatie in of verminderde aanmaak van PC1 of 2 vanaf de gezonde kopie, respectievelijk de zogenaamde "second hit", of haploinsuffieciëncy genoemd.
Binnen de onderzoeksgroep waar ik gewerkt heb aan mijn promotieonderzoek, is een muismodel voor ADPKD gemaakt waarin in de cellen van de nierbuisjes van deze muis het gezonde *Pkd1*-gen

op een willekeurig moment kan worden uitgeschakeld. Dit model wordt het induceerbare *Pkd1*-deletie model genoemd. Op deze manier is het mogelijk om het dodelijke effect van volledige uitschakeling te omzeilen en cystenvorming te bestuderen.
Uit experimenten met dit diermodel bleek dat het belangrijk was of de cellen in het nierbuisje aan het delen waren of niet. In hele jonge muizen is de nier nog aan het groeien, en worden de nierbuisjes langer door deling van de cellen die het buisje bekleden. Als in deze hele jonge muizen het tweede *Pkd1* kopie wordt uitgeschakeld, krijgen deze muizen zeer ernstige cystennieren. Wanneer het gen in volwassen muizen, waarin de cellen van de nierbuisjes nauwelijks nog delen, wordt uitgeschakeld, ontstaan er nauwelijks cysten in de nieren en duurt het bovendien erg lang voordat deze ontstaan. Hieruit volgde de hypothese dat de status van de mate van celdeling van de cellen die de nierbuisjes bekleden, belangrijk is voor de snelheid waarmee cystennieren ontstaan.
Hoofdstuk 3 van dit proefschrift beschrijft een test van deze hypothese. In volwassen muizen werd eerst het gezonde *Pkd1* kopie uitgeschakeld. Vervolgens hebben we celdeling van de cellen in de nierbuisjes veroorzaakt. Er werd met een chemische stof, genaamd DCVC, schade aangebracht aan de cellen van de nierbuisjes. Hierdoor gaan er cellen dood en gaan de overgebleven cellen deze schade vervolgens repareren door te delen en de lege plaatsen weer op te vullen. De door de schade veroorzaakte celdeling bleek inderdaad de cystenvorming in de nieren aanzienlijk te versnellen. Daarnaast hebben we aangetoond dat er na volledige uitschakeling van het *Pkd1*-gen er een aantal vroege veranderingen optreden in bepaalde signaleringsroutes.
Voor het goed functioneren van een cel is het belangrijk dat de informatie van buiten de cel verwerkt wordt in de cel en dat deze daar op de juiste manier op reageert, door bijvoorbeeld bepaalde eiwitten te produceren. Vaak wordt in het lichaam informatie verstuurd via chemische stoffen die kunnen binden aan de "ontvangers" aan de buitenkant van de cel. De "ontvangers" aan de buitenkant van de cel worden receptoren genoemd, en de stoffen die eraan binden, liganden. Deze liganden en receptoren werken volgens een sleutel-slot principe. Alleen met de goede sleutel gaat het slot open en volgt er een cascade van reacties in de cel die tot de benodigde reactie van de cel leidt. De eiwitten en processen die nodig zijn voor een specifieke cascade van reacties op een bepaald ligand, worden samen een signaaltransductie route of signaleringsroute genoemd.
Als vroege verandering na uitschakeling van het *Pkd1*-gen werd verhoogde activatie van de Wnt-signaleringsroute gevonden. Deze Wnt-signaleringsroute is belangrijk tijdens de embryonale ontwikkeling.Verhoogde activiteit van deze route zorgt o.a. voor verhoogde celdeling. Een andere verandering is een verstoring in de planar cell polarity. De cellen die de nierbuisjes bekleden, hebben een boven- en een onderkant. De onderkant is de kant waarmee de cel vast zit aan de wand van het nierbuisje. De bovenkant van de cel is naar de ruimte aan de binnenkant van het nierbuisje gericht.
Naast deze vorm polariteit, die haaks op de wand van het nierbuisje staat, is er ook polariteit van de cellen die parallel loopt met de wand van het nierbuisje. Deze polariteit, planar cell

polarity, geeft de cel informatie over wat de lengte- en breedterichting van het nierbuisje is. Dit is belangrijk om te zorgen dat bijvoorbeeld tijdens de ontwikkeling van de nierbuisjes de buisjes langer worden, maar dat de diameter gelijk blijft. Ook bij herstel zorgt planar cell polarity ervoor dat het nierbuisje de goede vorm blijft houden. In **hoofdstuk 4** wordt een techniek die wij gebruikt hebben om de planar cell polarity te bestuderen uitgebreid beschreven.
De vroege veranderingen na het uitschakelen van het *Pkd1*-gen zijn (gedeeltelijk) nodig voor de vorming van cysten, maar zijn op zichzelf niet genoeg; er is nog een additionele factor nodig. De verstoorde opbouw van nieuwe cellen na celdeling in afwezigheid van PC1 zou die factor kunnen zijn. Deze verstoorde opbouw zorgt ervoor dat nog meer signaleringsroutes ontregeld raken en de cellen beginnen te delen en een uitstulping vormen in het nierbuisje. Uit deze uitstulping ontstaat uiteindelijk een afgesloten cyste die in grootte verder toeneemt.

Een van de onderzochte genen, waarvan het product in de regulatie van planar cell polarity een rol speelt, wekte onze interesse. Dit eiwit, genaamd "fourjointed", maakt niet alleen deel uit van de signalering die planar cell polarity reguleert, maar ook van de Hippo-signaleringsroute. De Hippo-signaleringsroute speelt een rol bij het controleren van de grootte van organen in de fruitvlieg en is ook van belang bij verschillende vormen van kanker in de mens. In **hoofdstuk 5** is onderzocht of de Hippo-signaleringsroute een aandeel heeft in het proces van cystenvorming. Er werd geen verandering gevonden in de Hippo-signaleringsroute vóór de initiatie van cystenvorming. Echter in verwijde nierbuisjes en cysten werd wel een verandering waargenomen in de Hippo-signalering. Hieruit kan geconcludeerd worden dat de Hippo signaleringsroute geen rol speelt in de initiatie van cystenvorming in de nieren, maar samen gaat met de groei van cysten en zeer waarschijnlijk ook bijdraagt aan die groei.

Naast de initiatie van cystenvorming en de groei van cysten komt ook de progressie van ADPKD in dit proefschrift aan bod. **Hoofdstuk 6** beschrijft factoren die belangrijk zijn bij de progressie van cystennieren naar levensbedreigende uitval van de nierfunctie. Verschillende muismodellen, zoals het induceerbare *Pkd1*-deletie model, zijn beschikbaar om de vorming en daaropvolgende groei van cysten te bestuderen. Echter, er zijn weinig modellen beschreven die het uiterlijk, fenotype, van de humane cystennieren in een gevorderd stadium van de ziekte weerspiegelen. In hoofdstuk 6 wordt een muismodel dat maar 15-20% van de normale hoeveelheid PC1 aanmaakt, het $Pkd1^{nl,nl}$ model, beschreven. Deze muizen hebben bij de geboorte verwijde nierbuisjes en in een periode van 4 weken ontwikkelen ze grote cystennieren maar ze kunnen 12 maanden oud worden. In de eerste 4 weken werd een grote toename in het volume van de nieren waargenomen, daarna nam het niervolume weer af. Tegelijkertijd was er sprake van regressie van cysten, ze werden kleiner, ze stortten als het ware in. Deze afname in niervolume en collaps van cysten, ging gepaard met een toename in fibrose, de vorming van littekenweefsel, en later een toename van het aantal ontstekingscellen. Op een leeftijd van 4 weken, als het niervolume maximaal is, is ook gecontroleerde celdood het hoogst. Dit betekent dat gecontroleerde celdood een rol zou kunnen spelen in de regressie van de cysten.

De collaps en het verdwijnen van cysten in het *Pkd1*^{nl,nl} muismodel wordt ook waargenomen in nierweefsel van ADPKD patiënten, echter op veel minder grote schaal.
Met betrekking tot de karakteristieke aspecten van het ziektebeloop van ADPKD, fibrose en ontsteking laat het *Pkd1*^{nl,nl} muismodel grote overeenkomsten zien met de nieren van ADPKD patiënten. Daarnaast heeft dit model laten zien dat regressie van niervolume en cysten plaatsvindt, wat impliceert dat het volume van de nier geen goede voorspellende factor is voor het ontwikkelen van volledige uitval van de nierfunctie.
Uit de resultaten beschreven in dit proefschrift kunnen we concluderen dat de mate van celdeling van de cellen van de nierbuisjes belangrijk is voor de vorming van cysten in de nier.

De vroege veranderingen die optreden direct na het uitschakelen van het *Pkd1*-gen maken de cellen vatbaar voor cystenvorming, maar zijn alleen niet voldoende om tot cystenvorming te leiden. Celdeling van de cellen van de nierbuisjes is noodzakelijk om deze cellen daadwerkelijk tot cystenvorming aan te zetten. Afwijkende opbouw van de nieuw gevormde cellen zou hier een belangrijke rol in kunnen spelen. De basis van deze afwijkende opbouw ligt in het herstel na schade en het zou interessant zijn om het herstelproces na schade in meer detail te bekijken.
Vervolgens hebben we laten zien dat de Hippo-signaleringsroute samen gaat met de groei van cysten en mogelijk ook bijdraagt aan die groei. Vervolg experimenten zijn nodig om te laten zien dat deze signaleringsroute daadwerkelijk bijdraagt aan de groei van cysten door in te grijpen in deze signaleringsroute in één van de muismodellen voor ADPKD. Als blijkt dat de Hippo-signaleringsroute inderdaad bijdraagt aan cystengroei, is dit een nieuw aangrijpingspunt voor therapie om de cystengroei te remmen.
Ten slotte blijkt het *Pkd1*^{nl,nl} muismodel grote overeenkomst te vertonen met de humane pathologie van ADPKD. Dit muismodel laat een afname van het niervolume en collaps van de cysten zien, die gepaard gaat met de vorming van littekenweefsel.
De waargenomen afname van niervolume impliceert dat niervolume geen goede voorspellende factor is voor het ontwikkelen van volledige uitval van de nierfunctie en zou niet als enige parameter gebruikt moeten worden in klinische trials om de effectiviteit van een kandidaat geneesmiddel vast te stellen.
Dit proefschrift laat zien dat cystenvorming, cystengroei en ADPKD ziekteprogressie complexe processen zijn, die door veel factoren beïnvloed worden. Dit biedt niet alleen veel aangrijpingspunten voor therapeutische interventie, maar is tegelijkertijd een moeilijkheid. Therapeutische interventie op slechts één aangrijpingspunt zal hoogst waarschijnlijk niet succesvol zijn. Voor de behandeling van ADPKD is eerder een "multi-target" aanpak nodig.
Dit promotieonderzoek heeft bijgedragen aan het inzicht in het onstaan en de groei van cysten en de progressie van ADPKD. Dit is slechts een kleine stap vooruit in de zoektocht naar een behandeling voor ADPKD. Zoals gebruikelijk in wetenschappelijk onderzoek levert een beantwoorde vraag minstens één nieuwe vraag op: meer onderzoek is nodig.

9

Curriculum Vitae

Curriculum Vitae

Hester Happé werd geboren op 9 oktober 1981 te 's-Hertogenbosch. Van 1994 tot 2000 volgde zij het VWO op het d'Oultremontcollege te Drunen, waar haar voorkeur uitging naar de vakken biologie, scheikunde en natuurkunde. Na het behalen van haar eindexamen studeerde zij Biofarmaceutische Wetenschappen aan de Universiteit van Leiden waar zij in 2001 haar propedeuse behaalde. Tijdens haar studie was Hester actief in verschillende commissies binnen de studievereniging "Aesculapius" en vervulde daar tevens een bestuursfunctie. In december 2005 behaalde zij haar doctoraal diploma waarna zij in januari 2006 begon aan haar promotieonderzoek naar erfelijke cystennieren bij de afdeling Humane Genetica en Pathologie van het LUMC. Tijdens haar promotieonderzoek mocht zij haar resultaten verschillende malen presenteren tijdens nationale en internationale congressen.
Het promotieonderzoek resulteerde in 2012 in het proefschrift getiteld: "Cyst initiation, cyst expansion and progression in ADPKD". Tijdens het afronden van haar proefschrift werkte Hester bij Stichting C3, waar zij projectmedewerker was bij de promotie van procestechniek onder jongeren. Tevens werkte zij als onderzoeker op een samenwerkingsproject van de afdeling Humane Genetica en Roche waarbij onderzoek werd gedaan naar het remmen van cystengroei.
Sinds december 2011 is zij werkzaam als postdoc onderzoeker bij de afdeling ouderengeneeskunde, waar zij onderzoek doet naar de cellulaire mechanismen achter veroudering.

10

List of Publications

List of Publications

Happé H, de Heer E, and Peters DJ**.** Morphometric analysis of centrosome position in tissues. *Methods Mol Biol. 2012;839:249-55.*

Happé H, de Heer E, and Peters DJ. Polycystic kidney disease: The complexity of planar cell polarity and signaling during tissue regeneration and cyst formation. *Biochim Biophys Acta. 2011 Oct;1812(10):1249-55. Epub 2011 May 27.*

Happé H, van der Wal AM, Leonhard WN, *et al.* Altered Hippo signalling in polycystic kidney disease. *J Pathol. 2011 May;224(1):133-42. Epub 2011 Mar 7.*

Happé H, Leonhard WN, van der Wal A, *et al.* Toxic tubular injury in kidneys from *Pkd1*-deletion mice accelerates cystogenesis accompanied by dysregulated planar cell polarity and canonical Wnt signaling pathways. *Hum Mol Genet. 2009 Jul 15;18(14):2532-42. Epub 2009 Apr 28.*

Streefland M, van de Waterbeemd B, **Happé H**, van der Pol LA, Beuvery EC, Tramper J, Martens DE. PAT for vaccines: the first stage of PAT implementation for development of a well-defined whole-cell vaccine against whooping cough disease.*Vaccine. 2007 Apr 20;25(16):2994-3000. Epub 2007 Jan 22.*

van Wanrooij EJ, **Happé H**, Hauer AD, de Vos P, Imanishi T, Fujiwara H, van Berkel TJ, Kuiper J.HIV entry inhibitor TAK-779 attenuates atherogenesis in low-density lipoprotein receptor-deficient mice. *Arterioscler Thromb Vasc Biol. 2005 Dec;25(12):2642-7. Epub 2005 Oct 20.*

11

Dankwoord

Dankwoord

Een promotieonderzoek is iets dat je niet alleen kunt doen, ik ben dan ook veel mensen mijn dank verschuldigd. Als eerste wil ik mijn "lab-Peters" collega's bedanken voor de fijne tijd. Wouter, bedankt voor al je hulp met expressieanalyses en *in vivo* experimenten en de (wetenschappelijke) discussies die we zo tussendoor voerden. Hans, ik dank je voor je interesse en hulp, als ik raad en daad nodig had en je kon me helpen, dan deed je dat. Irma, je was een goede collega en stond altijd klaar voor een goed gesprek. Ook Jeroen, Paola, Nanna, Sabrin en Zlata, dank jullie wel voor de fijne tijd op het lab. Daarnaast ben ik ook mijn studenten Marlon, Irene en Steven dankbaar voor hun inzet op het lab en de dingen die ik van hen heb kunnen leren. Verder wil ik ook mijn collega PhD-studenten en andere collega's van Humane Genetica bedanken. Sjoerd, Antoine en Silvia, *partners in crime*, bedankt voor de leuke tijd tijdens de MGC Promovendi Workshops, en jullie verdere steun.

Deels hoorde ik ook bij de afdeling pathologie. Ondanks dat ik daar niet mijn werkplek had, voelde ik me daar als verse promovenda meteen welkom. Daphne, Marije, Marian, Klaas, Suzanne, Idske en later Hanneke, Annelies en Antien, en ook de anderen van de AIO-kamer: ontzettend bedankt voor jullie steun en interesse in mijn "hardcore" onderzoek. Ook tijdens de projectbesprekingen bij pathologie hoorde ik er helemaal bij. Professor Bruijn, Professor van Es, Ingeborg, Hans en alle anderen, het was mij een waar genoegen om met jullie van gedachten te wisselen over mijn hypothesen en onderzoeksresultaten. Ik heb er van genoten! Jan Anthonie, ik waardeer je enthousiasme enorm, het gaf me energie en motiveerde me op momenten dat ik het nodig had.

Verder wil ik nog aantal collega's van de afdeling Patholgie persoonlijk noemen. Beste Frans, uren hebben we gespendeerd achter de confocale microscoop en macro's maken voor Image J. Bedankt voor al je hulp en het meedenken. Jij bent een belangrijke ondersteuning geweest bij de totstandkoming van dit proefschrift. Beste Annemieke, ik mocht je nooit bedanken voor het werk dat je gedaan had, jij vond dat je immers gewoon je werk deed. Tot groot verdriet van ons allemaal ontviel je ons onverwacht en veel te vroeg het afgelopen jaar. Ontzettend bedankt voor al je inzet en de prettige samenwerking. Zonder jouw kennis en deskundigheid had de inhoud van mijn proefschrift er heel anders uitgezien. Ik zal nooit vergeten wat voor een fijne collega en mooi persoon je was.

Ook de mensen die ondersteuning boden bij mijn onderzoek wil ik niet vergeten. Ik heb een aantal mensen getroffen die vaak een stapje extra gezet hebben om toch mogelijk te maken wat eigenlijk niet haalbaar was. Van de collega's van de dierverzorging van het PDC wil ik graag Michel speciaal bedanken voor de hulp bij de strak geplande experimenten en het luisterend oor. Daarnaast ben ik ook Daniela en Saskia mijn verschuldigd voor hun hulp bij de laatste *in vivo* experimenten van mijn promotieonderzoek.

Dr. Emile de Heer en dr. Dorien Peters, ik wil jullie heel erg bedanken voor de begeleiding tijdens de afgelopen jaren en de waardevolle discussies tijdens onze werkbesprekingen. Beste Emile, bedankt voor je steun en goede raad op de moeilijke momenten. Beste Dorien, ik heb veel plezier gehaald uit onze discussies en gedachtewisselingen, vaak nog even aan het einde van de dag. Met plezier denk ik terug aan de keren dat een koffiemok en pen onmisbaar bleken.

Lieve vrienden, Emmani, Willem, Elke, Dennis, Jenina en Anne, dank jullie wel voor alle belangstelling voor mijn proefschrift en steun de afgelopen jaren. Bedankt voor het steeds aanhoren van mijn proefschrift frustraties. Linda, ook jij hebt me de afgelopen jaren minder vaak gezien dan ik had gewild, maar je bent er als ik je nodig heb. Mijn hardloopmaatjes, Monique, Bart, Boudewijn, Mariska en alle anderen, de afgelopen twee jaar bleven jullie onvermoeid vragen hoe het mijn proefschrift ging. Dank jullie wel voor jullie luisterend oor. Lieve Acception meiden, Josine, Monique, Jorine, Brenda, Willemieke Michelle en de "nieuwe" garde: dank jullie wel voor jullie geduld, steun en begrip. Ook wil ik mijn verschillende danspartners Han, Piotr en Emmani bedanken. Het dansen zorgde voor de broodnodige afleiding en (poging tot) ontspanning, hoe vaak was leiden lijden?

Luuk natuurlijk wil ik jou ook bedanken, jij was mijn wetenschappelijke sparringpartner, bedankt voor het begrijpelijk houden van mijn manuscripten en de verhelderende discussies. Dank je wel voor al je steun de afgelopen 5,5 jaar, je hebt me door veel moeilijke momenten heen geholpen.

Tot slot wil ik ook mijn ouders bedanken. Pap en mam, bedankt voor jullie steun en luisterend oor. Bedankt voor jullie interesse in mijn werk en jullie geduld. Dit proefschrift is ook een beetje voor jullie.